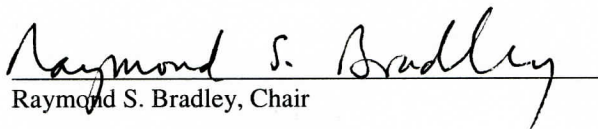**CLIMATE AND ENVIRONMENTAL CHANGE IN ARCTIC CANADA: OBSERVATIONS FROM UPPER AND LOWER MURRAY LAKES, ELLESMERE ISLAND, NUNAVUT**

A Dissertation Presented

by

TIMOTHY COOK

CLIMATE AND ENVIRONMENTAL CHANGE IN ARCTIC CANADA: OBSERVATIONS FROM UPPER AND LOWER MURRAY LAKES, ELLESMERE ISLAND, NUNAVUT

A Dissertation Presented

by

TIMOTHY COOK

Approved as to style and content by:

_____
Raymond S. Bradley, Chair

_____
Robert Deconto, Member

_____
David P. Ahlfeld, Member

_____
Al Werner, Member

_____
Michael L. Williams, Department Head
Department of Geosciences

ACKNOWLEDGEMENTS

ABSTRACT

CLIMATE AND ENVIRONMENTAL CHANGE IN ARCTIC CANADA: OBSERVATIONS FROM UPPER AND LOWER MURRAY LAKES, ELLESMERE ISLAND, NUNAVUT

SEPTEMBER 2009

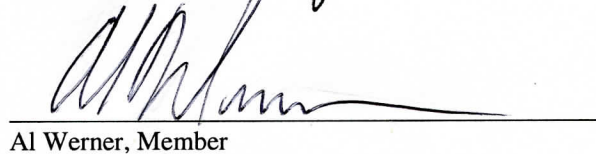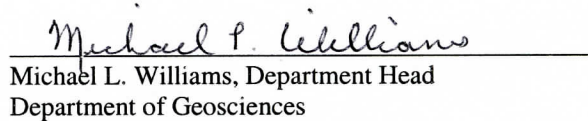TIMOTHY COOK, Sc.B., BROWN UNIVERSITY

M.S., UNIVERSITY OF DELAWARE

Ph.D., UNIVERSITY OF MASSACHUSETTS AMHERST

Directed by Professor Raymond S. Bradley

This study was designed with the overriding goal of improving our understanding of the nature, causes, and impacts of past climatic conditions in the High Arctic and to evaluate the potential impacts of future climatic warming. Specifically, the focus of this project was centered on Upper and Lower Murray Lakes (81° 21' N, 69° 32' W) on northern Ellesmere Island, Nunavut, Canada. Sediment cores were collected from each of the lakes in order to reconstruct past climate and environmental variability and space-borne synthetic aperture radar (SAR) data were used to evaluate recent variability in the ice cover of these lakes.

The climatic setting and physical characteristics of Lower Murray Lake has led to the formation and preservation of annually laminated sediments (varves). Varve deposition began ca. 5200 calendar years BP and continued through 2004 AD, providing an annual record of sediment accumulation spanning the past 5200+ years. Annual mass accumulation was correlated to regional July temperatures providing a means of quantitatively evaluating past temperature changes in the region. The temperature reconstruction suggests that recent temperatures are ~2.6°C higher than minimum temperatures observed during the Little Ice Age, maximum temperatures during the past 5200 years exceeded modern values by ~0.6°C, and that minimum temperatures observed approximately 2900 varve years BC were ~3.5°C colder than recent conditions.

SAR observations of the ice cover Upper and Lower Murray Lake were used to assess the potential effects of past and future temperatures on lake-ice conditions. Under current climatic conditions the lakes average several weeks of ice-free conditions in August and early September, although in some

years a continuous ice cover persists throughout the year. The relationship between summer temperature and ice melt at the lakes suggests that recent warming in the High Arctic has forced the lakes across a threshold from a state of perennial ice cover to seasonal melting. Projected future warming will significantly increase the duration of ice free conditions on Upper and Lower Murray Lakes. Ice-out is predicted to occur between 6 and 28 days earlier for every 1°C of warming.

TABLE OF CONTENTS

LIST OF FIGURES

CHAPTER 1

INTRODUCTION

<u>Context of the study</u>

In light of projected changes in the global climate system stemming from human activity it is important that we understand the causes and impacts of past, present, and future climatic changes. Knowledge of how the climate system has responded to various forcing mechanisms in the past is useful for assessing how the climate system may respond to anticipated changes in future conditions. In addition, reconstructions of past climatic conditions and coincident environmental impacts can help guide potential mitigation and adaptation strategies to future changes. The Arctic is a region that is particularly sensitive to global climate change and it makes up an important component of the global climate system. These factors make the Arctic an important site for studies of past climate and environmental conditions.

The significance of the Arctic within the global climate system and its enhanced sensitivity to global climate change results from the complex interactions and feedbacks of a variety of processes. The contrast in albedo between snow or ice and bare land or open water creates a positive feedback mechanism where increased air temperatures cause melting and a reduction in the extent of snow and ice cover which in turn leads to increased absorption of solar radiation at the Earth's surface and further warming (e.g. Manabe and Stouffer, 1980; Robock, 1980). Changes in sea-ice thickness and extent also influence the thermal inertia of the ocean and alter heat and moisture transfer between the ocean and atmosphere (Holland and Bitz, 2003). Increased cloud cover resulting from more open water can create a positive feedback scenario by increasing the downward longwave radiation at the surface (Holland and Bitz, 2003). Changes in snow, ice, vegetation and soil conditions in the Arctic can in turn influence the global climate system through a variety of processes. Reduced sea-ice extent in the Arctic Ocean has the potential to create a significant sink for atmospheric CO_2 which is readily absorbed in cold water (Laxon et al., 2003). However, warming of the Arctic may accelerate the rate of soil decomposition and cause the region to change from a net carbon dioxide sink to a net source (Oechel et al., 1993). Ice sheets in the Arctic exert a topographic influence on atmospheric circulation and alter the pattern of synoptic systems (Barry, 2002). In

addition, increased freshwater runoff and iceberg calving rates resulting from higher temperatures in the Arctic may influence the freshwater flux to the North Atlantic and in combination with warmer surface ocean conditions lead to a reduction in meridional overturning circulation, which in turn influences global heat transport and climatic conditions (Stocker and Wright, 1991; Solomon et al., 2007). Thus, an improved understanding of the Arctic climate system is critical to our comprehension of the causes and impacts of global climate change.

According to climate model simulations using a range of emissions scenarios, globally averaged surface temperatures are projected to increase by 1.1 to 6.4°C during the 21st century (Solomon et al., 2007). Model simulations suggest that warming over most land areas will occur even more rapidly than the global average and that high northern latitudes in particular will see some of the most extreme warming (Solomon et al., 2007). For example, Holland and Bitz (2003) compared projections of Arctic and global temperature changes based on output from 15 different climate models. All of the model projections show significantly amplified warming at high northern latitudes, with warming from 75-90° N that is typically two to three times the global average (Holland and Bitz, 2003).

The impacts of global warming on humans and the environment are likely to be particularly severe in Arctic regions. In particular, indigenous communities are dependant on climate-sensitive resources for food, commerce, and transportation and a warmer climate will cause considerable cultural and economic impacts. Reduced sea ice is likely to create new opportunities for shipping and resource exploration in Arctic waters, but also increases the threat of waves and storm surges on coastal areas. In addition, a number of different species will be influenced by a warmer Arctic, with some species being pushed towards extinction. Specifically, reductions in sea-ice extent reduce critical habitat necessary for the survival of polar bears, ice-inhabiting seals, and some seabirds. (ACIA, 2004)

Despite the potential impacts of global warming on the Arctic and the significance of the Arctic to the global climate system our understanding of the Arctic climate system is severely limited by a lack of information pertaining to past climatic conditions. The instrumental record is very short, spanning only the past 50-100 years in most regions and provides limited spatial coverage. In addition, limited daylight and extremely low temperatures reduce the potential for paleoclimate reconstructions based on many proxy indicators used in other regions, such as tree rings, fossil pollen, and plankton assemblages. The few long-

term proxy records that are available provide limited geographic coverage and typically demonstrate low temporal resolution (e.g. Gajewski and Atkinson 2003), thus there is a significant need for additional high-resolution paleoclimatic data from the Arctic.

Objectives and Hypotheses

In light of the sensitivity of the Arctic to climatic changes, the importance of the Arctic as a component of the global climate system, and the considerable uncertainty which remains in our knowledge of the Arctic climate system, both past and future, this study was designed with the overriding goal of improving our understanding of the nature, causes, and impacts of past climatic conditions in the High Arctic and to evaluate the potential impacts of future climatic warming. Specifically, this project utilized lake sediments as archives of past environmental conditions in the High Arctic and examined the impacts of climate change on High Arctic lake systems. The focus of this project was centered on Upper and Lower Murray Lakes (81° 21' N, 69° 32' W) on northern Ellesmere Island, Nunavut, Canada.

In order to meet the goals outlined above, this study tested three main hypotheses:

1. The physical characteristics of annually laminated sediments in high Arctic lakes are a sensitive indicator of past climate variability.

2. Changes in summer climate in the High Arctic are related to shifts in radiative forcing caused by variations in solar irradiance, explosive volcanism, and the concentration of greenhouse gases in the atmosphere.

3. Ice cover on high arctic lakes is sensitive to small temperature changes and recent warming has caused a significant reduction in the duration of ice cover on High Arctic lakes.

Research Strategy and Thesis Organization

The research strategy of this project involved multiple components that are reflected in the organization of this thesis. First, field observations and long sediment cores were used to characterize the modern environment of Upper and Lower Murray lakes and to trace their evolution following deglaciation

(Chapter 2). This information provides essential context for understanding and evaluating the significance of the paleoclimate record preserved in the lake sediments. The second component of the study involved investigating the climatic processes controlling sedimentation in the Murray Lakes and using this information to identify the major climatic variations recorded in Murray Lake sediments over the past 5000+ years and to evaluate the mechanisms responsible for these variations (Chapter 3). Chapter 4 summarizes the current understanding of Holocene climate change in the Canadian High Arctic and evaluates the significance of the Lower Murray lake record and other varve-based climate reconstructions within this regional context. Finally, recent instrumental and satellite based observations were used to identify the effects of recent temperature changes on ice cover on Upper and Lower Murray lakes and to evaluate the impacts of continued warming on these lakes (Chapter 5). Chapter 6 provides a summary of the major conclusions derived from this study, describes the need for continued research on Arctic environmental change, and evaluates the potential for further research focused on Upper and Lower Murray lakes.

CHAPTER 2

**CHARACTERIZATION OF THE MODERN AND ANCIENT ENVIRONMENT
OF UPPER AND LOWER MURRAY LAKES**

Introduction

Lake sediments provide an important archive of past environmental conditions and comprise a valuable resource for climate and global change studies. The utility of lakes in studies of arctic environmental change is based on a number of factors, including: (1) lakes and ponds are widely distributed in arctic regions; (2) lake basins often contain continuous records of environmental change spanning thousands of years; (3) local human activity has had little or no impact on most arctic lakes; and (4) biological, chemical, and physical processes occurring in arctic lakes are closely linked to climate and meteorological variability at a variety of timescales (Pienitz et al., 2004).

This chapter describes field observations at Upper and Lower Murray lakes and discusses the subsequent analysis of sediment and water samples that were collected in the field. This information is used to characterize the modern environment of the study site. In addition, a discussion of the physical and inorganic geochemical characteristics of the sediment is used to trace the evolution of Upper and Lower Murray lakes after regional deglaciation. The purpose of this section is to provide context for the subsequent evaluation of the paleoclimatic signal preserved in the sediments of Lower Murray Lake, as described in Chapter 3. These lakes were originally identified as a potential study site for reconstructing past climate and environmental change by researchers from the University of Massachusetts while conducting field work on a pair of small icecaps located on the plateau adjacent to the lakes (cf. Braun, 2006). Reconnaissance work in 2000 and additional work in 2001 recovered the first sediment cores from the two lakes and identified annually laminated sediments which have proven to be useful indicators of past climatic conditions at other sites in the Arctic (e.g. Hardy et al., 1996; Lamoureux and Bradley, 1996; Hughen et al., 2000; Moore et al., 2001). The results of the preliminary work were described by Besonen et al. (2008) who established a ~1000 year record of climate change based on the characteristics of laminated sediments in Lower Murray Lake. The present study has extended this climate record through the past

5,000 years and has defined a quantitative relationship between July temperatures and the amount of annual sediment accumulation in Lower Murray Lake (cf. Chapter 3).

Description of the study area

Physical Setting

Upper and Lower Murray Lakes are located within the Hazen Plateau region of northeastern Ellesmere Island, Nunavut, Canada (81°21' N, 69°32' W; Figure 2.1). The long, narrow lakes occupy a glacially carved valley within an extensive upland plateau (Figure 2.2). Upper Murray Lake is ~7.5 km long and has a surface area of ~7.5 km^2; Lower Murray Lake is ~6.5 km long with a surface area of ~5 km^2. The drainage basin of the two lakes is characterized by considerable relief, with the majority of the watershed located on adjacent upland plateaus. Lower Murray Lake has a total drainage basin of 261 km^2. However, the majority of this area (184 km^2) first drains into Upper Murray Lake which is connected to the lower lake by a shallow stream. The elevation of the upper and lower lakes are 107 and 106 m, respectively, while the adjacent plateau has a maximum elevation between ~1100 and 1300 m at the summits of several small ice caps located partially within the drainage basin. Runoff associated with snow and ice melt in the upland areas drains into the lakes via several short, high gradient streams. The main tributary entering Upper Murray Lake drains an approximately 55 km^2 ice cap located southwest of the lakes. Two small, stagnant ice caps located east of the lakes drain directly into Lower Murray Lake at its extreme north and south ends. Apart from the outlet stream which runs from the upper lake into the lower lake, the largest tributary entering Lower Murray Lake is found at its southeast corner, near its outflow stream. Streamflow in the outlets of Upper Murray Lake (~1.5 m^3/s) and Lower Murray Lake (~2.9 m^3/s) was estimated in early August of 2006 using the Embody (1927) method. These results suggest that 50% or more of the total runoff into Lower Murray Lake first flows through the upper lake. At the time of the survey the stream connecting the two lakes was ~33 m wide and <0.2 m deep. Upper Murray Lake has a single deep basin in its northeast corner with a maximum depth of 83 m. The remainder of the lake is typically less than 30 m deep. Lower Murray Lake has a central basin with a maximum depth of 46 m. This basin is separated from the southern portion of the lake and the main inlet stream by an approximately 300

m wide channel of unknown depth. Table 2.1 provides a summary of the main physiographic characteristics of the two lakes.

Geologic Setting

The bedrock geology of the Murray Lakes region and surrounding Hazen Plateau consists mainly of calcareous-dolomitic sandstone and slaty mudrock of the Danish River Formation, deposited during the Lower Silurian to Lower Devonian in a deep water setting (Trettin, 1994). Compositionally the Danish River Formation is rather homogenous, with the silicate fraction of the sandstones consisting mainly of quartz (mean content ~ 52%) with lesser proportions of feldspar (albite 8%, K-feldspar 4%), phyllosilicates (muscovite, chlorite and biotite combined 4%), low grade metamorphic rock fragments (3%), and chert (1%). The balance of the material (~28%) consists of carbonate grains mixed with the silicates (Trettin, 1994). Weathered bedrock and colluvium are the dominant surficial deposits within the lake basin, with fluvial and gelifluction processes the dominant agents of erosion. Weathering of the Danish River Formation provides a regular source of carbonate and siliciclastic material for transport to and deposition within the lakes.

Modern Climatic Setting

Long term observations of climatic conditions in the Canadian High Arctic are of limited duration (~60 years) and sparsely distributed, thus our ability to fully characterize the local climatic setting of Upper and Lower Murray Lakes is somewhat limited. The two nearest permanent weather stations are located at Alert, approximately 180 km north of the Murray lakes, and at Eureka, approximately 325 km to the west. While the two stations provide a useful record of climatic conditions, caution must be used when making regional generalizations due to the effects of local influences at each station. Specifically, Alert is influenced by cold air advection from the Arctic Ocean and the blocking of solar radiation by frequent low clouds and fog while Eureka is subject to the rainshadow effect of surrounding mountains (Maxwell, 1981). Keeping these limitations in mind, northern Ellesmere Island and the region surrounding the Murray Lakes can be characterized by extreme seasonality in temperatures and low annual precipitation totals (Maxwell, 1981). For the period 1971-2000, mean annual temperatures at Alert and Eureka were -18° C and -20° C,

respectively. Temperatures above freezing are typically experienced only during the months of June, July, and August, with mean daily maximum temperatures during the summer of 3.6° C at Alert and 6.1° C at Eureka. Total annual precipitation at Alert and Eureka are extremely low, averaging only 154 and 76 mm water equivalent (weq), respectively. The majority of this precipitation occurs as snow, with total annual rainfall at Alert and Eureka averaging only 16 and 26 mm, respectively (Table 2.2)

In addition to the observations from the permanent stations at Alert and Eureka, ~24 months of local observations (during 1999-2001) were recorded on the Hazen Plateau adjacent to the Murray Lakes and provide additional details about the local climatic setting (Braun, 2006). These data are particularly relevant to our understanding of the processes influencing the Murray Lakes, as much of the drainage basin is located on the upper plateau, within the focus area of the study by Braun (2006). Comparison of mean monthly temperatures on the Hazen plateau with the measurements from Alert and Eureka confirmed that these long term stations can provide a reasonable approximation of temperature conditions near the Murray Lakes, (Braun, 2006). Based on snow accumulation measurements on Murray and Simmons ice caps, and nearby St. Patrick Bay ice caps, Braun (2006) concluded that high elevation regions of the Hazen Plateau probably receive, on average, about 100 to 125 mm weq of winter snow accumulation and 125 to 150 mm weq total annual precipitation. Approximately 80 percent of the annual precipitation typically occurs during the fall, winter and spring as snow.

Methods

Field work

Upper and Lower Murray Lake were visited in June 2005 and August 2006 to conduct coring and to survey the lake environment. The bathymetry of the lakes was determined by drilling a hole through the ice and lowering an echosounder into the hole to measure water depth. Occasional spot checking with a tape measure and weight confirmed the accuracy of the echosounder to within 10 cm (Figure 2.2). A suite of cores were collected from the deepest point in each of the lakes: 83 m water depth in Upper Murray Lake at 81.39872° N, 69.81638° W and 46 m water depth in Lower Murray Lake at 81.34175° N, 69.55204° W (Table 2.3; Figure 2.2). Two overlapping, long cores were collected at each site using an

Uwitec piston corer. Special care was taken to collect an undisturbed record of the upper-most sediments and to preserve an intact sediment-water interface using an Aquatic Research Instruments gravity corer and an Ekman dredge-type sampler. Both the Aquatic Research and Ekman cores displayed clear water overlying the sediment, confirming that an undisturbed sediment water interface was recovered. The Ekman samples were subsampled by inserting a 6 cm diameter polycarbonate tube into the sediment and then sealing both ends of the tube. Table 2.4 contains a complete list of the sediment cores collected from both Upper and Lower Murray Lakes and a description of the analyses performed on the individual cores. Water samples were collected from a number of depths at each of the coring locations and from each of the main streams draining into or out of the lakes (Table 2.3). Water column measurements of temperature, pH, conductivity, and dissolved oxygen were recorded using a Hach Corporation Hydrolab MiniSonde. In June 2005, water column measurements were recorded at the coring site (deepest basin) in each lake. In August, 2006 access to the deepest points in the lakes was limited by ice conditions, so profiles were recorded at the deepest location that was accessible through leads in the ice (Table 2.3: Fig 2.2).

A process monitoring program was planned in order to better understand the connection between local meteorological conditions and sedimentation within the lakes. Two Onset Computer Corporation HOBO Pro Temp H08-030-08 air temperature loggers were placed in the watershed to record local temperature conditions. The temperature loggers were configured with a 1 hr sampling interval and placed within a solar radiation shield located 2 m above the ground surface. One logger was located near the lake shore at the north end of Lower Murray Lake; the second logger was located on the upper portion of the slope leading to the plateau east of the lakes (Table 2.3; Figure 2.2). The temperature loggers were deployed in early June 2005 and recovered in early August 2006. According to the manufacturer, the stated accuracy of the loggers is better than $\pm$ 0.5 °C for temperatures between 0 and 40 °C. Between 0 and -40 °C temperature accuracy decreases to approximately $\pm$1.25 °C. No additional verification of the accuracy of the temperature loggers was conducted.

In addition, moorings were deployed at the coring sites in both lakes in order to monitor sediment accumulation and lake-water temperature. Each mooring consisted of two automated sediment accumulation sensors (Lamoureux, 2005) located ~1.2 m above the lake bottom and 10 m below the lake surface and an Onset Computer Corporation HOBO U22 Water Temp Pro v2 water temperature logger

located 10 m below the surface. Mooring recovery was planned for August of 2006. At this time however, the lakes remained more than 80% covered by a severely candled ice surface that prohibited boat travel and proved unsafe as a working platform, thus the sediment accumulation sensors were never recovered. This situation underscores the challenges associated with field work on remote high-arctic lakes.

Laboratory Analysis

All cores were split, photographed and described in the lab in order to facilitate further analysis and interpretation of the sedimentary record. The initial core descriptions were used to guide targeted physical and geochemical analysis of sediments with the goal of producing a continuous record of environmental change using the least disturbed sections of the cores. Preliminary analytical results and chronological data were then used to refine the sampling scheme throughout the process. Due to the overall poor quality of the cores recovered from Upper Murray Lake (UML sediments contained high concentrations of gas vesicles and considerable disturbances likely originating from core recovery), the primary focus of the laboratory work became the analysis of Lower Murray Lake sediments.

Dry bulk density of the sediment was measured by extracting 1 cc sub samples using a cutoff syringe, drying the sediment for 16 hours at 105°C and then measuring the mass. Dry bulk density was calculated by dividing the dry mass of the sediment by the initial sampling volume. Organic carbon content was then estimated by percent loss-on-ignition (LOI) using the same samples analyzed for bulk density. Dried samples were placed in a preheated 550°C muffle furnace for 4 hours and then allowed to cool in a dessicator. Percent LOI was estimated by dividing the mass difference between the dry sediment sample and the post ignition sample by the mass of the dry sample (Dean, 1974; Heiri, et al. 2001). Bulk density and LOI were measured on Lower Murray Lake sediments at 1 cm interval for the uppermost 15 cm, 2 cm intervals from 15 to 500 cm depth, and 10 cm intervals from 500 to 1340 cm depth.

Sediment grain size was analyzed using a Beckman Coulter LS200 particle size analyzer. Sample sizes ranged from 0.1 to 0.8 g depending on the grain size distribution of the sample. Coarser sediment required larger sample sizes in order to meet the obscuration requirements of the instrument. Prior to particle size analysis, sediment sub samples were pretreated to digest organic material. Two mL of Hydrogen Peroxide (H_2O_2) solution was combined with the sediment sample in a 25 mL centrifuge tube.

The mixture was initially broken-up using a test tube shaker for ~20 seconds and then placing the tube in an ultrasonic bath for 60 seconds. Samples were then left for 24 hours in a cold (tap water) bath with the centrifuge tube loosely capped. After 24 hours the tubes were tightly capped, mixed for ~ 20 seconds, sonicated for 60 seconds and placed in an oven at 50° C for at least 48 hours. After 48 hours in the oven but not more than 24 hours prior to being analyzed 1 mL of dispersant solution (consisting of 30 g of $NaPO_3$ and 7 g of $NaCO_3$ per 1 L of solution) was added to the samples. Samples were again mixed for ~ 20 seconds and sonicated for 60 seconds before being analyzed. Particle size was analyzed at 1 cm intervals for the uppermost 500 cm and at 10 cm intervals from 500 to 1340 cm depth.

Subsamples for paleomagnetic analysis were recovered from the split cores using rigid u-shaped plastic channels with a 2 cm x 2 cm cross section. Paleomagnetic analyses were conducted at Institut des Sciences de la Mer de Rimouski, Québec, Canada. The primary purpose of the paleomagnetic measurements in the present study was to provide an independent means of verifying the varve chronology by comparing the paleomagnetic record from Lower Murray Lake with other independently dated regional records (Chapter 3). The following measurements were used in this study: characteristic remanent magnetization (ChRM) declination; ChRM inclination; relative paleointensity estimated using the mean of the natural remanent magnetization (NRM) intensity normalized by anhysteretic remanent magnetization (ARM) over a range of progressive alternating field demagnetization steps; and the ratio of ARM after 30 mT demagnetization to the ARM before demagnetization. Refer to Stoner and St-Onge (2007) for a detailed explanation of these measurements. Further analysis and interpretation of the paleomagnetic data is being conducted by Maureen Davies and Joseph Stoner at Oregon State University.

High resolution geochemical analysis of the sediments was carried out using an ITRAX X-ray flouresence (XRF) core scanner at Institut national de la recherche scientifique, Centre Eau, Terre et Environment, Québec, Canada. The ITRAX scanner provides a rapid non-destructive technique for acquiring continuous geochemical measurements at a maximum resolution of 100 μm (Croudace et al., 2006). The XRF was configured with a 3 kW molybdenum target tube operating at 30 kV and 30 mA. A wide range of elements can be detected by the ITRAX XRF and geochemical data for individual elements are output as counts related to their relative abundance. Detection limits for individual elements vary based on atomic number and the acquisition time of the analysis; under ideal conditions concentrations as low as

5 ppm can be detected for certain elements. Analyses were performed on either split core halves or u-channel subsamples. Measurements were acquired using various sampling intervals ranging from 100 to 1000 μm and acquisition times of 1, 5 or 10 sec depending on the characteristics of the sediments (Table 2.5). Finely laminated portions of the sediment were targeted for higher resolution (100 μm) measurements with a 1 sec acquisition time. One second acquisition times provided unsatisfactory detection limits, so the longer 5 sec measurements, recorded at 500 and 1000 μm intervals were utilized for the construction of a composite down core record of sediment geochemistry. One core section (LML-05-C1-B2) was inadvertently analyzed with a 10 sec acquisition time. The count totals from this section were divided by two so that the values were comparable with the rest of the data obtained using a 5 sec acquisition time.

Quantitative measurements of the chemical composition of sediments were acquired by inductively coupled plasma-atomic emission spectrometry (ICP-AES; Boyle, 2001). Three subsamples, representing different sedimentary facies found in the Lower Murray Lake record were analyzed for 26 different major, minor, and trace elements. Analyses were conducted on a Varian Instruments Vista AX CCO Simultaneous ICP-AES at Institut national de la recherche scientifique, Centre Eau, Terre et Environment, Québec, Canada. Sample LML-05-C1-E1-1 came from a depth of 6 cm, sample LML-05-C1-E1-2 came from a depth of 8 cm, and sample LML-05-C1-C1-1 came from a depth of 573 cm.

Water samples were analyzed for both anion and cation concentrations. Anions were analyzed via Ion Chromatography using a Lachat IC 5000 instrument using a setup based on EPA method 300.0. Anions were separated based on their affinity for an ammonium resin column, identified based on their retention times, and quantified using a calibration curve based on the analysis of known standards. Cations were analyzed via ICP-OES using a Spectro M120 sequential instrument. Aqueous samples were made into a mist and then introduced into an Argon plasma. Light emissions given off by individual elements were measured by photomultiplier tubes and quantified using a calibration curve. Individual samples were measured three times by the instrument with the average value reported.

Chronological Control

Recent sedimentation rates were evaluated by measuring the activity levels of ^{210}Pb and ^{137}Cs in surface cores LML-05-C1-E5 and UML-05-A4. Cores were sub-sampled by removing 0.5 or 1.0 cm (LML and UML, respectively) slices of sediment from the split core tube. Individual samples were then freeze-dried and powdered. Twelve samples from LML-05-C1-E5 and eight samples from UML-05-A4 were analyzed by gamma spectroscopy using Canberra ultra low background well-style germanium detectors at the University of Florida.

Radiocarbon dating was used to provide additional age control on sediments in Upper and Lower Murray Lakes. A total of seven samples from Upper Murray Lake cores and one sample from Lower Murray Lake cores were collected (Table 2.6). The samples, consisting of terrestrial organic macrofossils, were isolated from the sediments and sent to the University of Pittsburgh Radiocarbon Laboratory for cleaning and preparation following standard acid/alkaline/acid pretreatment methods (Abbott and Stafford, 1996). Dating of the samples was conducted at the University of California Irvine Keck Accelerated Mass Spectrometry Radiocarbon Laboratory. Radiocarbon ages were calibrated to calendar years AD/BC using CALIB 5.0.1 (Stuiver and Reimer, 1993; Reimer et al, 2004).

Additional age control was provided by counting annual laminations (varves) in the upper 2.3 m of Lower Murray Lake sediments. Varve counts utilized digital images of thin sections made from epoxy impregnated sediment slabs. The annual nature of the individual lamina and the accuracy of the long term varve chronology were assessed by comparing paleomagnetic variations in Lower Murray Lake sediments to the independently dated paleomagnetic record from South Sawtooth Lake. A thorough discussion of the techniques used to construct and verify the varve chronology, and an assessment of its uncertainty is presented in Chapter 3.

Results

Surface Air Temperatures

Approximately 14 months of surface air temperature data were acquired from June 10, 2005 through August 8, 2006 (Figure 2.3). The maximum temperatures during this period were recorded on July

23, 2005 and reached 19.5 °C at lake level, and 14.2 °C on the upper slope. The minimum temperature at lake level, -41.2 °C, was recorded on March 14; the minimum temperature recorded on the upper slope, -40.1 °C occurred on February 11, 2006. During summer (June, July and August), temperatures were generally warmer at lake level than on the upper slope. Temperature inversions (defined by mean daily temperatures on the upper slope which were higher than mean daily temperatures at lake level) were observed during 40 % of the days during the summer months. In contrast, temperature inversions were observed 76 % of the time during the remainder of the year (September through May). During the most extreme cases temperatures on the upper slope were as much 15 °C warmer than lake level temperatures. Because the two temperature loggers spanned a 500 m elevation range, the difference in mean daily air temperature at each of the stations was used to estimate the surface air temperature lapse rate. Considering only those days on which temperature inversions were not observed the average surface air temperature lapse rate was -4.2 °C / 1000 m during the observation period.

Lake and Stream Water Properties

Hydrolab profiles in the two lakes from June 2005 and August 2006 provide an indication of vertical changes in water column characteristics in addition to seasonal variations between early and late summer (Figure 2.4). In June, surface temperatures in both lakes were ~0 °C and increased to ~3 °C at depth. In Upper Murray Lake this transition occurs gradually over the upper 20 m of the water column, whereas in Lower Murray Lake temperatures increase rapidly in the upper 7 m of the water column and then remain constant below that depth. In contrast, August 2006 temperature profiles indicate a water column without thermal stratification and near uniform temperatures around 3.5 °C. Dissolved oxygen (DO) concentrations in June 2005 ranged from ~13 mg/L at the surface of both lakes to 0.1 mg/L at maximum depth in Upper Murray Lake and 3.3 mg/L at maximum depth in Lower Murray Lake. August 2006 DO concentrations were nearly uniform with depth and slightly higher overall, ranging from ~16 to 17 mg/L. Based on these profiles, anoxic and suboxic conditions appear to be confined to only the bottom few meters of the water column in the deepest part of each lake. A second hydrolab cast in June 2005 at a location where water depth was only 79.2 m (as opposed to 83 m at the deepest point) did not encounter anoxic water, and helps to confirm this interpretation. Specific conductivity (SPC) in both lakes is nearly

constant with depth until within ~5 m of the bottom. In Lower Murray Lake, SPC ranges from ~140 µs/cm at the surface to ~170 µs/cm at the bottom. In Upper Murray Lake, SPC ranges from ~130 µs/cm at the surface to ~160 µs/cm at the bottom. These conductivity values correspond to salinity values ranging from 0.05 to 0.07 ppt. Both Upper and Lower Murray Lakes display elevated pH levels. June 2005 pH values ranged from ~8.2 at the surface to ~7.4 at maximum depth; whereas August, 2006 pH values were slightly higher, ranging from 8.4 to 8.5 and displayed minimal variation with depth.

Chemical analysis of lake water samples indicate an increase in the concentration of major dissolved anions and cations in the deepest samples from each lake (Table 2.7; Figure 2.5) which is consistent with the slight increase in conductivity observed at the bottom of the lakes. The one exception to this is the concentration of Sulfate (SO_4^{2-}) which decreases in the bottom waters of both lakes. The concentration of dissolved ions in runoff into the lakes is consistent with the concentration in the lakes' surface waters, with dissolved calcium being most abundant (20.8 to 30.7 mg/L) followed by magnesium (2.6 to 8.2 mg/L) and sulfate (1.1 to 21.0 mg/L). The concentration of dissolved ions in the deepest waters (below ~70 m in UML and below 40 m in LML) is enriched relative to runoff into the lakes.

Core Stratigraphy & Physical Characteristics

Two overlapping Uwitec percussion cores were recovered from the deepest basin in each of the lakes, with sediment recovery in Upper Murray Lake extending 8.4 m below lake bottom and sediment recovery in Lower Murray Lake extending 13.4 below lake bottom (Figures 2.6a and 2.6b). An additional suite of Ekman dredge samples and short gravity cores provided coverage of the sediment water interface and correlate with the longer percussion cores in each lake (Figure 2.6a and 2.6b).

Initial description of Upper Murray Lake sediments identified fine (<1 mm) to coarsely (>1 cm) laminated clastic sediment of clay, silt, and sand size. Upper Murray Lake sediment contained numerous gas vesicles of unknown origin and displayed considerable deformation which likely originated during core recovery.

Initial description of Lower Murray Lake sediment cores again identified predominantly clastic sediment, with quantitative particle size analysis providing further details about changes in the style of sedimentation (Figure 2.7a). The upper 240 cm of sediment are characterized by finely laminated (<1 mm)

silt and clay sized particles (Figure 2.8a; Figure 2.9) interspersed with occasional coarse (up to 1 cm thick) layers of silt and very fine sand (Figure 2.8b). A distinct transition marking the bottom of the laminated sediments occurs at 240 cm, below which the sediment consists predominantly of well sorted clay (Figure 2.8c) consisting of extremely faint bedding of approximately 1 cm scale (Figure 2.10a). Particle size gradual increases between depths of 310 cm to 400 cm and is characterized by massive or indistinct bedding. Between 400 cm and 1250 cm the sediment consists of faintly bedded silt and clay sized particles (Figure 2.8e) with indistinct bedding of approximately 1 cm scale and intermittent very fine sand layers (Figure 2.8d). A distinct sequence of medium sand mixed with organic fragments and silt and clay layers punctuates the sequence between 1250 cm and 1320 cm (Figures 2.8f, 2.8g, and 2.10b). The sediment below 1320 cm is again characterized by faintly bedded silt and clay sized particles.

Dry bulk density measurements range from less than 1.0 g/cm^3 near the sediment water interface to nearly 2.0 g/cm^3 at the bottom of the core (Figure 2.7b). The large scale pattern of sediment bulk density largely follows changes in particle size. The upper 240 cm of the core are characterized by sediment of relatively low dry bulk density punctuated by spikes associated with coarse deposits of silt and very fine sand. As mean particle size increases below 300 cm, dry bulk density similarly increases and then maintains relatively higher values until the bottom of the core is reached.

Percent loss-on-ignition (LOI) ranges from 1-2 % in the lowest part of the core (below ~ 400 cm) to 3-5 % in the upper part of the core (Figure 2.7c). Although percent LOI can provide an estimate of the organic carbon content of the sediment, actual carbon content in Lower Murray is likely even lower than LOI values indicate because the dehydration of clay minerals continues at temperatures above 105°C (Dean 1974) such that some of the observed mass loss is due to continued removal of water from the sediment during ignition at 550°C and possibly from the additional loss of volatile salts and/or inorganic carbon (Heiri et al., 2001).

Comparison of the LOI results from adjacent Lower Murray lake cores, LML-05-C1 and LML-05-C2, suggests that small variations in core stratigraphy are consistently identified by LOI analysis (Figure 2.11). The dominant feature in the LOI data is an apparent cyclicity displaying a pattern of increasing and decreasing percent LOI which repeats every ~100 cm. Close review of the procedure of the LOI analysis in comparison with the observed results indicated that the cyclicity in the LOI values resulted from a bias in

the results associated with the laboratory procedure. Specifically, the furnace used for the LOI analysis held two trays of 25 crucibles, one on an upper shelf and the other on a lower shelf, for a total run of 50 samples per analysis. Because the LOI analyses were carried out on samples spaced at 2 cm intervals a single batch of samples represented 100 cm of core sequence. Consequently, a consistent pattern of core sampling and crucible placement in the furnace resulted in the observed pattern in the LOI measurements, with samples placed on the lower rack consistently producing elevated percent LOI values relative to those crucibles placed on the upper rack. This interpretation is consistent with other studies which have reported the effects of sample placement on LOI values (e.g. Heiri et al., 2001). Whereas the differences may be small and relatively inconsequential when dealing with organic rich sediments, the results from the LOI analysis of Lower Murray Lake sediments indicate that extreme caution should be used when interpreting the results of LOI data from sediments with extremely low organic content. In these cases errors inherent in the LOI measurement procedure may be larger in magnitude than variations in LOI associated with actual changes in the content of organic carbon in the sediment.

Geochemical Data

Three samples from Lower Murray Lake sediments were analyzed for bulk chemical composition by ICP-AES. Each of the three samples represented different sedimentary facies. Consequently, the results of the chemical analyses should be treated as only an approximation of the potential range in the chemical composition of the sediments. The three samples do show distinct chemical differences, however without replicate analyses on multiple samples it is not known whether the individual samples are truly representative of the facies from which they were sampled. Nonetheless the results highlight some important characteristic of the composition of the sediments in Lower Murray Lake (Table 2.8). Overall, SiO_2 is the dominant chemical component comprising 56.2-69.5% of the sediment, followed by Al_2O_3 (12.9-20.5%), CaO (2.47-15.8%), Fe_2O_3T (3.1-7.6%), MgO (3.2-4.4 %), and K_2O (1.2-4.3 %). Thus, the composition of the sediments is consistent with that of the calcareous-dolomitic sandstone and slaty mudrock of the Danish River Formation which characterizes the regional bedrock and acts as the source of clastic material transported into the lake. Sample LML-05-C1-E1-1 was recovered from a typical section of the laminated upper portion of the sediment core, whereas sample LML-05-C1-E1-2 was recovered from

anomalous, coarse deposit within this same region of the core (Figure 2.9). Interestingly, the anomalous, coarse deposit contained significantly less CaO (only 2.47%) and more Al_2O_3 than the surrounding finely laminated sediments. Sample LML-05-C1-C1-1, collected from the non-laminated portion of the record at 573 cm contains more SiO_2 and less Al_2O_3 and Fe_2O_3T.

Whereas the ICP-AES analyses produced quantitative geochemical data from a few locations within the cores, the ITRAX scanning XRF provided continuous, high-resolution (0.5 or 1.0 mm) data spanning the entire sedimentary record. The theoretical detection limit of the ITRAX instrument is inversely related to the atomic number of the element of interest and the count time used during the analysis (Cox Analytical Systems, *personal communication*; Figure 2.12). Based on a comparison of the quantitative results from ICP-AES analysis with the detection limits presented in Figure 2.12, interpretation of ITRAX data was limited to the following elements that were found in concentrations above the detection limit of the instrument: Si, K, Ca, Ti, Mn, Fe, Rb, Sr, and Zr.

Down-core profiles of ITRAX data are largely consistent with the variations observed in the physical characteristics of the sediments (Figure 2.13). Specifically, the sedimentary record can be divided into two distinct units, the upper finely laminated, fine-grained portion above 240 cm depth and the more coarse-grained section below 400 cm. Despite considerable high frequency variation within both of these sections, mean conditions are relatively stable. In contrast, the region between 240 and 400 cm is characterized by a gradual transition between the two end member states. The similarity in the pattern of variability in the ITRAX geochemical data and the physical characteristics of the sediment are consistent with the limitations of the X-ray fluorescence analytical technique. Specifically, variations in particle size, mineralogy, density, water content, and organic content all influence the amplitude of the signal recorded by the instrument (Croudace et al., 2006). Consequently it is difficult to unequivocally distinguish between those variations in the ITRAX data caused by changes in chemical composition versus those related to changes in the physical characteristics of the sediment.

In general, the down-core ITRAX profiles fall into two categories. The first category, including Si, Ca, Sr, and Zr is characterized by those elements that start out with higher count values at the bottom of the core, show decreasing counts between 400 and 240 cm, and have generally low count values above 240 cm. The second category, including Ti, K, Rb, and Fe shows the inverse pattern with low count values below

400 cm, increasing values between 400 and 240 cm, and generally high values above 240 cm. Correlation coefficients determined between each of the elements revealed a similar pattern of two groupings (Table 2.9). The strongest correlations coefficients were generally associated with either K or Ca, with Ti, Fe, and Rb positively correlated with K and Si, Sr, Zr positively correlated to Ca. Thus, the ITRAX data reveal a consistent relationship in the relative abundance of the different elements in response to both large-scale trends in the down-core profiles as well as the high-frequency variability that prevails throughout the record. The one exception to these groupings is the element Mn, which is closest in behavior to the group containing Si, Ca, Sr, and Zr, but does not have a strong correlation with any of the elements.

Chronology

The short lived radioisotopes ^{210}Pb and ^{137}Cs provide a means of constraining the age of recent sedimentary deposits. The decay of ^{226}Ra ($t_{1/2}$ = 1602 yrs) in soil and rock produces ^{222}Rn ($t_{1/2}$ = 3.82 days), some of which escapes to the atmosphere and decays to form ^{210}Pb ($t_{1/2}$ = 22.3 yrs). The fallout of atmospheric ^{210}Pb leads to the deposition of *unsupported*, or excess ^{210}Pb in the sedimentary record, which is added to the *supported* ^{210}Pb that is produced in situ. Under idealized circumstances the total (supported + unsupported) ^{210}Pb activity in the sediments will be highest at the surface and decrease exponentially down core until reaching a constant activity level determined by the background activity of supported ^{210}Pb. With its short half life, ^{210}Pb is generally only useful for dating sediments through the past ~150 years (Wolfe et al., 2004).

^{137}Cs ($t_{1/2}$ = 30.1 yrs) is produced by human activity and was first introduced into the atmosphere with the onset of nuclear weapons testing ca. 1954. The fallout of atmospheric ^{137}Cs peaked in 1963 just prior to the signing of the nuclear test ban treaty with a secondary peak associated with the 1986 Chernobyl nuclear accident observed in some locations. Consequently, profiles of ^{137}Cs activity in sediments may include up to three stratigraphic markers associated with these events that can be used to verify the age model produced by the ^{210}Pb profile (Wolfe et al., 2004).

Age-depth models of recent Upper and Lower Murray Lakes sedimentation were constructed from the ^{210}Pb profiles using the constant rate of supply (CRS) model (Appleby and Oldfield, 1978). Comparison of the ^{210}Pb age models with the ^{137}Cs profiles indicate considerable uncertainty in the age

determinations based on these short lived radionuclides (Figure 2.14). Specifically, the ^{137}Cs peak occurs at a depth of 5.0-6.0 cm in Upper Murray Lake whereas the ^{210}Pb age model suggests that 1963 corresponds to a depth of less than 2.0 cm. The ^{137}Cs peak in Lower Murray Lake occurs at a depth of 1.5-2.0 cm in contrast to the ^{210}Pb age model which assigns 1963 to a depth of ~1.0 cm. A number of processes including turbidity currents, bioturbation, and mass movements can disturb ^{210}Pb profiles and produce errors in their associated age models (Wolfe et al., 2004). Further complications can arise in arctic regions due to reduced production of the parent isotope [222]Rn in frozen grounds and reduced ^{210}Pb deposition because of persistent ice cover on lakes, both of which lead to very low total ^{210}Pb activities in arctic lake sediments (Wolfe et al., 2004). Inspection of the uppermost sediments in the two lakes shows clear evidence of an erosive event in Lower Murray Lake (ca. varve year 1990) and possible evidence of erosion in Upper Murray Lake associated with the deposition of anomalously coarse sediment. Consequently, these deposits have likely produced unreliable ^{210}Pb age determinations.

Given the limitations of the ^{210}Pb and ^{137}Cs data, additional age control in Lower Murray Lake was provided by counting annual laminations (varves) which are preserved in the upper 2.4 m of core section. Confirmation of the varve chronology was established by comparing the record of paleomagnetic variations preserved in Lower Murray Lake with an independently dated paleomagnetic record from South Sawtooth Lake. A detailed description of the varve-based chronology and its uncertainty are discussed in Chapter 3. According to the varve chronology, the upper 240 cm of the sedimentary record from Lower Murray Lake spanned the interval from 2004 AD through 3236 BC providing a mean accumulation rate of 0.46 mm/yr (Figure 2.15). Only one organic sample suitable for radiocarbon dating, located at a depth of 1307 cm, was identified in Lower Murray Lake. The measured age of the sample was >50,800 ^{14}C years, beyond the useful limit of radiocarbon dating and most likely reflecting older tertiary material that remained on the landscape before eventually being washed into the lake. Consequently, no firm age control is available for sediments below 2.4 m in Lower Murray Lake. Nonetheless, the regional glacial history does provide some constraint on age of the sediments in the lake. Specifically, deglaciation of the Murray Lakes region occurred ~6900 ^{14}C years BP (~7700 calendar yrs BP; England 1983) providing a maximum age for post glacial sediments deposited in the lakes. Thus, the 11 m of sediment recovered below the base of the varve chronology at 2.4 m represent a maximum of ~2500 years of deposition. This indicates that deposition in

the early part of the record was occurring at a rate ~4.4 mm/yr or an order of magnitude faster than during the period of varve deposition (Figure 2.15).

A total of seven radiocarbon samples provided chronological control for the long-term sedimentary record in Upper Murray Lake (Table 2.6; Figure 2.15). These samples range in age from 1826 AD at a depth of 21.5 cm to 2409 BC at a depth of 634 cm. Based on these ages the long term rate of sedimentation in Upper Murray Lake is approximately 1.4 mm/yr, considerably higher than the rate of sedimentation in Lower Murray Lake over the same time interval. Although the radiocarbon ages from Upper Murray Lake indicate a relatively consistent rate of deposition over long time scales, the three youngest ages, spanning the upper 24 cm of the record indicate a lower sedimentation rate ~0.7 mm/yr. This may reflect erosion and redeposition of sediment elsewhere as suggested by the ^{210}Pb data.

Two of the radiocarbon samples came from the same stratigraphic unit at a depth of 21.5 cm, consisted of a coarse deposit containing numerous organic fragments. The two individual terrestrial organic macrofossils which were dated independently provide ages that differ by ~75 radiocarbon years. This discrepancy likely reflects the time lag associated with the transfer of terrestrial organic matter from the landscape into the sedimentary record, with temporary storage occurring for differing lengths of time along this transport pathway. Consequently, these results indicate that the uncertainty in ages determined by radiocarbon samples are in fact significantly greater than just the analytical error associated with the individual measurements.

Discussion

Modern Climatic Setting of the Murray Lakes

The hydrology of high arctic watersheds is dominated by meltwater production and ultimately driven by the surface energy balance (Woo, 1983). Surface air temperature data recorded at the Murray Lakes (Figure 2.3) reflect the extreme seasonality of the energy balance in the High Arctic and highlight the importance of temperatures on the annual hydrologic cycle. Because temperatures remain below freezing for 9 months of the year, stream flow is limited to the brief period spanning June through August when temperatures are above 0 °C. Observations from the permanent weather stations at Alert and Eureka

further indicate that summer rainfall on northern Ellesmere Island is limited, thus the primary source of surface runoff is meltwater derived from snow, ice, and frozen soil within the watershed. Consequently, seasonal temperatures influence both the timing and the magnitude of surface water runoff. The pronounced seasonal variability in surface water runoff will in turn influence the transfer of allochthonous sediment into the Murray Lakes, producing an annual cycle of sediment deposition. If sediments are allowed to accumulate in the absence of disturbances such as bioturbation or resuspension, then annual laminations are likely to be preserved in the sediment (Zolitschka, 2007). Consequently, the pronounced seasonal air temperature cycle at the Murray Lakes and its influence on streamflow and sediment transfer provides a mechanism to explain the formation of the annual laminations observed in the upper 240 cm of Lower Murray Lake sediments. (The significance of the relationship between air temperature and lamina formation is discussed in Chapter 3).

Given the significance of surface air temperatures in governing meltwater production, streamflow, and ultimately sediment transfer into the Murray Lakes it is important to evaluate the range of temperature variability within the Murray Lakes watershed. Daily and seasonal variations in the lake level and upper slope temperature records are highly correlated, yet significant differences are commonly observed between the mean daily temperatures at the two stations (Figure 2.3). These differences provide an estimate of the local surface air temperature lapse rate and the frequency of air-temperature inversions in the study area.

The -4.2 °C / 1000 m mean daily lapse rate observed at the Murray Lakes is consistent with near surface temperature lapse rates observed over the Prince of Wales Icefield on southern Ellesmere Island, where Marshall et al. (2007) observed a mean daily lapse rate during their study period of -4.1 °C / 1000 m and an average summer lapse rate of -4.3 °C / 1000 m. In contrast, Braun (2006) measured surface air temperature lapse rates on the Hazen Plateau just east of the Murray Lakes that ranged from -6.8 to -7.9 °C / 1000 m. The difference between the lapse rate determined in the present study and those reported by Braun (2006) may be a function of the limited (100 m) elevation range of the temperature observations used by Braun (2006) or the higher elevation of the measurement (~935 to 1035 m) in a region where prolonged snow cover is likely to produce a different local energy balance and a different local air temperature lapse rate relative to that observed at the lower elevations evaluated in this study (cf. Marshall et al., 2007).

The frequent occurrence of air-temperature inversions observed at the Murray Lakes is consistent with the common incidence of inversions throughout the High Arctic. Air-temperature inversions at the study site were observed on 76 % of days during the months of September through May and 40 % of days during the summer months of June through August. Based on an analysis of radiosonde temperature data from permanent weather stations around the North American Arctic, Bradley et al. (1992) report a similar maximum in the frequency of inversions during winter months when inversions occurred on > 70 % of days. The frequent occurrence of air-temperature inversions in the Arctic is related to extended darkness during the winter months when a negative net radiation balance exists at the surface (Bradley et al., 1992).

Despite the limited temporal and spatial coverage of the air temperature data recorded in this study, these results highlight the range of temperature variability which can exist within small areas in the High Arctic. Consequently, an accurate evaluation of the role of temperature on meltwater production, streamflow, and sediment transfer in high arctic watersheds requires an understanding of the local temperature variation within that watershed. Because much of the Murray Lakes watershed and consequently the source region for meltwater production is located at high elevations, low-elevation surface-temperature observations (characteristic of the permanent weather stations in the High Arctic) are unlikely to provide an accurate indication of the processes driving surface runoff into the lakes. More specifically, variations in local surface air-temperature lapse rates and the frequent occurrence of temperature inversions necessitate caution when extrapolating air temperature measurements throughout a watershed for the purpose of understanding or predicting meltwater production.

Modern Limnology of the Murray Lakes

Although only two temperature profiles are available (Figure 2.4), the thermal structures of the Murray Lakes are consistent with classification as cold monomictic lakes in which water temperatures never exceed 4 °C and circulation is limited to one period during the summer (Wetzel, 2001). Cold monomictic lakes are typical of Arctic and mountain environments (Wetzel, 2001) and have been described elsewhere on Ellesmere Island (e.g. Francus et al., 2008). In these lakes the prolonged ice cover inhibits warming of surface waters and restricts wind driven mixing of the water column to brief ice-free intervals during late summer.

The observed oxygen depletion at depth in both Upper and Lower Murray Lakes (Figure 2.4) is puzzling given the oligotrophic status of the lakes and the presumed period of overturning which should occur when thermal stratification breaks down in late summer. However, similar dissolved oxygen profiles are observed in other cold monomictic lakes on northern Ellesmere Island including South Sawtooth Lake (Francus et al., 2008) and Lake C3 (Cook, *unpublished field data*). Francus et al. (2008) hypothesize that extended ice cover on South Sawtooth Lake isolates the water body from the atmosphere allowing biota within the lake to gradually consume oxygen through respiration and the oxidation of organic matter (Ellis and Stefan, 1989; Wetzel, 2001). Over extended time periods this process can lead to anoxic conditions in ice-covered water bodies (Golosov et al., 2007). It is plausible that a similar mechanism is responsible for the oxygen depletion observed in the bottom waters of Upper and Lower Murray Lakes.

As dissolved oxygen concentrations decrease with depth in Upper and Lower Murray Lakes and South Sawtooth Lake, simultaneous increases in conductivity/salinity are observed in each lake (Figure 2.4). Several mechanisms are capable of increasing the concentration of dissolved ions in arctic lakes, including: evaporative enrichment (e.g. Anderson et al., 2001); trapping of marine water through isostatic uplift (e.g. Van Hove et al., 2006); and the freeze-out of salt from saline groundwater or lake ice (e.g. Ouellet et al. 1987, 1989; Ferris et al, 1991; Davidge, 1994). High salinity levels caused by evaporative enrichment in West Greenland lakes are limited to a small number of closed basin (no outlet) lakes (Anderson et al., 2001). Given the significant inflow and outflow through the Murray Lakes, evaporative enrichment is an unlikely explanation for the observed salinity gradient. At an elevations of 107 and 106 m above sea level, Upper and Lower Murray Lakes are above the local marine limit (England, 1983) ruling out the possibility of seawater isolation. Furthermore, the role of ice exclusion of salts seems limited to those lakes that have preexisting high salinities, in which ice exclusion acts to concentrates salts and produce hypersaline bottom waters (e.g. Van Hove et al., 2006).

Francus et al. (2008) propose an additional mechanism to explain the conductivity profile in South Sawtooth Lake which may also apply to the Murray Lakes. Specifically, the dissolved ions causing the increase in conductivity near the sediment water interface may be the result of diffusion from the sediments themselves. The observed ~10 mg/L increase in the concentration of Ca^+ ions in the bottom waters of the Murray Lakes (Figure 2.5) is consistent with the dissolution of clastic sediments derived from the

surrounding carbonate bedrock and accounts for the majority of ~20 µs/cm increase in conductivity. Håkanson (2005) reports that while diffusion rates are low for many substances under oxic conditions, anoxia significantly increases diffusion rates. Thus, the increase in conductivity may actually be a product of the low oxygen concentration of the bottom waters.

The limited observations available from the Murray Lakes make it difficult to determine whether the slight increase in the salinity of the bottom waters acts as a density barrier to mixing, thus helping to maintain the existence of an anoxic zone, or if the salinity increase is simply a product of enhanced diffusion caused by the anoxic conditions. Nonetheless the existence of anoxic bottom waters, which tends to limit bioturbation of sediments (e.g. Zolitschka, 2006), appears critical to the preservation of the fine laminations observed in Lower Murray Lake. Besonen et al. (2008) describe several cores recovered from slightly shallower depths in Lower Murray Lake in which laminations are either more diffuse or completely absent. Thus, the preservation of laminations in Lower Murray Lake is closely linked to the oxygen content of bottom waters and any past or future changes in the physical processes acting within the lake are likely to significantly alter the characteristics of its sedimentary record.

Holocene Evolution of the Murray Lakes

The Holocene epoch in the High Arctic is characterized by significant environmental transitions driven by changing climate (e.g. Gajewski and Atkinson, 2003), the retreat of the Innuitian Ice Sheet (England et al., 2006), and the disappearance, emergence, and growth of local ice features (e.g. Smith, 1999). Deglaciation of the Murray Lakes region likely occurred ~6900 ^{14}C years BP (~7700 calendar years BP; England, 1983), with ice retreat continuing until margins close to or behind present conditions were reached by ~5000 ^{14}C years BP (~5700 calendar years BP; Smith, 1999). Plateau ice caps at favorable, high elevation locations likely persisted through the mid Holocene (Smith, 1999), but may have subsequently disappeared and later reformed following the Holocene thermal maximum (Koerner and Paterson, 1974). Thus the sediments preserved in the Murray Lakes provide a record of lake evolution during a period of profound environmental change.

The coarse grain size of the basal sediments recovered from Lower Murray Lake (Figures 2.7 and 2.8) suggests that they were deposited in a high energy environment possibly associated with discharge

from a locally receding glacier. The high rate of sedimentation inferred for the lower portion of the record (below 240 cm) further supports the notion of deposition in the vicinity of locally receding ice, whereas the transition to a significantly reduced rate of sedimentation in the upper, laminated portion of the record (Figure 2.15) likely indicates that runoff associated with a receding glacier was no longer draining into the Murray Lakes watershed. A marked contrast between deglacial and postglacial rates of lacustrine sedimentation is common in many lakes (Desloges and Gilbert, 1991; Gilbert and Desloges, 1992). Although these studies are based on seismic investigations unverified by core data or age constraints, the consensus interpretation portrays spectacularly rapid sediment accumulation in the wake of retreating glaciers followed by much lower sedimentation rates after deglaciation. The near constant sedimentation rates in Upper and Lower Murray lakes over the past ~5000 years further indicate that major changes in sediment production were not a significant consequence of changes in the size of local ice caps during this period. The higher mean rate of sedimentation in Upper Murray Lake relative to Lower Murray Lake is consistent with size of the tributaries draining into to the two lakes and the proximity of the deepest basins to these tributaries. Two large tributaries flow into the western side of Upper Murray Lake near the deep basin, whereas the main tributary draining into Lower Murray is located at the southern end of the lake near the outflow stream and is separated from the deepest basin in the lake by a narrow (and presumably shallow) constriction.

The down-core record of grain size variation in Lower Murray Lake sediments reflects a progressive transition between the deposition of coarse material in the early part of the record to the deposition of fine grained silt and clay particles during the most recent stage of lake evolution (Figure 2.7). In a proglacial environment characteristic of the early part of the Lower Murray Lake record, hyperpycnal flows (negatively buoyant density currents) caused by high concentrations of suspended sediment in inflowing stream water are capable of carrying large quantities of sediment into the deepest part of a lake (Smith and Ashley, 1985). Cold based ice caps in the High Arctic, like those presently adjacent to the Murray Lakes, are minimally erosive (Paterson, 1969). As a result, continued recession of ice to positions near or beyond present limits would have altered the production of sediment within the watershed and the concentration of suspended sediment in inflowing streams. The relatively stable pattern of fine grained silt and clay deposition which characterizes the upper 240 cm of laminated sediments in Lower Murray Lake

likely reflects this transition. Specifically, the last 5,000 years of sedimentation reflect decreased sediment production dominated by fluvial erosion. The resultant decrease in suspended sediment load limited the formation of hyperpycnal flows and deposition became dominated by the settling of finer grained particles which could be suspended in the upper part of the water column as they traverse the lake.

The importance of anoxia to the preservation of fine laminations in Lower Murray Lake reveals that anoxic conditions must have prevailed throughout the 5000+ year period in which laminations are observed. The continuous geochemical data produced from the ITRAX XRF analysis provided a useful for tool for evaluating the long term trends in the dissolved oxygen concentration of Lower Murray Lake bottom waters. Specifically, changes in the redox sensitive elements Mn and Fe (Wetzel, 2001) were used to investigate paleo-redox conditions (Figure 2.16). The general pattern of Fe variation in Lower Murray Lake sediments follows a similar pattern to changes in the physical characteristics of the sediment. As grain-size decreases Fe increases and then remains stable throughout the laminated portion of the record. Because the relative behavior of Mn and Fe differs under oxic and anoxic conditions, the Mn:Fe ratio is commonly used as an indicator of paleo-redox conditions (e.g. Davison, 1993; Koinig et al., 2003). Under oxic conditions Fe and Mn will behave in a similar fashion; in contrast Mn becomes more soluble under anoxic conditions resulting in decreased Mn:Fe ratio in the sediments when conditions are anoxic (Cohen, 2003). Thus the decrease in Mn:Fe ratio concomitant with the decrease in the particle size of Lower Murray Lake sediments suggests that the same factors contributing to changes in the physical characteristics of the sediments also influenced the dissolved oxygen concentration of the bottom waters.

Evidence for the onset of suboxic or anoxic conditions in Lower Murray Lake becomes clearer by examining the degree of correlation between Fe and Mn over different portions of the record. Figure 2.16 includes a profile of the correlation coefficient determined between Fe and Mn over a moving window of 101 measurements (10.1 cm). Although there is considerable variability in the profile, Mn and Fe are significantly correlated below 400 cm. In contrast there is essentially no correlation between Mn and Fe above 400 cm. This suggests that the onset of anoxia occurred early in the transition between the deposition of coarser sediment in the early part of the record and the fine, laminated deposits characteristic of the more recent part of the record.

Although the exact cause of the presently observed anoxic bottom water in Lower Murray Lake is not known, low dissolved oxygen concentrations necessitate a process of oxygen removal, such as respiration and the decay of organic matter, and minimal mixing of the water column. Consequently, the onset of anoxia as indicated by the behavior of Fe and Mn and the preservation of fine laminations in the sedimentary record likely reflects a change in one or both of these factors. A variety of factors including, but not limited to light availability, water temperature, and nutrient loading could lead to an increase in biologic activity (e.g. Cohen, 2003). Because lake waters remain near the freezing temperature today, it is unlikely that a significant increase in water temperature led to increased productivity. An increase in nutrient loading is possible and warrants further investigation. However, given the observed changes in the sedimentary record associated with the onset of anoxia, a simultaneous increase in light availability provides a reasonable mechanism for increased productivity. Specifically, high levels of suspended particulate matter significantly influence light penetration (e.g. Wetzel, 2001) and have been shown to directly influence lake productivity (e.g. Dokulil, 1994). The observed decrease in particle size and sediment accumulation rate were likely accompanied by a decrease in the turbidity of the lake water which would have promoted biologic activity and possibly initiated oxygen depletion in bottom waters as more organic matter was subject to decay. Concomitant with increased productivity, changes in inflow related to the retreat of local ice could further promoted the onset of anoxia by influence mixing. The amount of inflowing water is a significant factor influencing the mixing in many lakes (Imboden and Wuest, 1995). Thus reduced inflow could have led to reduced mixing of the water column and helped maintain anoxic conditions. Furthermore, reduced inflow, with a lower concentration of suspended sediment, would lead to fewer hyperpycnal flows and eliminate a primary mechanism for transporting oxygenated surface waters to depth.

Summary and Conclusions

The climatic setting of the Murray Lakes, characterized by extreme seasonality, and the physical characteristics of the lakes, including an extended ice cover, reduced mixing, and oxygen depleted bottom waters have led to the formation and preservation of annually laminated sediments (varves). Varved

sediments provide a valuable paleolimnologic tool because they provide precise chronological control and can be used as an indicator of past environmental conditions (Zolitschka, 2006). The physical and chemical characteristics of the sediments in Lower Murray Lake record the evolution of the lake basin following the retreat of the Innuitian Ice Sheet ca. 6000 ^{14}C years BP. These data indicate a period of rapid deposition of coarse clastic material during the early history of the lake, followed by a transitional period marked by decreasing grain size and sediment accumulation. These changes occur simultaneously with the onset of anoxia in bottom waters attributed to enhanced productivity and reduced mixing of the water column. Varve deposition began ca. 5200 calendar years BP and continued through 2004 AD. Relative to the earlier portion of the record, the physical and chemical characteristics of the sediments remain relatively stable throughout the period of varve deposition, suggesting that weathering, erosion, and sediment transport processes in the watershed, as well as physical, chemical, and biological conditions within the lake have not undergone major changes during this period.

Due to the much higher quality of the cores recovered from Lower Murray Lake the bulk of the discussion in this chapter and the following chapter (Chapter 3) focus on these sediments. Nonetheless, radiocarbon dating of organic material found in the sediments of Upper Murray Lake produced an absolute chronology spanning the past ~4500 years, a rarity in high-arctic lakes characterized by extremely low biologic activity. Although, the degree of deformation in the Upper Murray Lake cores precludes the development of a high-resolution paleolimnologic record, Upper Murray Lake sediments could potentially provide a valuable record if a suitable proxy was identified.

Table 2.1 Main physiographic characteristics of Upper and Lower Murray Lakes.

Characteristic	Upper Murray Lake	Lower Murray Lake
Elevation (m a.s.l.)	107	106
Drainage Basin Area (km^2)	184	261
Surface area of glacial ice draining directly into the lake (km^2)	9	4.5
Lake Surface Area (km^2)	7.5	5
Maximum Water Depth (m)	83	46

Table 2.2 1971-2000 Climate normals for Alert and Eureka.

Climate Variable	Alert	Eureka
Mean Annual Temp (°C)	-18	-19.7
Mean Daily Max Temp (°C) – Jun, Jul, & Aug	3.6	6.1
Mean Daily Min Temp (°C) – Dec, Jan & Feb	-35.5	-40.3
Average # of days with max temp > 0°C	77.5	94.2
Total Annual Precip (mm water equivelent)	153.8	75.5
Total Annual Rainfall	16.1	26.2

Table 2.3 Key locations discussed in the text.

Description	Location (Lat/Lon)	Elevation (m)	Water Depth (m)
2005 Upper Murray Lake Core & Hydrolab Site	81.39872° N 69.81638° W	-	83
2005 Lower Murray Lake Core & Hydrolab Site	81.34175° N 69.55204° W	-	46
2005 Upper Murray Lake Water Samples	81.39872° N 69.81638° W	-	5, 15, 25, 50, 70, 80, 81.5, 83
2005 Lower Murray Lake Water Samples	81.34175° N 69.55204° W	-	15, 25, 45
2005 Upper Murray Lake Hydrolab Site	81.3984° N 69.78576 W	-	79.2
2006 Upper Murray Lake Hydrolab Site	81.35953° N 69.54603° W	-	25
2006 Lower Murray Lake Hydrolab Site	81.34615° N 69.52150° W	-	32
UML Outlet Stream Water Sample	81.35566° N 69.53293° W	107	-
UML Southeast Tributary Water Sample	81.36290° N 69.54940° W	107	-
UML Main Tributary Water Sample	81.37767° N 69.63303° W	107	-
LML Northeast Tributary Water Sample	81.34999° N 69.50971° W	106	-
LML Southeast Tributary Water Sample	81.30428° N 68.96979° W	897	-
LML Outlet Water Sample	81.30109° N 69.51566° W	106	-
Lake Level Air Temperature Logger	81.35492° N 69.53679° W	111	-
Upper Slope Air Temperature Logger	81.35610° N 69.42322° W	611	-
Upper Murray Lake Mooring	81.3987° N 69.81564° W		
Lower Murray Lake Mooring	81.3417° N 69.55247° W		

Table 2.4 List of cores collected from Upper and Lower Murray Lakes and associated analyses.

Core ID	Length (cm)	Start Depth (cm)	Photo	Gamma Density	Mag. Susc.	Paleo-mag.	XRF	X-Ray	LOI & Bulk Density	Grain Size	Thin Section
LML-05-Ekman1	17.5	0	X				X	X			
LML-05-Ekman3	18	0	X								
LML-05-Ekman4	17	0	X						X	X	X
LML-05-Ekman5	12.5	0	X								X
LML-05-Ekman6	10.5	0	X								
LML-05-AR1	35	0	X	X			X	X			X
LML-05-AR2	56	0	X	X			X	X	X	X	X
LML-05-C1-A1	140	21	X	X		X	X	X	X	X	X
LML-05-C1-A2	144	161	X	X		X	X	X	X	X	X
LML-05-C1-B1	104	305	X	X	X	X	X	X		X	
LML-05-C1-B2	78	409	X	X	X	X	X	X		X	
LML-05-C1-B3	85	487	X	X	X	X	X	X		X	
LML-05-C1-C1	141	572	X	X	X		X	X		X	
LML-05-C1-C2	98	713	X	X	X		X	X		X	
LML-05-C2-A1	108	5	X	X		X	X	X	X		X
LML-05-C2-A2	144	113	X	X		X	X	X	X		X
LML-05-C2-B1	136	257	X	X	X	X	X	X	X	X	
LML-05-C2-B2	130	398	X	X	X	X	X	X	X	X	
LML-05-C2-C1	127	539	X	X	X		X	X	X		
LML-05-C2-C2	138	667	X	X	X		X	X	X		
LML-05-C2-D1	133	805	X	X	X		X	X	X	X	
LML-05-C2-D2	143	938	X	X	X		X	X	X	X	
LML-05-C2-E1	121	1081	X				X	X	X	X	
LML-05-C2-E2	139	1202	X	X	X		X	X	X	X	
UML-05-Ekman1	10	0	X				X	X			
UML-05-Ekman2	9	0	X				X				X
UML-05-AR3	22.5	0	X	X			X	X			
UML-05-AR4	27	0	X				X	X	X		X
UML-05-A1-A1	128	3	X								
UML-05-A1-A2	127	132	X								
UML-05-A1-B1	146	262	X								
UML-05-A1-B2	147	408	X								
UML-05-A1-C1	137	555	X								
UML-05-A1-C2	146	692	X								
UML-05-A2-A1	89	0	X				X	X			
UML-05-A2-A2	58	89	X								
UML-05-A2-A3	61	147	X								
UML-05-A2-B1	146	208	X								
UML-05-A2-B2	145	354	X								
UML-05-A2-C1	145	499	X								
UML-05-A2-C2	145	644	X								

Table 2.5 ITRAX analyses of Lower Murray Lake Cores. Cores labeled in bold were used to construct the composite geochemical record.

Core	Sampling Interval (μm)	XRF Duration (sec)	XRF Voltage (kV)	XRF Current (mA)	X-Ray Resolution (μm)	X-Ray Exp. Time (sec)	X-Ray Voltage (kV)	X-Ray Current (mA)
LML-05-Ekman1	100	1	30	30				
LML-05-Ekman1	1000	10	30	30				
LML-05-AR1	100	5	30	30	100	800	45	45
LML-05-AR2	100	1	30	30				
LML-05-AR2	1000	10	30	30				
LML-05-C1-A1	100	1	30	30				
LML-05-C1-A1	1000	5	30	30				
LML-05-C1-A2	100	1	30	30				
LML-05-C1-A2	1000	5	30	30				
LML-05-C1-B1	1000	5	30	30				
LML-05-C1-B2	500	10	30	30				
LML-05-C1-B3	500	5	30	30				
LML-05-C1-C1	500	5	30	30				
LML-05-C1-C2	500	5	30	30				
LML-05-C2-A1	200	5	30	30	200	400	45	45
LML-05-C2-A2	200	5	30	30	100	400	45	45
LML-05-C2-B2	1000	5	30	30	100	400	45	45
LML-05-C2-C1	1000	5	30	30	100	400	45	45
LML-05-C2-C2	1000	5	30	30	100	400	45	45
LML-05-C2-D1	1000	5	30	30	100	800	45	45
LML-05-C2-D2	1000	5	30	30	100	800	45	45
LML-05-C2-E1	1000	5	30	30	1000	800	45	45
LML-05-C2-E2	1000	5	30	30	100	800	45	45

Table 2.6 AMS radiocarbon data from Upper & Lower Murray Lakes. Radiocarbon ages were calibrated using Calib 5.0.1 (Reimer et al., 2004).

Core Section	Section Depth (cm)	Composite Depth (cm)	Material	Lab #	Measured Age (years BP)	Median Calibrated Age (AD/BC)	1 Sig Lower Limit	1 Sig Upper Limit
UML-05-A1-A2	44	176	Plant Matter	UCI-23048	1515±15	557	546	585
UML-05-A2-A1	24	24	Plant Matter	UCI-23049	270±15	1646	1644	1647
UML-05-A2-B1	40	248	Plant Matter	UCI-23050	2025±15	-23	-44	-36
UML-05-A2-B1	110	318	Plant Matter	UCI-23051	2530±20	-683	-772	-761
UML-05-A2-C1	135	634	Plant Matter	UCI-23052	3905±30	-2409	-2466	-2453
UML-05-A4	21.5	21.5	Twig	UCI-23053	105±20	1826	1697	1708
UML-05-A4	21.5	21.5	Plant Matter	UCI-23054	180±15	1717	1669	1677
LML-05-C2-E2	105	1307	Plant Matter	UCI-23055	>50800±	out of range	-	-

Table 2.7 Water sample anion and cation concentrations (mg/L).

Sample	Cl^-	NO_3^-	SO_4^{2-}	Na^+	Mg^+	K^+	Ca^+	Si^+
UML 5m depth	0.5	0.1	2.8	0.1	4.2	0.3	25.8	0.3
UML 15m depth	0.5	0.1	2.7	0.1	4.5	0.3	27.3	0.3
UML 25m depth	0.5	0.1	2.6	0.1	4.5	0.3	27.0	0.3
UML 50m depth	0.5	0.1	2.7	0.1	4.5	0.3	27.9	0.4
UML 70m depth	0.5	0.1	2.7	0.1	4.5	0.3	28.1	0.4
UML 80m depth	0.5	0.2	2.6	0.1	4.6	0.3	29.7	0.7
UML 81.5m depth	0.6	0.2	2.4	0.2	4.8	0.3	32.4	1.2
UML 83m depth	0.6	0.8	1.3	0.2	5.0	0.4	35.5	2.5
LML 15m depth	0.6	0.1	3.9	0.2	5.2	0.3	30.7	0.4
LML 25m depth	0.6	0.1	3.9	0.2	5.4	0.3	31.0	0.4
LML 45m depth	0.6	0.2	3.5	0.2	5.8	0.4	36.7	1.6
UML-06 Outlet Stream	0.6	0.1	3.0	0.1	4.7	0.3	27.3	0.3
UML-06 SE Tributary	0.4	0.4	5.8	0.1	5.2	0.3	27.5	0.4
UML-05 Main Delta 1	2.5	0.4	21.0	0.6	8.9	1.6	20.8	0.9
UML-05 Main Delta 2	1.5	0.3	11.2	0.3	8.1	0.9	22.5	0.8
LML-06 NE Tributary	0.4	0.3	5.9	0.1	4.8	0.2	28.0	0.4
LML-06 SE Tributary	0.3	0.2	1.1	0.0	2.6	0.1	21.4	0.2
LML-06 Outlet Stream	0.5	0.1	4.0	0.2	4.8	0.3	26.1	0.3

Table 2.8 Chemical composition of Lower Murray Lake sediments based on ICP-AES analysis.

Element/Oxide	LML-05-C1-E1-1	LML-05-C1-E1-2	LML-05-C1-C1-1	Unit	Analytical Limit
Total	99.76	99.18	99.59	%	
Al_2O_3	12.9	20.5	7.72	%	0.00003
CaO	15.8	2.47	12.9	%	0.000003
Fe_2O_3T	6.37	7.57	3.12	%	0.00004
K_2O	2.29	4.33	1.18	%	0.00001
MgO	4.20	4.44	3.20	%	0.00005
MnO	.0986	.0267	.0478	%	0.000001
Na_2O	.915	.626	1.17	%	0.000005
P_2O_5	.158	.127	.131	%	0.00005
S	< 0.01	< 0.0094	< 0.007	%	0.00001
SiO_2	56.2	58.1	69.5	%	0.00001
TiO_2	.72	.84	.50	%	0.000001
As	< 122.3	< 112.6	< 83.5	ppm	0.12
Ba	416	684	206	ppm	0.002
Cd	10	11	< 7	ppm	0.01
Co	< 20.4	26	< 13.9	ppm	0.02
Cr	85	158	58	ppm	0.02
Cu	43	127	25	ppm	0.01
Ni	< 50.9	107	69	ppm	0.05
Sc	13	20	7	ppm	0.0005
Sr	159	38	141	ppm	0.002
V	76	135	39	ppm	0.02
Zn	82	128	53	ppm	0.006
Y	33	28	25	ppm	0.004
Zr	205	163	245	ppm	0.006
Pb	< 101.9	< 93.9	< 69.6	ppm	0.1
La	43	35	30	ppm	0.01

Table 2.9 Correlation coefficients determined between different elemental intensities measured by ITRAX XRF.

	Si	K	Ca	Ti	Mn	Fe	Rb	Sr	Zr
Si	1.00								
K	-0.11	1.00							
Ca	0.56	-0.53	1.00						
Ti	0.12	0.62	-0.03	1.00					
Mn	0.18	0.12	0.39	0.30	1.00				
Fe	-0.20	0.93	-0.54	0.63	0.18	1.00			
Rb	-0.32	0.81	-0.73	0.42	-0.08	0.84	1.00		
Sr	0.44	-0.62	0.85	-0.19	0.28	-0.64	-0.75	1.00	
Zr	0.31	-0.60	0.50	-0.31	-0.06	-0.63	-0.58	0.53	1.00

Figure 2.1 Regional map of the Canadian Arctic showing the location of the Murray Lakes field site on Northern Ellesmere Island.

Figure 2.2 Map of the Murray Lakes watershed indicating the position of local ice caps, the boundary of the watershed, and the location of air temperature loggers installed as part of this study. Shown at right is the general bathymetry of Upper and Lower Murray Lakes and the locations where sediment cores were collected.
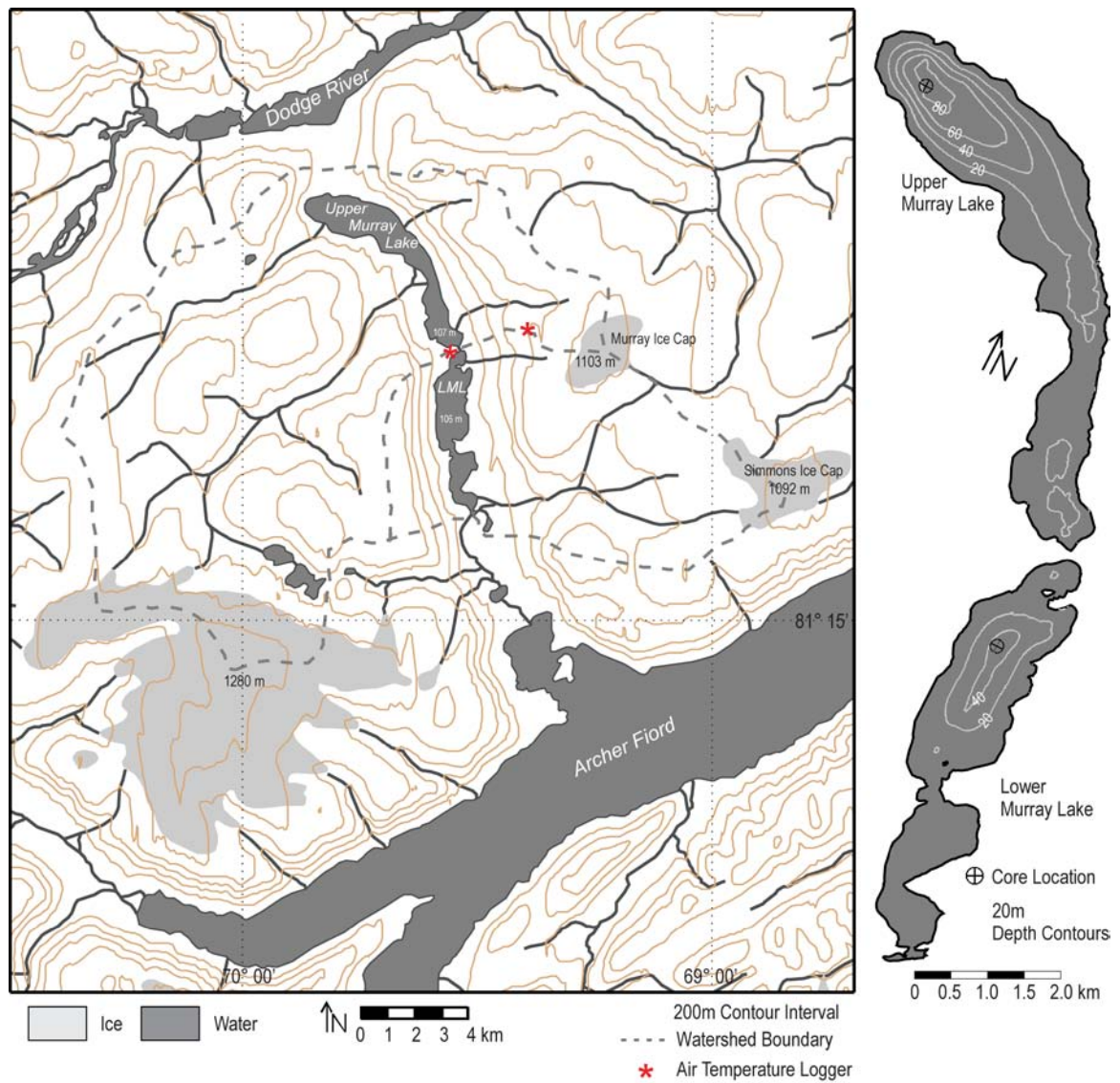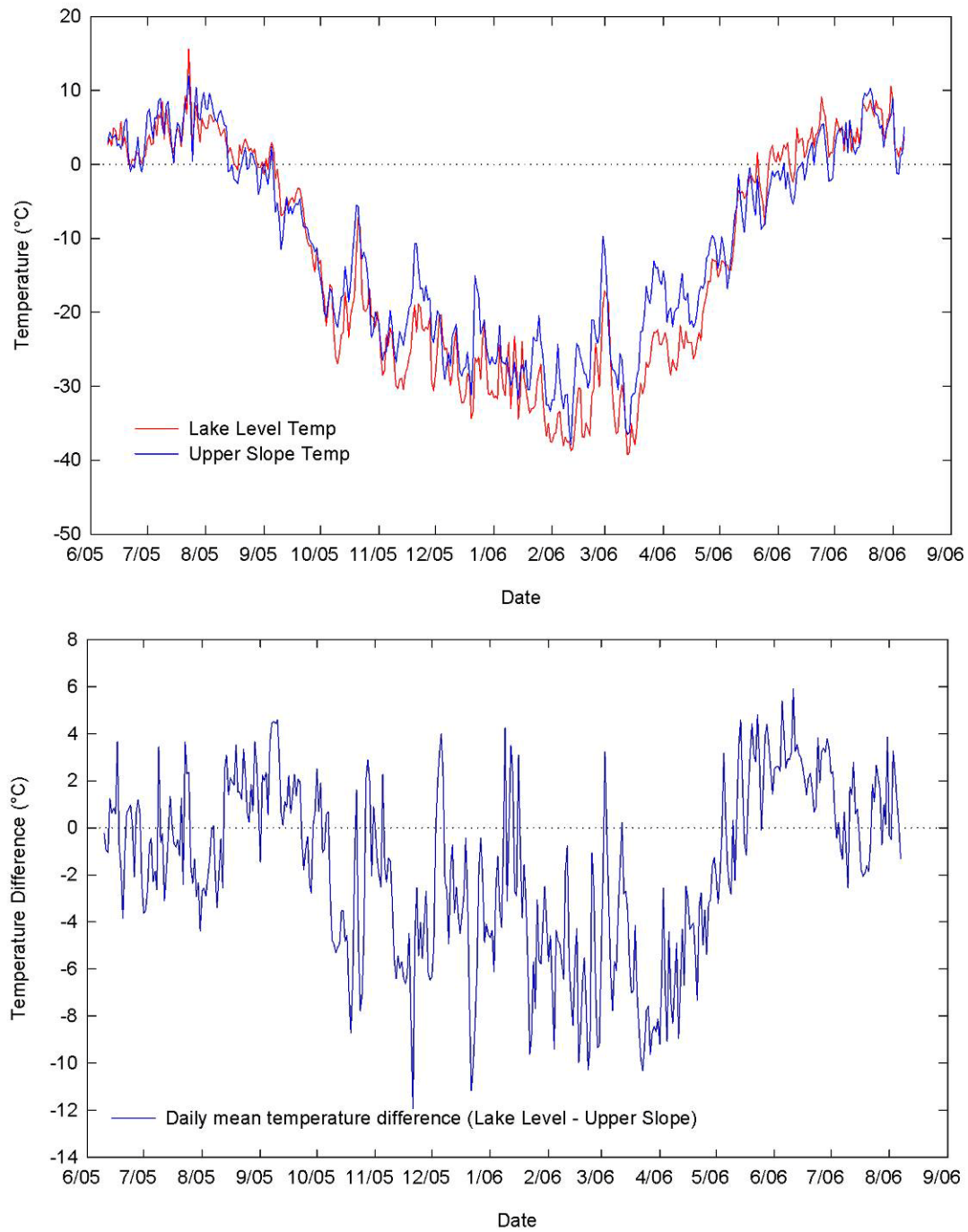
Figure 2.3 (Top) Mean daily air temperature recorded at lake level (113 m elevation) and on the upper slope adjacent to Lower Murray Lake (611 m elevation). Bottom panel indicates the difference between the mean daily temperatures recorded by the two loggers.
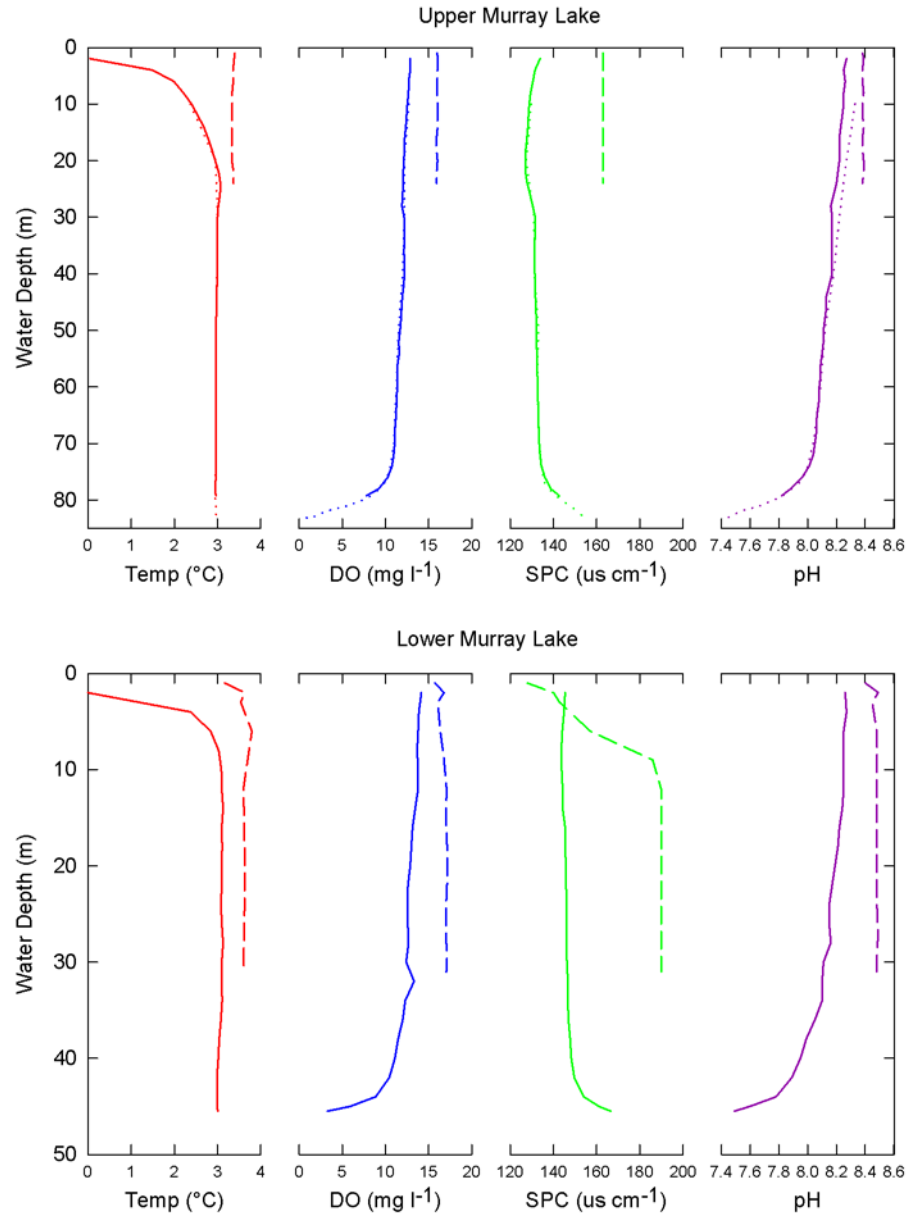
Figure 2.4 Water column properties measured in Upper and Lower Murray Lakes. Solid lines indicate data obtained in June 2005; dashed lines are from August 2006; dotted lines are from a repeat profile in Upper Murray in June 2005.
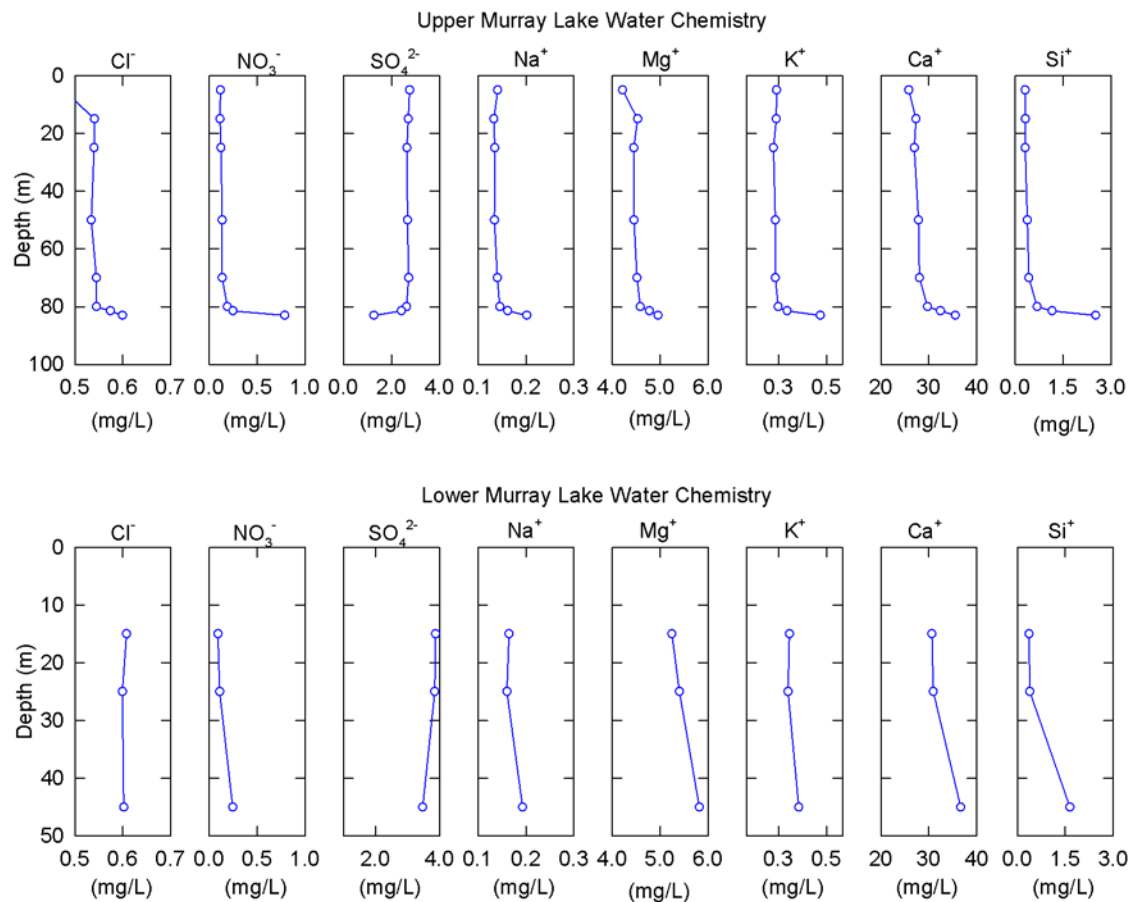
Figure 2.5 Profiles of dissolved ion concentrations in Upper and Lower Murray Lakes.
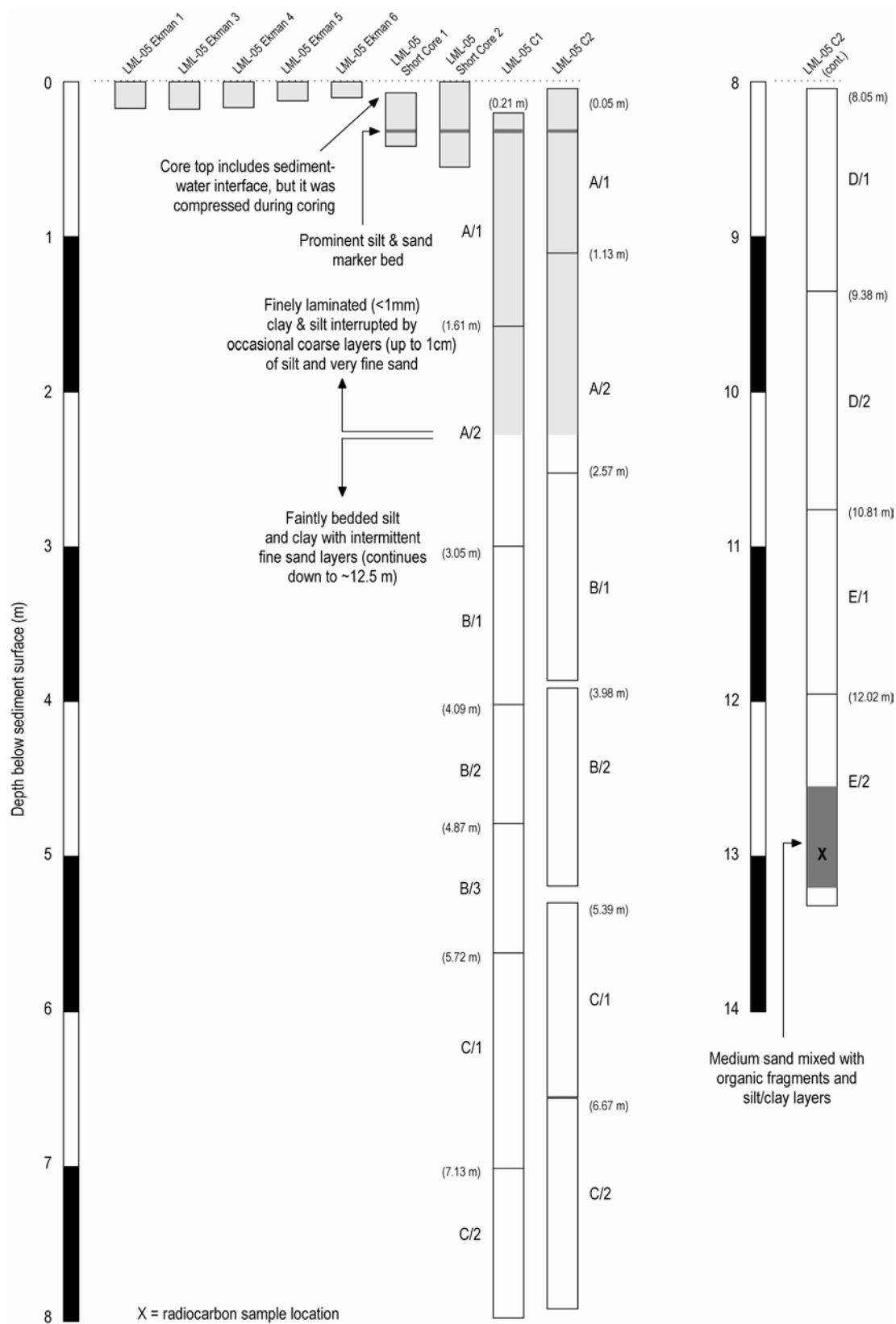
Figure 6a Brief description and correlation of the sediment cores recovered from Lower Murray Lake.

Figure 6b Brief description and correlation of the sediment cores recovered from Upper Murray Lake.
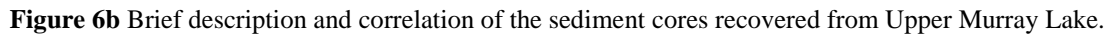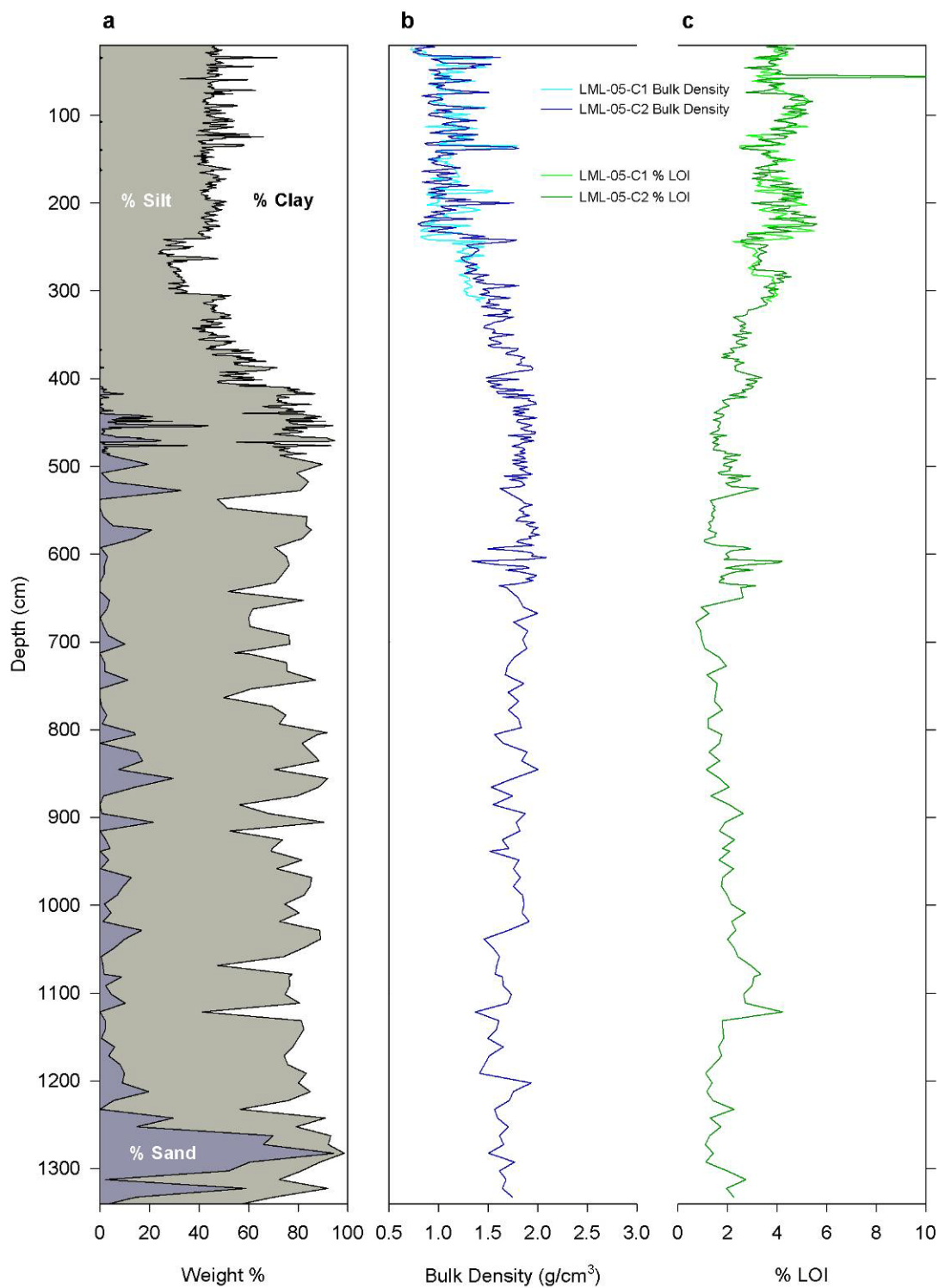
Figure 2.7 Down core variations in grain size, bulk density, and percent loss on ignition (LOI) in Lower Murray Lake.
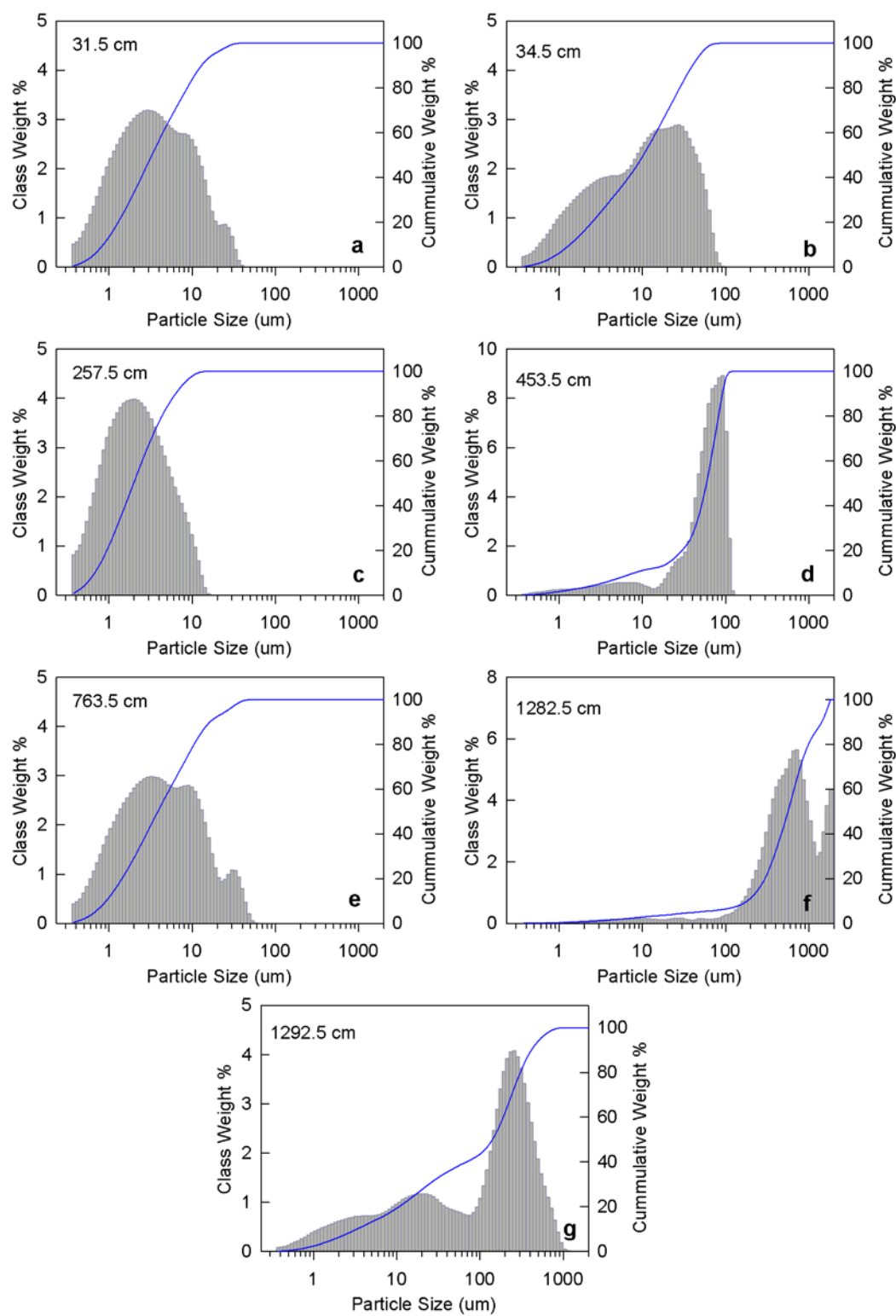
Figure 2.8 Size distribution plots illustrating the range of particle sizes characterizing different portions of the Lower Murray Lake sedimentary record.
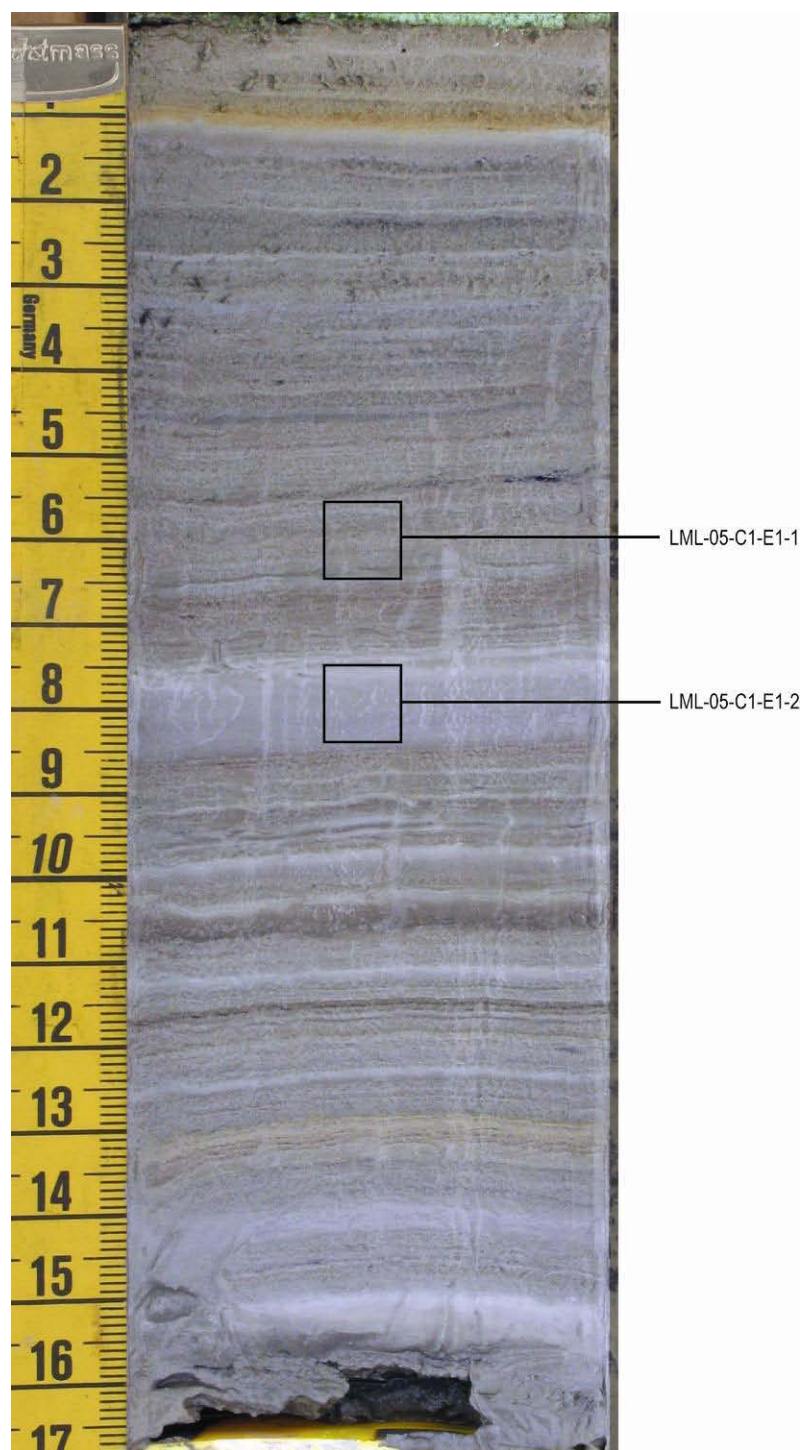
Figure 2.9 Photograph of core LML-05-C1-E1 illustrating fine laminations characteristic of the upper 240 cm of Lower Murray Lake sediments. Boxes indicated the location of sub samples utilized for ICP-AES analysis.
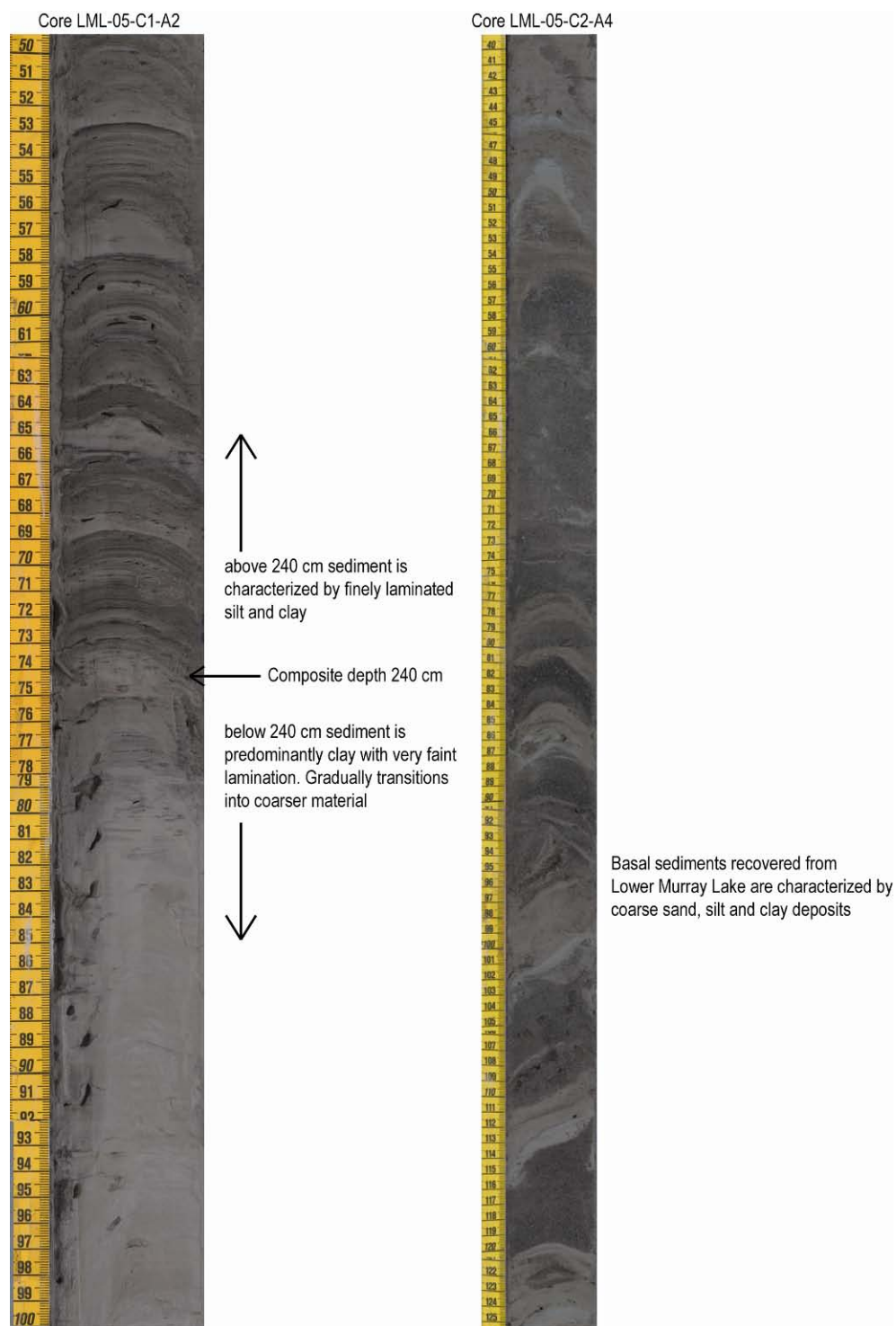
Figure 2.10 Subsection of core photos indicating the major transition to finely laminated sediments at a depth of 240 cm (core LML-05-C1-A2) and the variable, coarse deposits recovered in the basal core section (core LML-05-C2-E2).

49
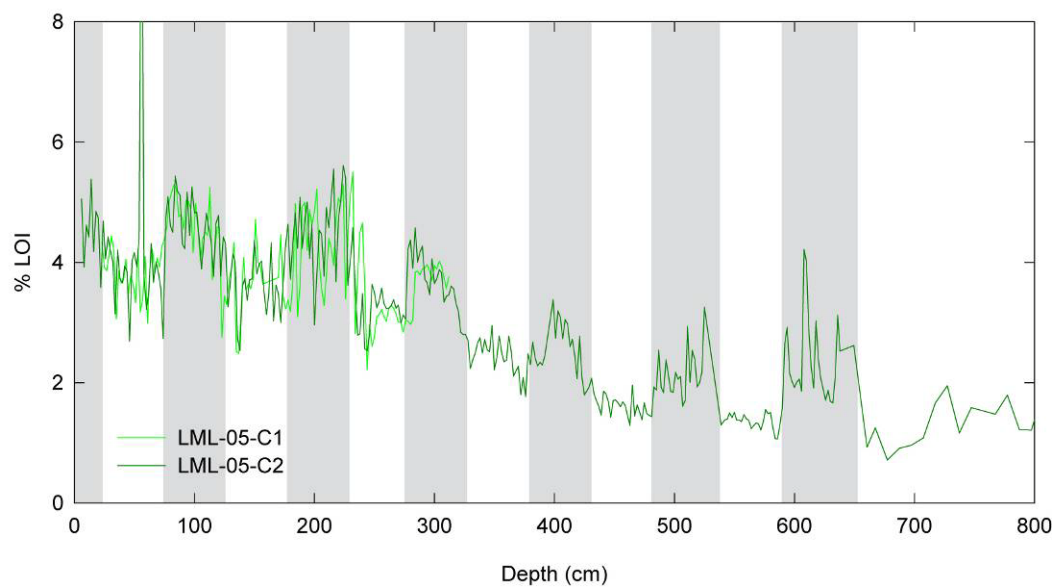
Figure 2.11 Percent loss-on-ignition (LOI) results from Lower Murray Lake Sediments. Apparent cyclicity in the % LOI values reflects errors associated with the placement of samples in the furnace during analysis. Shaded regions correspond to samples placed on the lower shelf of the furnace that consistently produced higher percent loss-on-ignition values relative samples on the upper rack.
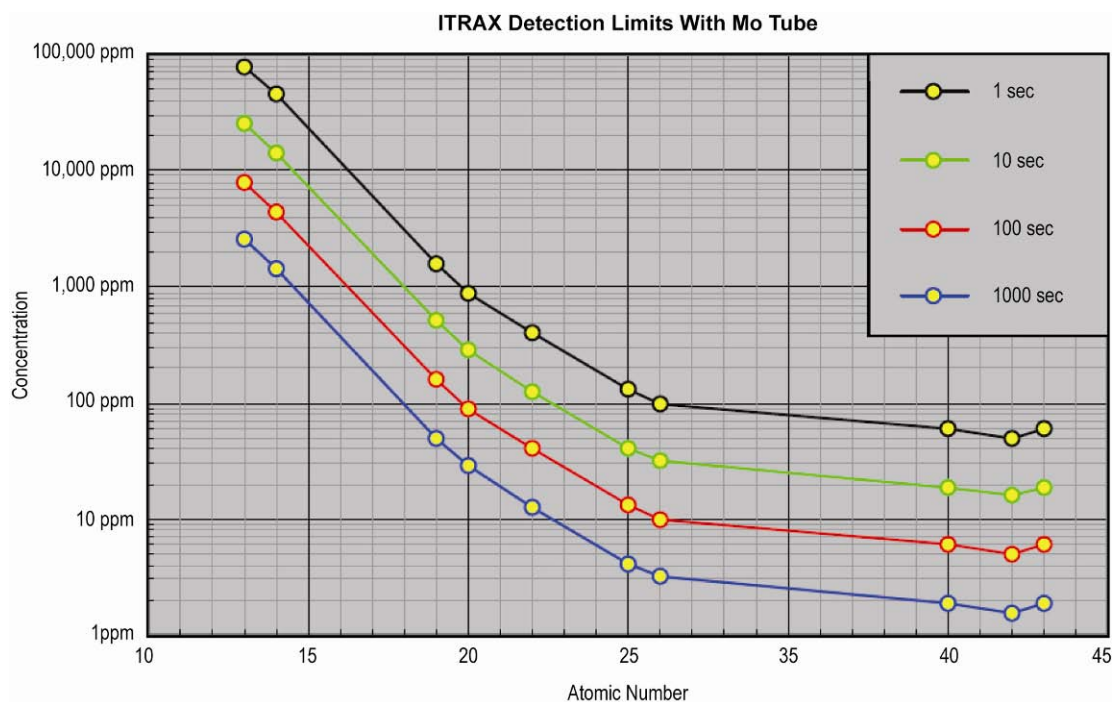
Figure 2.12 Minimum detection limits of the ITRAX X-ray fluorescence (XRF) instrument for elements of various atomic numbers based on acquisition times of 1, 10, 100, and 1000 sec (original figure provided by Cox Analytical Systems).
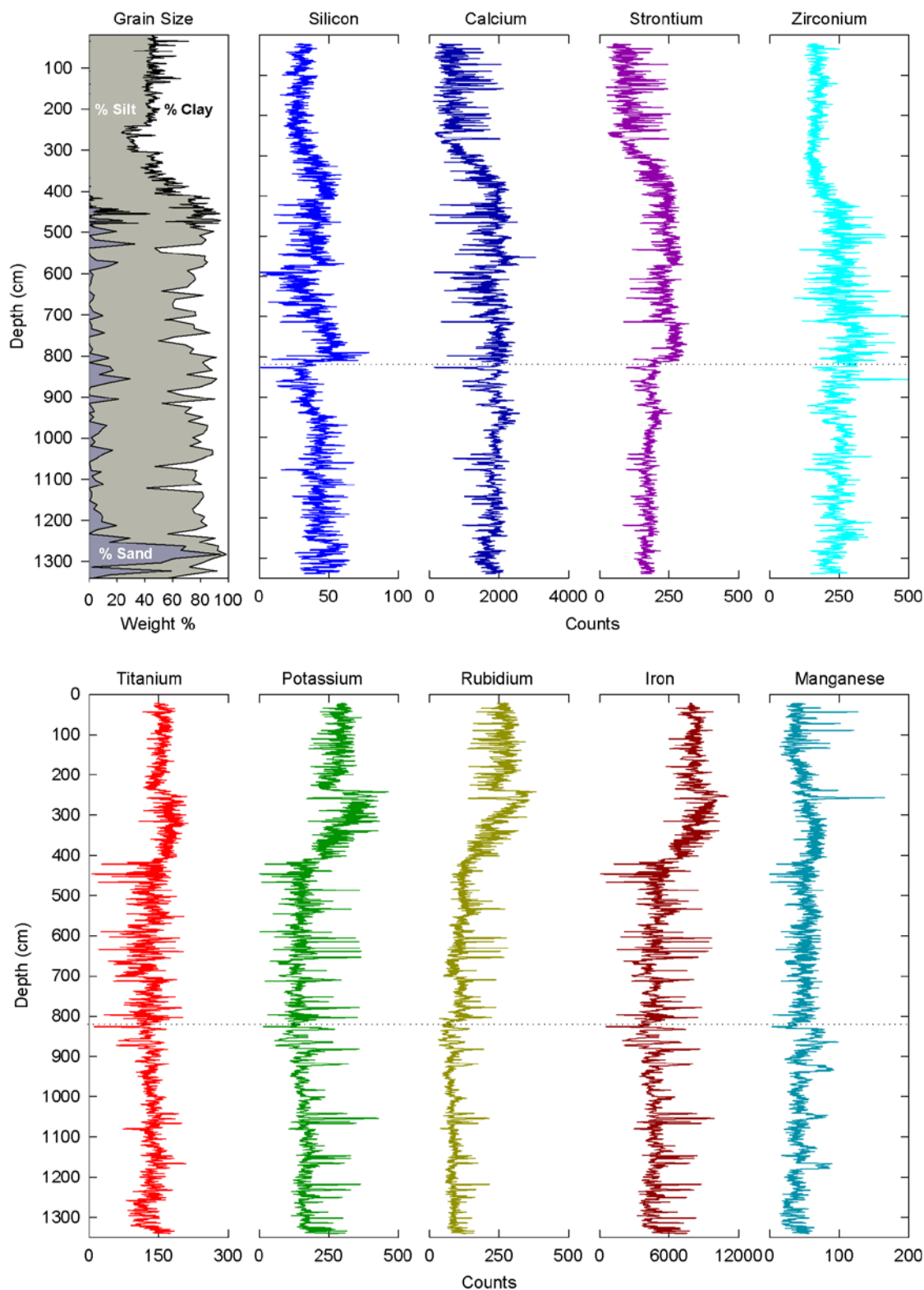
Figure 2.13 ITRAX XRF profiles of major chemical elements compared to down core variations in particle size. Dotted line indicates a break in the timing of sample analysis. Data from below the dotted line were recorded more than a year after the original analyses were performed, introducing the potential for analytical bias associated with the desiccation of the cores over time.
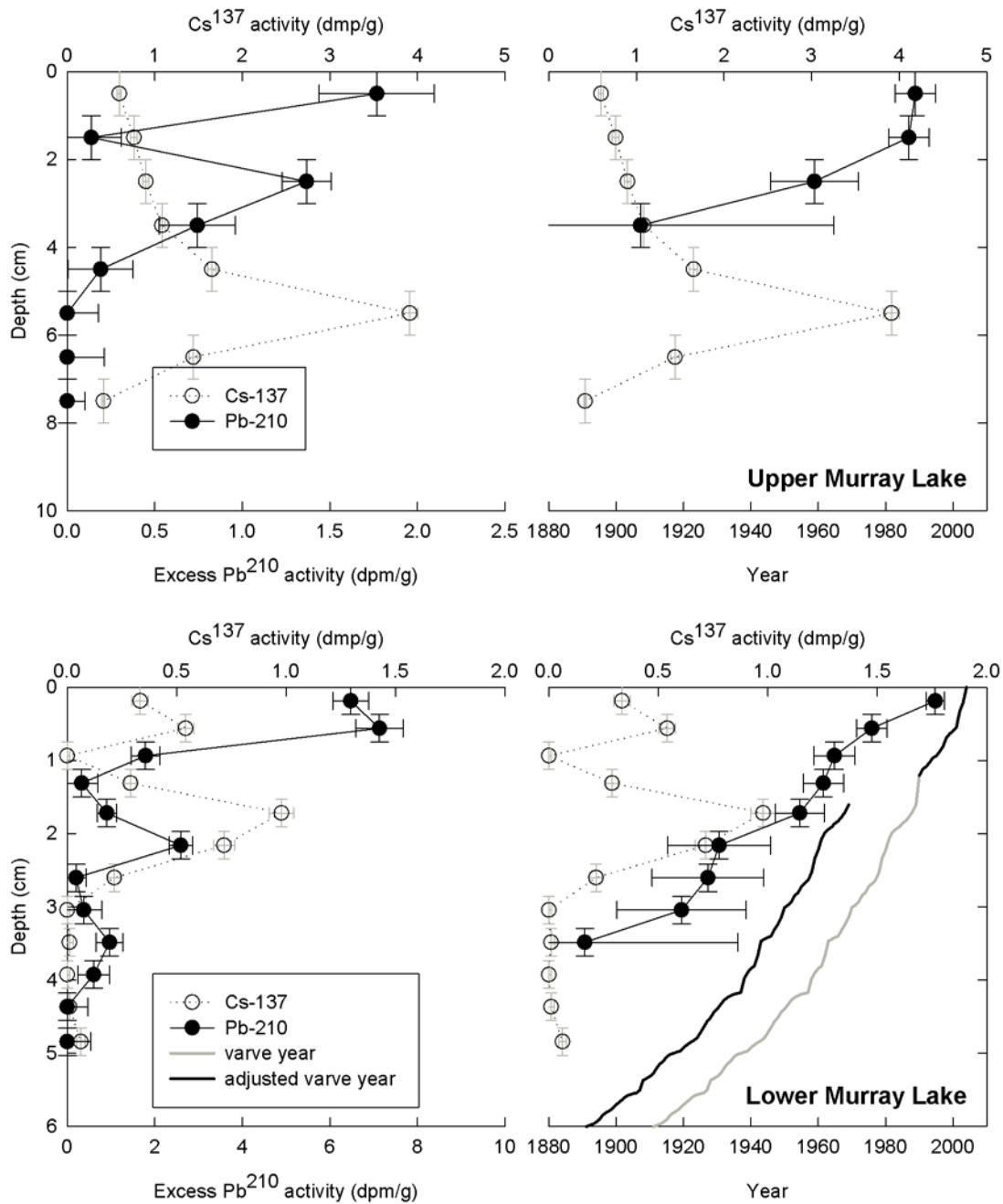
Figure 2.14 Results from ^{210}Pb and ^{137}Cs analyses of Upper (top panel) and Lower (bottom panel) Murray sediments. Plots on the left depict ^{210}Pb and ^{137}Cs activity versus depth. Plots on the right show ^{210}Pb data interpreted according to the constant rate of supply (CRS) plotted as age versus depth. The bottom right plot also shows the raw varve chronology and adjusted varve chronology as described in Chapter 3. Discrepancies between the ^{210}Pb age mode, the ^{137}Cs stratigraphy, and the Lower Murray varve chronology reflect likely disturbances in the upper most deposits sediments of the two lakes.
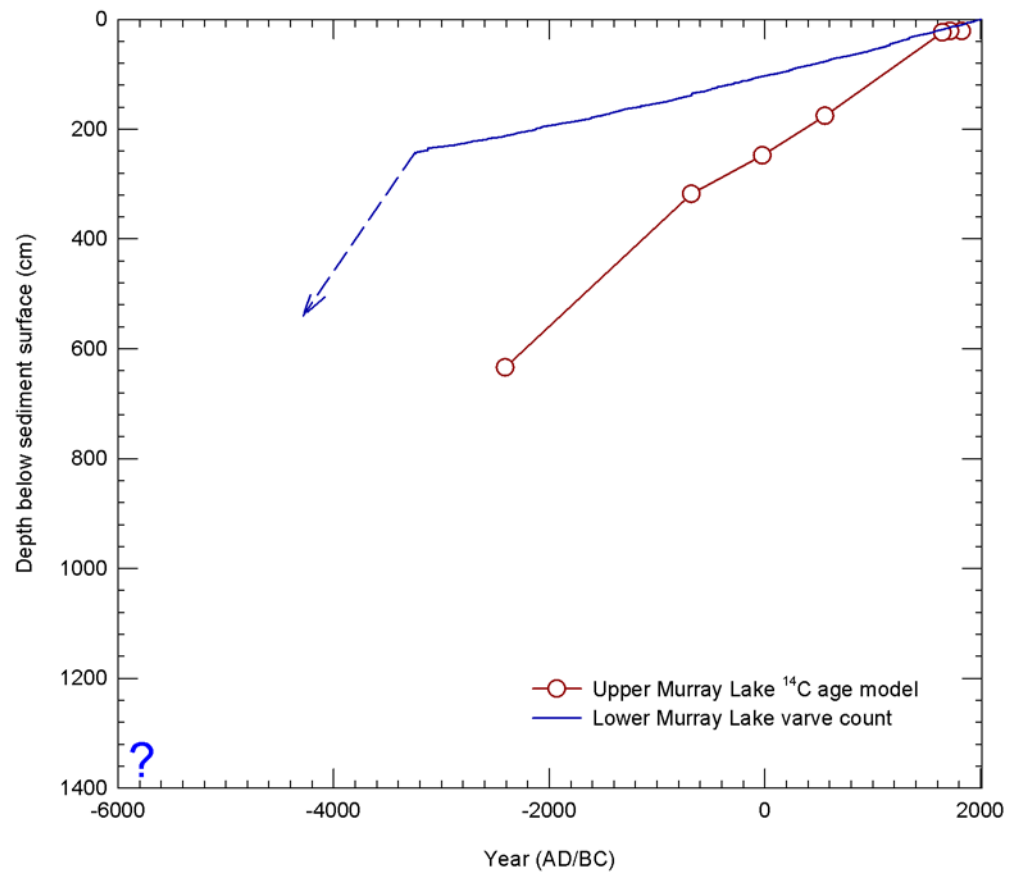
Figure 2.15 Age model for Upper and Lower Murray lake sediment accumulation. Lower Murray Lake age model is based on the varve chronology for the past 5200 years. The dashed line indicates a presumed increase in the rate of sediment accumulation prior to the varved portion of the record. Upper Murray Lake age model based on calibrated radiocarbon ages.
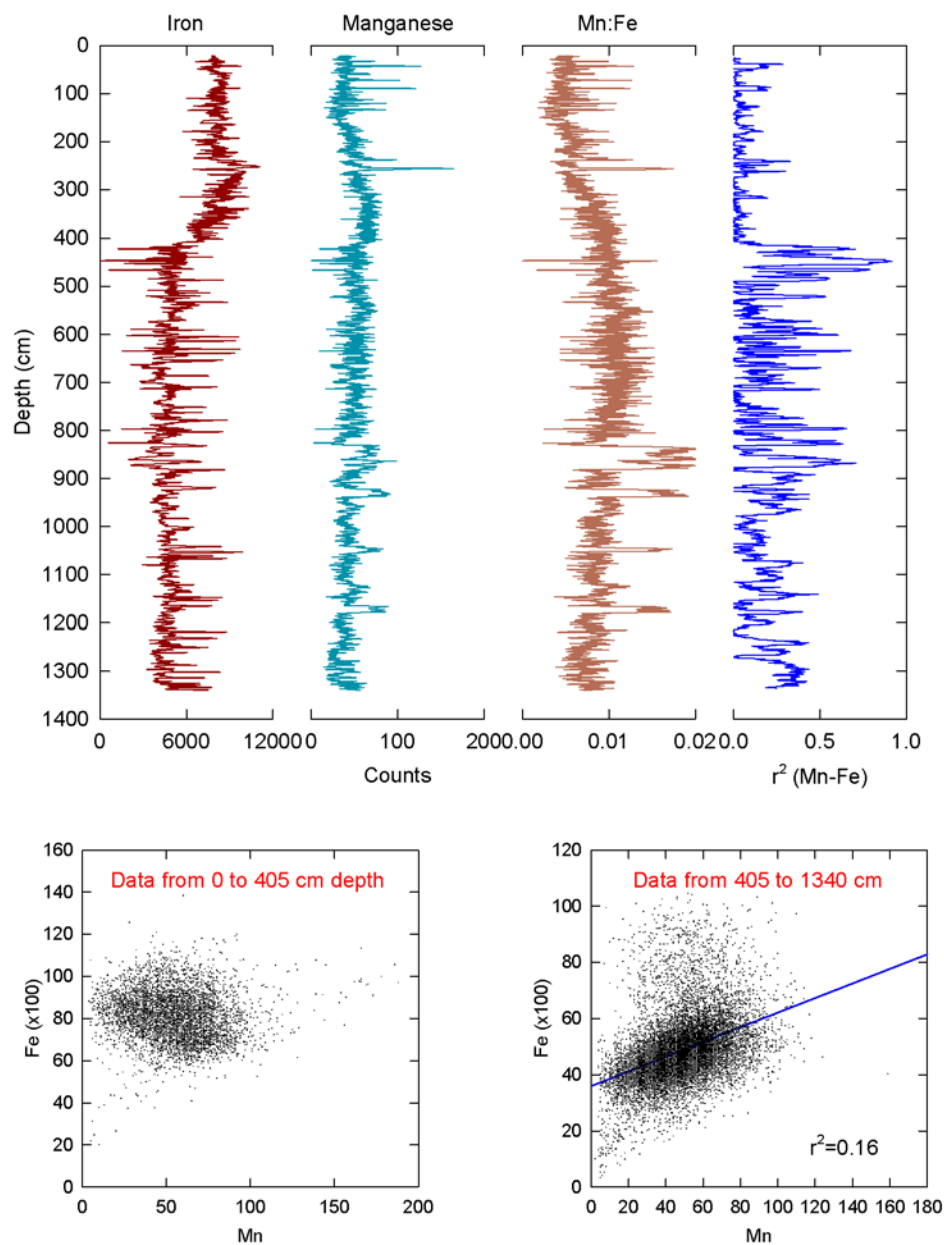
Figure 2.16 XRF profiles of redox sensitive elements Mn and Fe. The decrease in Mn:Fe ratio above ~ 405 cm likely indicates the onset of anoxia in the bottom waters of Lower Murray Lake. Determination of the correlation coefficient between of Mn and Fe over a moving 10 cm (101 point) window highlights this transition. Under oxic condition Mn and Fe are more likely to behave in a similar fashion, whereas Mn becomes more mobile under anoxic conditions, leading to poor correlation in the behavior of the two elements.

CHAPTER 3

ORIGIN, CHRONOLOGY, AND CLIMATIC SIGNIFICANCE OF
VARVED SEDIMENTS IN LOWER MURRAY LAKE

Abstract

Sediments in Lower Murray Lake, northern Ellesmere Island, Nunavut Canada (81°21' N, 69°32' W)

contain annual laminations (varves) that provide a record of sediment accumulation through the past 5000+

years. Annual mass accumulation was estimated based on measurements of varve thickness and sediment

bulk density. Comparison of Lower Murray Lake mass accumulation with instrumental climate data, long-

term records of climatic forcing mechanisms and other regional paleoclimate records suggests that lake

sedimentation is positively correlated with regional melt season temperatures driven by radiative forcing.

The temperature reconstruction suggests that recent temperatures are ~2.6°C higher than minimum

temperatures observed during the Little Ice Age, maximum temperatures during the past 5200 years

exceeded modern values by ~0.6°C, and that minimum temperatures observed approximately 2900 varve

years BC were ~3.5°C colder than recent conditions. Recent temperatures were the warmest since the

fourteenth century, but similar conditions existed intermittently during the period spanning ~4000–1000

varve years ago. A highly stable pattern of sedimentation throughout the period of record supports the use

of annual mass accumulation in Lower Murray Lake as a reliable proxy indicator of local climatic

conditions in the past.

Introduction

The High Arctic, surrounded by sea ice and snow covered much of the year, is a region where global climate changes are expected to be amplified by positive feedback processes (Holland and Bitz, 2003). The elevated climatic sensitivity of the Arctic makes it an ideal location for examining the causes and impacts of climate variability in the past, including both recent changes attributed to human activity and past changes associated with natural forcing mechanisms. However, our understanding of the climate system in the High Arctic is severely limited by a lack of long-term climate observations. In particular, the instrumental record is very short, generally less than 60 years in the Canadian Arctic, and provides limited spatial coverage. Additionally, limited daylight and severe temperatures reduce the potential for paleoclimate reconstructions based on biological proxies such as tree rings, pollen, and plankton assemblages. The few long-term proxy records that are available provide limited geographic coverage and typically demonstrate low temporal resolution (e.g. Gajewski and Atkinson, 2003). Therefore, there is a significant need for additional high-resolution paleoclimatic data for the High Arctic.

Due to their widespread occurrence, annually laminated (varved) lake sediments are increasingly being utilized as an important source of paleoclimatic information in the High Arctic. Climate reconstructions from laminated lake sediments are based on the relationship between the characteristics of an individual lamination, such as thickness or grain size, and some aspect of the weather during the corresponding year. Considerable effort has focused on correlating varve characteristics with instrumental climate records (Hughen et al., 2000; Moore et al., 2001; Francus et al., 2002; Hambley and Lamoureux, 2006) and monitoring the meteorological and hydrological processes controlling sediment transfer and deposition in arctic lakes (e.g. Hardy, 1996; Hardy et al., 1996; Cockburn and Lamoureux, 2007; 2008). These studies have described and quantified process linkages between climatic conditions, stream flow, sediment transfer and lake sedimentation. However, they have also highlighted the complexity of the climate-sedimentation system and the uncertainty associated with paleoclimatic reconstructions based on laminae characteristics. Because varve-climate correlations are limited by the length of local instrumental observations and detailed process studies have been limited to only a few seasons of monitoring, one of the

largest uncertainties in varve records relates to assumptions about the long-term stability of linkages between climate and sedimentation under varying climatic and geomorphic conditions.

In this paper, we report the results from a study of laminated sediments in Lower Murray Lake in the Canadian High Arctic, building upon results previously reported by Besonen et al. (2008). The results presented here extend the record of annual sedimentation in Lower Murray Lake through the past 5000+ years, making it the longest varve record yet produced from the High Arctic. This paper aims to identify how sediment delivery to the lake has varied through time and to evaluate the validity of inferred climate-sedimentation linkages over long time scales that include changes in external forcing mechanisms related to climate variability.

Study Area

Lower Murray Lake is a relatively large (~5 km^2), deep (~47 m) lake located along the eastern margin of the Hazen Plateau, northern Ellesmere Island, Nunavut, Canada (81°21' N, 69°32' W; Figure 3.1). The region is characterized by an extensive upland plateau that contains several small ice caps at an elevation of approximately 1000 m. Lower Murray Lake is one of two lakes occupying a glacially carved valley within the plateau region. The lake lies at an elevation of 106 m, which is above the local Holocene marine limit (England 1983), and most of its surface inflow is derived from the upper plateau. Lower Murray Lake has a total drainage basin of 261 km^2; however, the majority of this area (184 km^2) first drains into Upper Murray Lake, which is connected to the lower lake by a shallow spillway that is less than 1 m deep. Runoff associated with snow and ice melt in the upland areas drains into the lakes via several short, high-gradient streams. The main tributary into Upper Murray Lake drains a ~55 km^2 icecap located southwest of the lakes. Two small, stagnant ice caps drain directly into Lower Murray Lake at its extreme north and south ends. Apart from the spillway connecting the two lakes, the largest tributary enters Lower Murray Lake at its southeast corner, near its outflow stream. The southern portion of the lake is separated from the central, deep basin by a ~300-m-wide channel of unknown depth.

Climatically, the region is a polar desert with a mean annual temperature around -19°C, and mean annual precipitation, which occurs mostly in the form of snow, is less than 150 mm water equivalent (Maxwell 1981). Above-freezing temperatures occur from early June through late August, with daily maximum temperatures occasionally exceeding 15°C. The extreme seasonality of temperatures produces a brief period of runoff and sediment transfer into Lower Murray Lake and is highly conducive to the formation of annual laminations in the sedimentary record. A 1.5- to 2-m-thick (or thicker) ice cover lasts throughout much of the year, with open water generally occurring only from mid August through early September. This brief period of open water reduces wind and wave action and limits mixing of the water column leading to near anoxia at the sediment water interface (Besonen et al. 2008). In combination, these factors are highly conducive to the preservation of individual laminations in the lake sediments. Besonen et al. (2008) concluded that individual lamina in Lower Murray Lake were annual, and established a varve chronology for the past 1000 years from the upper ~55 cm of sediment.

Methods

Field work

Lower Murray Lake was visited in June 2005 and August 2006 to conduct coring and to survey the lake environment. A suite of cores was collected from the deepest basin (water depth 46.13 m) at 81.34175°N, 69.55204° W. Two overlapping, long cores were collected using an Uwitec piston corer (cores LML-05-C1 & LML-05-C2). Special care was taken to collect an undisturbed record of the upper-most sediment and to preserve an intact sediment-water interface using an Aquatic Research Instruments gravity corer (cores LML-05-C1-AR1 & LML-5-C1-AR2) and an Ekman dredge-type sampler (cores LML-05-C1-E4 & LML-05-C1-E5). Both the Aquatic Research and Ekman cores displayed clear water overlying the sediment, confirming that an undisturbed sediment-water interface was recovered. The Ekman samples were subsampled by inserting a 6-cm-diameter polycarbonate tube into the sediment and then sealing the ends of the tube.

Core analysis

        All cores were split and photographed in the lab in order to identify the most complete and

undisturbed sections suitable for further analysis. Dry bulk density of the sediment was measured at fixed

intervals of 1 cm in core LML-05-C1-E4, and at 2-cm spacing in all other cores by extracting 1 cc samples

using a cutoff syringe, drying the sediment for 16 h at 105°C, and then measuring the mass. Bulk density

was calculated by dividing the dry mass of the sediment by the initial sampling volume. Organic carbon

content was then estimated by percent loss-on-ignition (LOI) using the same samples analyzed for bulk

density. Dried samples were placed in a preheated 550°C muffle furnace for 4 h, and then allowed to cool

in a desiccator. Percent LOI was calculated by dividing the mass difference between the dry sediment

sample and the post-ignition sample by the mass of the dry sample (Dean, 1974; Heiri et al., 2001). Particle

size was analyzed at 1 cm increments after pre-treating samples with a 30% hydrogen peroxide solution to

digest organic material. Samples were analyzed using a Beckman Coulter LS200 particle-size analyzer.

Paleomagnetic samples were recovered from the split cores using rigid u-shaped plastic channels with a 2

cm × 2 cm cross section. Paleomagnetic analyses were conducted at Institut des Sciences de la Mer de

Rimouski, Québec, Canada. In order to analyze and interpret fine-scale laminations, thin sections of epoxy-

impregnated sediment slabs were produced in a manner similar to that described by Francus and Asikainen

(2001). Slabs of sediment were removed from the split core halves using 18 cm × 2 cm × 0.7 cm aluminum

trays inserted into the sediment. Overlapping the trays provided continuous stratigraphic coverage. The

slabs were then flash frozen in liquid nitrogen, dehydrated in a freeze dryer, and impregnated with epoxy

under vacuum using a low viscosity resin. After the epoxy had cured, the slabs were cut into three sub-

blocks from which 2.5 cm × 7.5 cm polished thin sections were prepared. Cutting the slabs at an angle

across the laminations ensured that none of the sequence was lost to the saw kerf.

        Detailed analysis of the laminations was carried out using digital images of the thin sections. Each

thin section was scanned at 2400 dpi under plain transmitted and cross polarized light using an Epson V750

flatbed scanner. A composite sequence of images providing continuous coverage of the sediment record

was created by selecting individual thin sections from the different cores which showed the least

disturbance for that portion of the record (Table 3.1; Appendices 1 and 2). Counting and quantitative

measurement of individual laminae was performed using image acquisition and analysis software

developed at Institut National de la Recherche Scientifique, Québec. This software calculates and records

the thickness and depth of individual laminae along a vertical axis. However, down-warping along the

edges of the core barrel and/ or misalignment of sediment slabs on the thin sections resulted in laminae that

were not consistently oriented perpendicular to the measurement axis. In these cases the angle of the

laminae was recorded and used to adjust the thickness measurements. The complete lamination sequence

was counted and measured three times in an iterative manner, where the previous count was used as a

starting point for refining further observations. An assessment of the reproducibility of the Lower Murray

Lake lamination record was possible by comparing the results produced during this study with

measurements previously reported by Besonen et al. (2008) who independently examined a different core,

ML-00, collected at 81.3334° N, 69.54216° W from the same basin in Lower Murray Lake.

Radioisotope analysis

Surface core LML-05-C1-E5 was subsampled for ^{210}Pb and ^{137}Cs analysis by removing 0.5 cm

slices of sediment from the split core tube. Sediment samples were freeze dried and powdered. Twelve

samples spanning the upper 6 cm of the deposit were analyzed by gamma spectroscopy using a Canberra

ultra-low background well-type germanium detector at the University of Florida.

Results

Core stratigraphy

Core LML-05-C2, the longest core recovered from Lower Murray Lake, penetrated ~13.9 m. The

bottom of this core consists of massive 5- to 10- cm-thick units of fine- to coarse-grained sand interspersed

with silt and clay units (Figure 3.2). The large grain size of these basal sediments suggests that they were

deposited in a high-energy environment. We infer that the source of this energy was fluvial discharge from

a locally receding glacier. This would suggest that core LML-05-C2 contains a nearly complete post-glacial

lacustrine sedimentary sequence from Lower Murray Lake. The sediment sequence consists predominantly

of fine-grained, siltand clay-sized clastic material with very little organic matter. Mean loss-on-ignition was

~4.3%, although the actual organic content is likely lower because the dehydration of clay minerals continues at temperatures above 105°C (Dean, 1974). The upper 245 cm of the core are characterized by fine laminations (<1 mm thick), consisting of alternating silt and clay couplets (Figure 3.3). This upper portion of the core is punctuated by occasional, thicker units of silt and fine sand that are up to 1 cm thick (Figure 3.3). Below 245 cm, laminations are less distinct and grain size is more variable. We interpret the transition to laminated sediments to reflect the retreat of glacial ice from the Murray Lakes valley and the evolution of the lake to its current water level. Relatively uniform grain size and lamination characteristics throughout the upper 245 cm suggest that the lake and its surroundings had reached steady-state conditions prior to this time. The remainder of this paper focuses only on the upper, finely laminated portion of the record where lake sedimentation follows a consistent pattern.

Chronology

Due to the pronounced seasonality of the processes controlling sediment transfer and deposition in Lower Murray Lake, and to patterns of sedimentation that are consistent with varved deposits, including fining upwards laminae topped by clay caps, we hypothesized that the silt-clay laminations observed in the sediments reflected annual units. Indeed, sediment cores collected in 2005 contained five additional laminae relative to those cores retrieved in 2000, confirming that recent laminae are annual. Further confirmation of this hypothesis was attempted by comparing ^{210}Pb and ^{137}Cs profiles to the varve chronology. However, disturbance from turbidity currents, bioturbation or mass movements can influence the inventory of ^{210}Pb in surface sediments (Wolfe et al., 2004). The application of ^{210}Pb dating in the Arctic is further complicated by very low ^{210}Pb activities in high-latitude lake sediments. Low radionuclide concentrations reflect a combination of reduced production because frozen soil retards the release of the parent isotope ^{222}Rn, and reduced deposition because persistent lake-ice cover limits the efficiency with which atmospheric ^{210}Pb is transferred to lake sediments (Wolfe et al., 2004). The Lower Murray Lake ^{210}Pb profile shows low activity levels characteristic of the Arctic, and erratic variations that likely reflect disturbance of the upper sediments (Figure 3.4a). Visual inspection of the sediment confirms that an erosive turbidite layer was deposited during varve year 1990 (1.5 cm depth). Modeling of the sedimentation rate based on the ^{210}Pb profile using the constant rate of supply (CRS) model (Appleby and Oldfield, 1978)

produces an age depth curve which is inconsistent with the varve chronology (Figure 3.4b). The lowest

sample in the ^{210}Pb age model assigns a date of 1890 to a depth of 3.5 cm, which corresponds to varve year

1944. This discrepancy would suggest large inaccuracies in the varve chronology which we believe are

unreasonable and can more easily be explained by errors associated with low ^{210}Pb inventories in Arctic

lake sediments, and by the erosive turbidite which would have removed and deposited elsewhere a portion

of the radionuclide inventory. The anthropogenic radionuclide ^{137}Cs provides two stratigraphic age

horizons, corresponding to the onset of nuclear weapons testing ca. ~1954, and a peak in 1963 associated

with maximum atmospheric fallout immediately prior to the implementation of the nuclear test ban treaty

(Wolfe et al., 2004). The Lower Murray Lake radionuclide profile shows the first occurrence of ^{137}Cs at

~2.6 cm and a distinct peak at ~1.7 cm, corresponding to varve years ~1977 and 1988 respectively (Figure

3.4). We propose that the discrepancy between the varve chronology and the known timing of these ^{137}Cs

stratigraphic horizons was due to erosion of underlying varves associated with the turbidite in varve year

1990. Consequently the varve located in the middle of the interval of peak ^{137}Cs activity was assumed to be

varve year 1963 and the varve chronology below the turbidite was reestablished from this point. The

number of varves counted between the onset and subsequent peak in ^{137}Cs is consistent with the known age

of these stratigraphic horizons. However, the large sampling interval used for radionuclide measurements

relative to the low sedimentation rate in Lower Murray Lake precludes a precise determination of the

number of laminae between the first occurrence and peak ^{137}Cs intervals. Counting varves upwards from

the 1963 varve to the base of the turbidite suggests that varves from ~1970 through 1989 were eroded. This

finding is consistent with the previous varve chronology established in Lower Murray Lake by Besonen et

al. (2008).

Confident interpretation of the long-term sedimentary record in Lower Murray Lake requires

validation of the consistency of the varve chronology throughout the time scale to be investigated.

However, biological productivity in Lower Murray Lake is low both within the lake and in the surrounding

drainage basin, and no suitable material for radiocarbon dating was identified in the lake sediments.

Consequently, the long-term accuracy of the varve chronology was confirmed by comparing a record of

paleomagnetic secular variation from Lower Murray Lake sediments in core LML-05-C2 with an

independently dated paleomagnetic record from South Sawtooth Lake (Figure 3.5). South Sawtooth Lake

was cored as part of a separate study by coauthors of this paper. While analysis of the South Sawtooth record is ongoing, varve characteristics and limnological and sedimentary processes have been discussed in Francus et al. (2002; 2008). Despite differing rates of sedimentation, distinctive sedimentary characteristics and unique magnetic properties for each record, consistent patterns can be correlated among the different time series. In particular, both records show a large, coeval shift in declination and relative paleointensity and in-phase variations in the environmental magnetic ratio of anhysteretic remanent magnetization (ARM) after 30 mT demagnetization to the ARM before demagnetization. These similarities in the timing of paleomagnetic secular variations and environmental magnetic parameters help to confirm the accuracy of the individual chronologies.

Sources of error in varve chronologies can result from a number of factors including: (1) technical problems associated with coring and sub-sampling of the sediments; (2) unconformities caused by erosive events; (3) changes in varve preservation; and (4) either very high or very low sedimentation rates, which often make it difficult to distinguish seasonal events from the annual cycle (Zolitschka, 2007). Technical problems in the Lower Murray Lake chronology were minimized by collecting multiple sediment cores and carefully selecting the least disturbed portions from each core to create a single composite varve sequence. All of the cores used in the composite record were from the same coring site, within a radius of \5 m, thus local variations in sedimentation should not be a factor. Although evidence for erosion during the ca. 1990 turbidite is unequivocal, only three other erosive turbidites were identified in the rest of the record. Additional unconformities may exist, but without further evidence, it seems likely that erosive events occur infrequently in this part of the lake. If erosive events were a common feature of the record, a continuously increasing offset would be expected between the timing of paleomagnetic variations in Lower Murray Lake sediments versus those in South Sawtooth Lake. However, this type of offset is not observed.

An estimate of the uncertainty associated with the subjective nature of varve identification and delineation was possible because Lower Murray Lake was the site of a previous varve study. Comparison of the overlapping portions of the varve records established in this study and by Besonen et al. (2008) demonstrates a high degree of consistency between chronologies established by separate individuals on different cores (Figure 3.6). Despite relying on different sources of information (plain and cross-polarized scanned images in this study, and plain-light scans and backscattered SEM images in the previous study)

the two independent chronologies are offset by only 17 varve years at the end of the 1000 year period. Close examination of the individual chronologies isolated most of the offset to a single, short (~4 cm) portion of the record, between varve years 1550 and 1600 AD, where laminae were particularly diffuse and difficult to distinguish. There was no clear justification for favoring one chronology over the other, and as a result this discrepancy provides an error estimate of ~2% for the reproducibility of the varve chronology. The largest remaining sources of chronological error relate to either over-counting of sub-annual laminae, or under-counting eroded or poorly preserved laminae. Without more precise age control for the long record from either radiocarbon or tephra dating it is difficult to precisely quantify the full level of chronological uncertainty from all sources in the Lower Murray Lake varve record.

Lamina characteristics

A total of 5221 individual varves were identified. After accounting for the estimated ~20 varves eroded during the ca. 1990 turbidite, but without taking into account the additional uncertainties described above, the laminated portion of the Lower Murray Lake record spans the period from varve year 2004 AD through 3236 BC. No adjustment was made for the three additional erosive events because there was no way of determining how many laminae were removed. The composite time series of varve thickness is shown in Figure 3.7. Mean laminae thickness throughout this period is 0.46 mm, although the record shows considerable high-amplitude variability. Typical laminae are characterized by a fining-upward silt unit topped by uniform clay caps. These units fit the classic description of clastic varves typical of cold environments (Sturm, 1979; Zolitschka, 2007). Punctuating this sequence are a number of anomalously thick (up to 1 cm), coarser grained (silt to fine sand), graded deposits, which occasionally contain planar sub laminae. The larger grain size of these deposits necessitates an alternative, higher-energy transport mechanism relative to the typical varves. The genesis of these deposits is difficult to decipher without additional process monitoring; however, similar deposits in other arctic lakes have been attributed to turbid underflows resulting from rain events and elevated stream flow (Lamoureux, 2000; Hambley and Lamoureux, 2006; Francus et al., 2008). A total of 124 of these anomalous beds were identified through visual inspection of the thin sections. To facilitate the interpretation of variations in mean sedimentation as

characterized by typical varves, the anomalous beds were removed from the time series and replaced by a unit equal in thickness to the series mean after excluding the graded beds (0.34 mm).

Evaluation of changes in sedimentation through time requires that varve thickness measurements are corrected for varying degrees of compaction. In general, sediment becomes more compacted with depth as it is compressed by the weight of the overlying material. In addition, differential compaction of sediments can occur during the coring process as sediment interacts with the surrounding sediment and core tube. This problem was addressed by converting varve thickness measurements to mass accumulation rates (MAR) using measurements of bulk density (Figure 3.7). The average mass accumulation rate for the period of record was 0.049 or 0.036 g cm^{-2} year^{-1} if the anomalous event beds are excluded. Correcting for variations in bulk density effectively compensated for the trend toward increasing varve thickness observed in the uppermost sediments. However, comparison of the grain size, bulk density, varve thickness, and mass accumulation records indicate that isolated, coarse-grained deposits are responsible for some of the largest peaks in mass accumulation. This result highlights the difficulty of relating discrete bulk density measurements to higher-resolution varve thickness measurements (cf. Besonen et al., 2008). Thus, when comparing rates of sedimentation between different periods of the record it is important to evaluate how and why mass accumulation rates differ from varve thicknesses within a given interval.

Varve thickness and mass accumulation data were smoothed with a 25-year running mean filter to aid identification of periods of consistently higher or lower sedimentation (Figure 3.7). The long-term record of mass accumulation shows distinct centennial-scale variations in addition to extended periods of reduced or enhanced mass accumulation relative to the long term mean. Twentieth-century mass accumulation rates fall at the upper end of the scale, and during the last 1000 varve years, were only exceeded in the twelfth and fourteenth centuries. A minimum in mass accumulation occurred around varve year 1800 AD; the only comparable period of low mass accumulation occurs from varve year 5200 BC through 4500 BC. Mass accumulation rates in the middle portion of the record, spanning varve years 2000 BC to 1000 AD, are predominantly near or above the 1000–2000 AD mean, and are characterized by considerable variability.

Discussion

Climatic controls on Lower Murray Lake sedimentation

Previous studies of High Arctic lake systems have demonstrated various quantitative relationships between lake sedimentation and meteorological conditions. In many cases, lake sedimentation and varve thickness are related to temperature during the summer melt season when the melting of ice and snow provides energy to transport sediment into lakes (Hardy, 1996; Hardy et al., 1996; Gajewski et al., 1997; Braun et al., 2000b; Hughen et al., 2000; Moore et al., 2001; Francus et al., 2002; Hambley and Lamoureux, 2006). In other systems, sediment delivery is controlled more by winter snow accumulation than by summer-melt conditions (Braun et al., 2000a; Lamoureux and Gilbert, 2004; Forbes and Lamoureux, 2005; Cockburn and Lamoureux, 2007). Additional controls on lake sedimentation can include rain-induced erosion (Lamoureux, 2000; Lamoureux et al., 2001), limited sediment availability (Braun et al. 2000a), spatial and temporal variations in the distribution of sediments within a lake (Lamoureux, 1999), mass movements (Lewis et al., 2005), variations in sediment availability (Lamoureux, 2002), and a variety of external catchment and within-lake processes that are often non-linear (e.g. Hodder et al., 2007). We examined the relationship between annual sedimentation in Lower Murray Lake and climatic conditions by comparing the time series of mass accumulation to instrumental climate data recorded at the two nearest permanent weather stations located at Alert, which is 180 km away along the north coast of Ellesmere Island, and at Eureka which is located 320 km west in a more continental setting. Because the frequency distribution of annual mass accumulation rates was heavily skewed towards smaller values the data were log transformed. This process yields a time series consisting of more normally distributed values which are better suited for correlation with climatic data that typically exhibits a Gaussian distribution (cf. Rittenour et al., 2000). Only mass accumulation data from the years 1990 through 2004 were used in the statistical analysis because the certainty of the varve chronology decreases prior to the ca. 1990 turbidite. Table 3.2 lists r^2 values obtained from calculating linear regressions between Lower Murray Lake MAR and various climatic variables for the period 1990–2004. In general, r^2 values generated from correlation with surface meteorological conditions were very low. However, mass accumulation rates were significantly correlated to radiosonde measurements (Durre et al., 2006) of mean July temperatures at 600 m at both Alert ($r^2 =$

0.61) and Eureka (r^2 = 0.50; Figure 3.8). Temperature data from 600 m were chosen for the analysis because this elevation corresponds to the approximate mean elevation of the Murray Lakes watershed.

A positive correlation between summer temperatures and sedimentation rates has been observed in several other lakes in the Canadian Arctic (e.g. Hardy et al., 1996; Hughen et al., 2000; Moore et al., 2001). In particular, Hardy et al., (1996) also identified a strong correlation between 600 m temperatures at Alert and daily sediment flux into Lake C2. Upper-air temperature measurements likely provide a better estimate of regional temperature conditions relative to surface measurements because they are not influenced by localized low-level temperature inversions which are common throughout the High Arctic. Furthermore, much of the runoff entering Lower Murray Lake is derived from snowmelt in the upper watershed which is at or above 600 m elevation. At other sites on northern Ellesmere Island where streamflow and sediment flux measurements have been recorded, peak streamflow and the majority of the seasonal sediment transport have occurred over a brief period of several days in July (e.g. Hardy et al., 1996; Braun et al. 2000b). Consequently, we suggest that sediment mass accumulation in Lower Murray Lake is dominantly influenced by July temperatures in the upper watershed which affect snowmelt, streamflow and sediment transport into the lake.

Because July air temperature at 600 m altitude at Alert showed the highest correlation with Lower Murray Lake mass accumulation, this relationship was used to calibrate the long-term record of MAR in terms of July temperature using the following equation:

$$\text{Temperature} = 8.49 + 1.95 \times \ln (\text{MAR}) \qquad \text{standard error} = \pm\ 1.04\ °C \qquad (1)$$

The temperature calibration does not change the major features of the mass accumulation record, but provides a quantitative estimate of the range of past temperature variations at Lower Murray Lake (Figure 3.9). The temperature reconstruction is plotted as anomalies relative to the 1001–2000 AD mean in order to account for differences in the absolute temperatures at Lower Murray Lake and the Alert calibration site. The 1001–2000 AD reference period, which is used in all subsequent figures and discussions, was chosen so that records of shorter duration could be compared to the Lower Murray Lake time series using a common interval as a reference for baseline conditions.

The temperature reconstruction suggests: (1) recent temperatures are ~2.6°C higher than minimum temperatures observed during the Little Ice Age, (2) maximum temperatures during the past 5,200 years exceeded modern values by ~0.6°C, (3) minimum temperatures observed approximately 2,900 varve years BC were ~3.5°C colder than recent conditions. The calibration period used to estimate these temperature changes is admittedly short and the distance between Lower Murray Lake and Alert adds additional uncertainty to the reconstruction that demands caution when interpreting the temperature calibration. Nonetheless, our confidence in the relationship between temperature and mass accumulation in Lower Murray Lake is enhanced by the similar relationships observed at Lakes Tuborg and C2 (Hardy et al., 1996; Braun et al., 2000b). The fact that MAR was significantly correlated to July temperatures at both Alert and Eureka suggests that sedimentation in Lower Murray Lake is responding to regional melt season temperatures. This allows us to compare the Lower Murray Lake time-series to independent proxy climate records and assess the veracity of inferred linkages between climate and sedimentation over long time scales.

As discussed previously, few high-quality paleoclimate reconstructions exist for the High Arctic. Therefore the sensitivity of Lower Murray Lake sedimentation to changes in temperature was evaluated by comparing the sedimentary sequence to records of climate forcing mechanisms known to contribute to changes in global temperatures (Figure 3.10; Crowley, 2000). Regional climate variations result from complex interactions among a variety of factors; nonetheless, changes in volcanic aerosols, solar output, and the concentration of greenhouse gases have a significant influence on temperature (Crowley 2000). Figure 3.10 indicates that periods of above average mass accumulation in Lower Murray Lake roughly coincide with periods of reduced volcanic activity, increased solar forcing, and increased greenhouse gas concentrations. In contrast, periods of below average mass accumulation generally coincide with periods of increased volcanic activity, reduced solar forcing, and reduced greenhouse gas concentrations. This relationship suggests that, over the last 1000 years decadal-scale variability in sedimentation in Lower Murray Lake is positively correlated with changes in regional temperatures that are driven by large-scale radiative forcing.

Over periods of several decades the relationship between temperature and sedimentation is likely strengthened by several factors specific to the Arctic. Przybylak (2002) demonstrated that, during the

instrumental period, increased temperatures coincided with higher precipitation totals in most regions of the Canadian Arctic. Warm periods in the past were therefore likely associated with elevated runoff resulting from a combination of increased precipitation throughout the year and enhanced melt production in the summer. In addition, warmer conditions should have increased sediment availability by increasing the depth of the active layer. Because sediment availability and runoff ultimately limit lake sedimentation, an increase in these variables due to warmer temperatures should have led to increased sediment accumulation in lakes. Indeed, a positive correlation between temperature and sedimentation rate has been observed in several other lakes in the Canadian Arctic (e.g. Hardy et al., 1996; Hughen et al., 2000; Moore et al., 2001).

Is there a consistent regional pattern?

Climatic controls on lake sedimentation were further examined by comparing Lower Murray Lake mass accumulation to other regional records of environmental change (Figure 3.11). Lake Tuborg is the nearest location from which another varve record has been produced (~110 km from Lower Murray Lake; Figure 3.11), and relative to Lower Murray Lake, likely reflects the most similar climatic setting of the available records. Similar patterns in each record, particularly relating to the timing of reduced sedimentation in each lake are evidence of an external (climatic) forcing mechanism. Process monitoring in the Lake Tuborg watershed by Braun et al. (2000b) demonstrated a relationship between summer temperature and sediment transfer to Lake Tuborg that is consistent with our interpretation of the climatic controls on Lower Murray Lake sedimentation. Although varve deposition in Lake Tuborg has been previously described by Smith et al. (2004), the Tuborg varve series shown here (Lewis et al., 2008) has not been independently dated past the last 150 years. In contrast, comparison of Lower Murray Lake mass accumulation with Lake C2 varve thickness (Lamoureux and Bradley, 1996) shows much less consistency. Lake C2 is located along the north coast of Ellesmere Island, adjacent to the Arctic Ocean and in a considerably different climatic setting. Thus differences in the two records may reflect either different local climatic conditions or the unique effects of site specific processes acting within the lakes and surrounding catchment. Lower Murray Lake mass accumulation, Lake Tuborg varve thickness, and Agassiz Ice Cap melt percentages (Fisher and Koerner, 1994; Fisher et al., 1995) all show a large increase in the twentieth century. Earlier peaks in Agassiz Ice Cap melt percentage frequently coincide with periods of elevated

sedimentation in Lower Murray Lake; however, the relative magnitude and timing of events is not always consistent. These discrepancies may reflect uncertainties in the chronology of both records, or differences in the way individual proxies respond to climate forcing. Anderson et al. (2008) identified two periods of widespread ice-cap expansion on northern Baffin Island around ~1280 and ~1450 AD (indicated by arrows in Figure 3.11a). These events coincide with episodes of reduced sediment accumulation in Lower Murray Lake and support the interpretation that cold periods in the past are associated with reduced sedimentation in Lower Murray Lake.

On longer time scales (Figure 3.11b) the period of extremely low sediment accumulation in Lower Murray Lake centered around 1800 AD is roughly consistent with the timing of lowest melt percentage and $\delta^{18}O$ values observed in the Agassiz Ice Cap (Koerner and Fisher 1990). Although $\delta^{18}O$ values in the Agassiz Ice Cap reflect the combined influence of changes in climate, ice-cap thickness, and wind scouring, low $\delta^{18}O$ values and melt percentages in the nineteenth century signify the culmination of the 'Little Ice Age' and likely reflect the coldest period of the last several thousand years in the High Arctic (Koerner and Fisher, 1990; Fisher et al., 1983). Thus, reduced sediment mass accumulation during this period is consistent with the inferred temperature control on lake sedimentation. Identifying the warmest periods in paleoclimate records from northern Ellesmere is less straightforward. $\delta^{18}O$ values and melt percentages in the Agassiz Ice Cap indicate that the warmest conditions were experienced in the early Holocene ~8000–10000 ^{14}C years BP, with temperatures generally decreasing until the end of the 'Little Ice Age' (Koerner and Fisher, 1990). In contrast, the earliest portion of the Lower Murray Lake record (~5200–4500 varve years) is characterized by extremely low rates of sedimentation. This difference may reflect regional climatic variability, the local influence of the waning Innuitian Ice Sheet at this time, or both. Indeed, Smith (2002) examined the abundance of diatoms in a series of lakes ~50 km from Murray Lake on the Hazen Plateau and identified evidence of a similarly delayed 'thermal maximum' ~4200–3000 ^{14}C years BP attributed to the effects of locally retreating glaciers. These differences illustrate the level of remaining uncertainty in the climatic history of the High Arctic and underscore the need for additional paleoclimate reconstructions so that local anomalies in individual proxy records can be separated from regional climatic trends.

Stability of the climate-sedimentation system

Quantitative reconstructions of past climatic conditions are strongly dependent on the data selection and calibration methods used (Esper et al., 2005). In the High Arctic, quantitative relationships between climate and varve characteristics have been based on either a few years of process monitoring or correlation of varve measurements with the instrumental record. The general assumption underlying the use of these models is that the relationships observed during the calibration period are stationary through time. In addition, previously published varve calibrations have largely relied on linear statistical models related to a single climate variable (e.g. Hardy et al., 1996; Hughen et al., 2000), whereas, the actual climate-varve process network as defined by Hodder et al., (2007) involves numerous variables which often interact in a non-linear fashion. Given these uncertainties, it is worth examining the long-term stability of the Lower Murray Lake system and its reliability as an archive of changing climatic conditions.

Blass et al., (2007) demonstrated that, in a glaciated alpine lake, a calibration model based on twentieth century observations was not valid for longer-term temperature reconstructions because of large-scale changes in the sediment transport system. Failure of the varve-climate calibration was coincident with distinct changes in mean sedimentation and in the amplitude of interannual variability (Blass et al., 2007). In contrast, several lines of evidence from the Lower Murray Lake record suggest that linkages within the climate-varve process network have remained relatively stable throughout the past several thousand years, including : (1) a reasonably consistent response to climate forcing mechanisms and similarities to other regional records during the last 1000+ years indicates that major processes linking the climatic conditions to lake sedimentation have been stable throughout this period; (2) mean sedimentation and the scale of variability in the long-term record of mass accumulation are nearly constant throughout the last 5000 years; (3) apart from the anomalous event deposits characterized by thick laminae and increased grain size and bulk density, median grain size is highly consistent throughout the period of record, suggesting that sediment transport has occurred under steady hydrodynamic conditions.

The apparent stability in the varve-climate process network at Lower Murray Lake has occurred despite considerable climate variability and substantial changes in the expanse of ice caps within the study area. Deglaciation of the Lower Murray Lake area occurred ~6900 ^{14}C years BP (England, 1983), with ice retreat continuing until margins close to or behind present conditions were reached by ~5000 ^{14}C years BP

(Smith, 1999). Plateau ice caps at favorable, high elevation locations likely persisted through the mid-Holocene (Smith, 1999), but may have subsequently disappeared and later reformed following the Holocene thermal maximum (Koerner and Paterson, 1974). Similarly, small plateau ice caps on northern Baffin Island are believed to have existed continuously since at least ~350 AD, and experienced significant expansion around 1280 AD and again around 1450 AD (Anderson et al., 2008).

Consistent controls on sedimentation in Lower Murray Lake are likely facilitated by several factors, including: the lake has a simple drainage basin that is characterized by short, high-gradient streams that lead to rapid transport of sediment from the catchment into the lake basin. Upper Murray Lake traps a significant portion of the sediment produced within the watershed and likely acts as a partial buffer to changes in Lower Murray Lake sedimentation. In addition, cold-based ice caps like those adjacent to Lower Murray Lake are minimally erosive (Paterson, 1969), and even at maximum extent covered less than ~10–15% of the Lower Murray Lake drainage basin. As a result, changes in ice expanse are not likely to have caused major changes in sediment production.

Conclusions

Lower Murray Lake varves contain an annual record of sediment mass accumulation spanning the past 5000+ years. In general, periods of elevated sediment accumulation coincide with periods of presumed warm conditions in the past. Likewise, suspected cold periods in the past are associated with low rates of sedimentation in Lower Murray Lake. Lower Murray Lake mass accumulation rates were positively correlated with mean July 600 m free air temperatures at the two nearest permanent weather stations at Alert and Eureka, with r^2 values of 0.61 and 0.50, respectively. Calibration of the MAR timeseries provided a quantitative estimate of the magnitude of past temperature variability. These results indicate that decadal-scale patterns of sedimentation in Lower Murray Lake are influenced by regional temperatures driven by radiative forcing. The lowest rates of sediment accumulation, and by inference the coldest periods occurred around varve year 1800 AD and prior to ~4200 varve years ago. In contrast, periods of increased sedimentation, and by inference the warmest conditions, occurred in the twelfth, fourteenth, and twentieth centuries, and throughout the middle portion of the record, approximately 1000 to 4200 varve years ago.

Lower Murray Lake sediments maintain a consistent pattern of deposition throughout the period of record and respond predictably to presumed climatic conditions in the past. Despite the complexity and inherent uncertainty in the varve-climate process network, the stability of the Lower Murray Lake sedimentary system supports the use of annual mass accumulation as a proxy indicator of climatic conditions in the past. Nonetheless, discrepancies between the Lower Murray Lake varve record and other regional paleoclimate records highlight the need to validate varve-based climate reconstructions using multiple lines of evidence from numerous locations. In the High Arctic, comparison of regional records is hindered by the limited number of high-quality paleoclimate reconstructions of any sort. Consequently, the acquisition of additional climate reconstructions from the High Arctic should be a priority.

Table 3.1 Ordered list of thin sections used to create the composite varve chronology from Lower Murray Lake. (Appendix 1 includes images of each of these thin sections including the marker beds used to tie the sequence between successive thin sections. Appendix 2 includes a list of all thin sections produced from Murray Lake sediments and a description of their corresponding depth interval.)

Sequence	Thin Section ID	Sequence	Thin Section ID
1	LML-001	30	LML-032
2	LML-080	31	LML-057
3	LML-002	32	LML-058
4	LML-010	33	LML-034
5	LML-003	34	LML-059
6	LML-083	35	LML-035
7	LML-084	36	LML-036
8	LML-004	37	LML-061
9	LML-005	38	LML-062
10	LML-006	39	LML-040
11	LML-007	40	LML-063
12	LML-008	41	LML-064
13	LML-009	42	LML-065
14	LML-093	43	LML-066
15	LML-094	44	LML-067
16	LML-095	45	LML-045
17	LML-024	46	LML-068
18	LML-096	47	LML-046
19	LML-097	48	LML-069
20	LML-098	49	LML-070
21	LML-099	50	LML-071
22	LML-100	51	LML-049
23	LML-101	52	LML-072
24	LML-029	53	LML-073
25	LML-102	54	LML-051
26	LML-030	55	LML-074
27	LML-055	56	LML-075
28	LML-031	57	LML-076
29	LML-056	58	LML-077

Table 3.2 Coefficient of determination (R2) values and their significance (p values) calculated for linear regressions between log-transformed Lower Murray Lake mass accumulation and assorted climatic data recorded at the Alert and Eureka weather stations.

Variable	Alert	Eureka
	r^2 (p value)	r^2 (p value)
June temp (°C)	0.02 (0.662)	0.01 (0.752)
July temp (°C)	0.15 (0.157)	0.06 (0.409)
August temp (°C)	0.23 (0.479)	0.13 (0.179)
Mean JJA temp (°C)	0.10 (0.240)	0.01 (0.767)
June 600 m temp (°C)	0.00 (0.992)	0.00 (0.961)
July 600 m temp (°C)	0.61 (<0.001)	0.50 (0.003)
August 600 m temp (°C)	0.02 (0.601)	0.02 (0.632)
Mean JJA 600 m temp (°C)	0.16 (0.136)	0.22 (0.080)
June rain (mm)	0.01 (0.732)	0.24 (0.023)
July rain (mm)	0.03 (0.582)	0.39 (0.017)
August rain (mm)	0.01 (0.732)	0.30 (0.041)
Total JJA rain (mm)	0.07 (0.446)	0.08 (0.323)
Total Sep-May snow (cm)	0.10 (0.102)	0.00 (0.479)
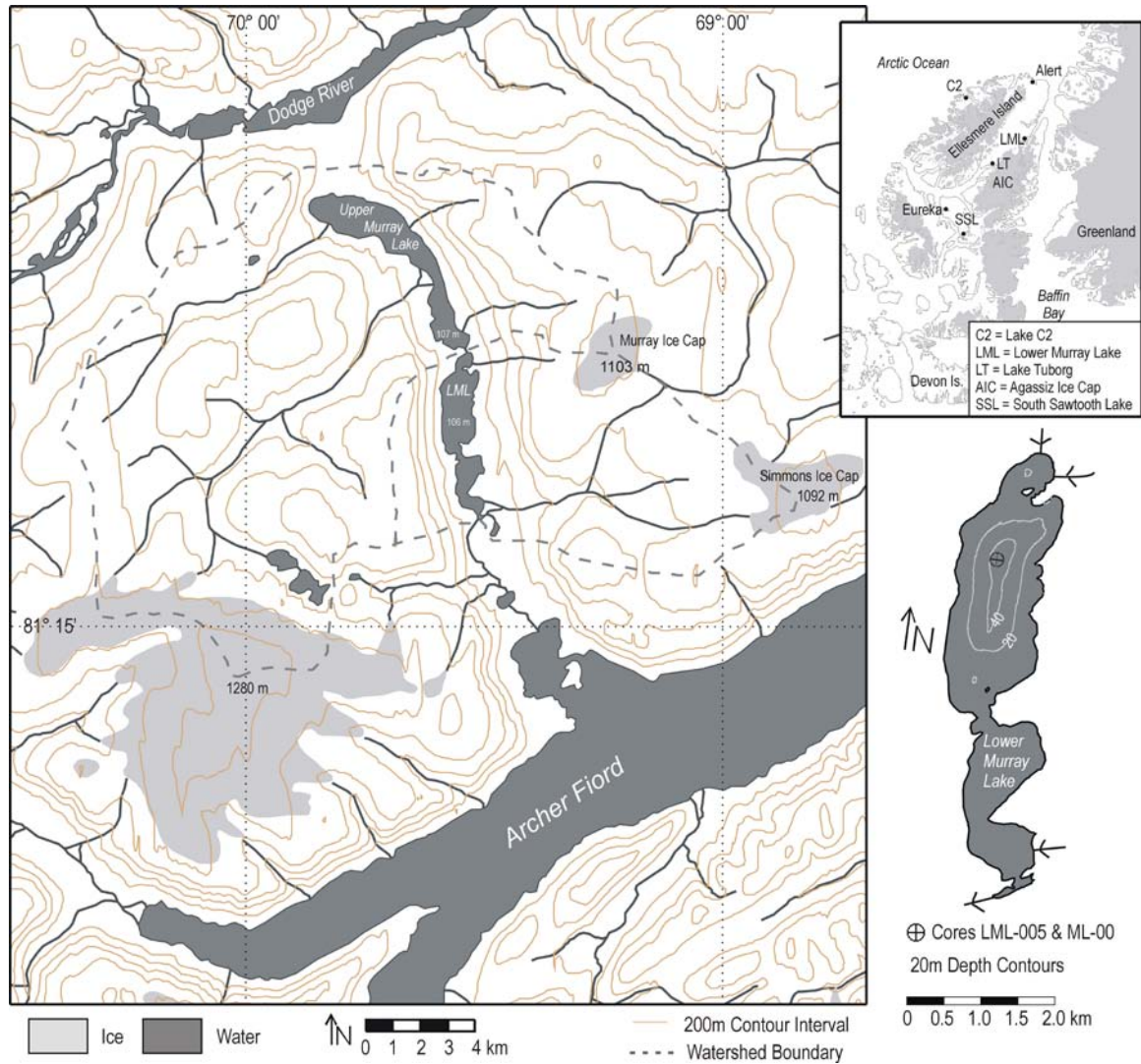
Figure 3.1 Map of Lower Murray Lake and surrounding region. The lower right panel shows a close up of Lower Murray Lake, including approximate bathymetry and the location of the coring site. Inset shows Ellesmere Island and surrounding region.
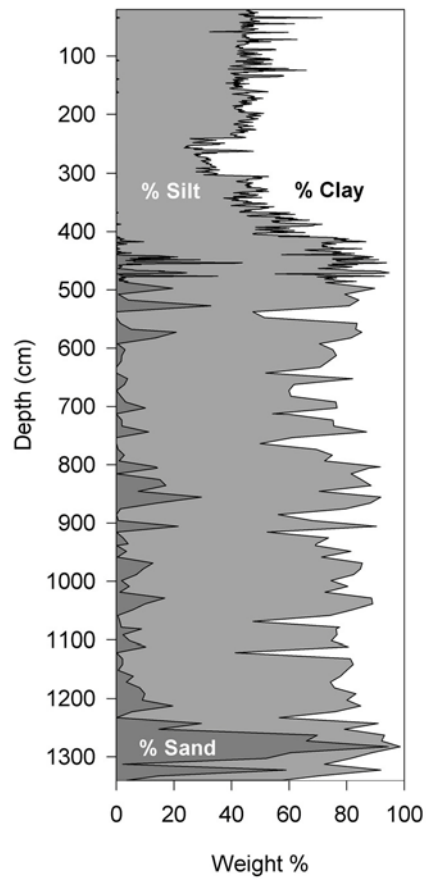
Figure 3.2 Down-core variations in grain size in Lower Murray Lake sediments. The distinct transition that occurs at ~245 cm depth marks the beginning of the laminated portion of the sequence.
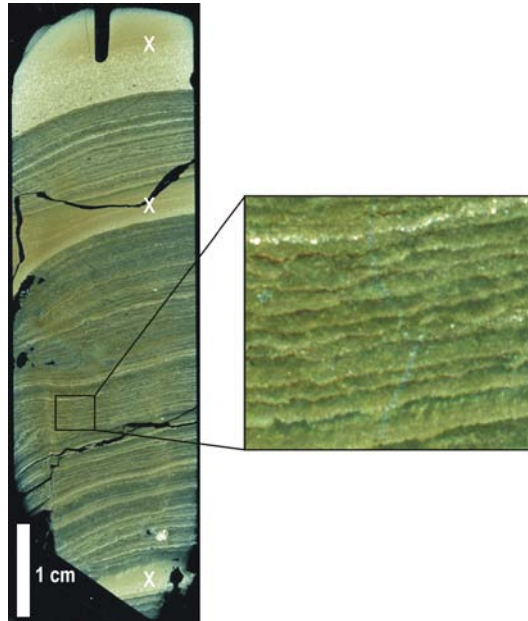
Figure 3.3 Scanned image of a thin section under cross-polarized light showing fine-scale laminations punctuated by coarse grained event deposits (marked X on thin section). Inset shows a sequence of fining-upwards silt and clay couplets that are characteristic of typical varves in Lower Murray Lake.
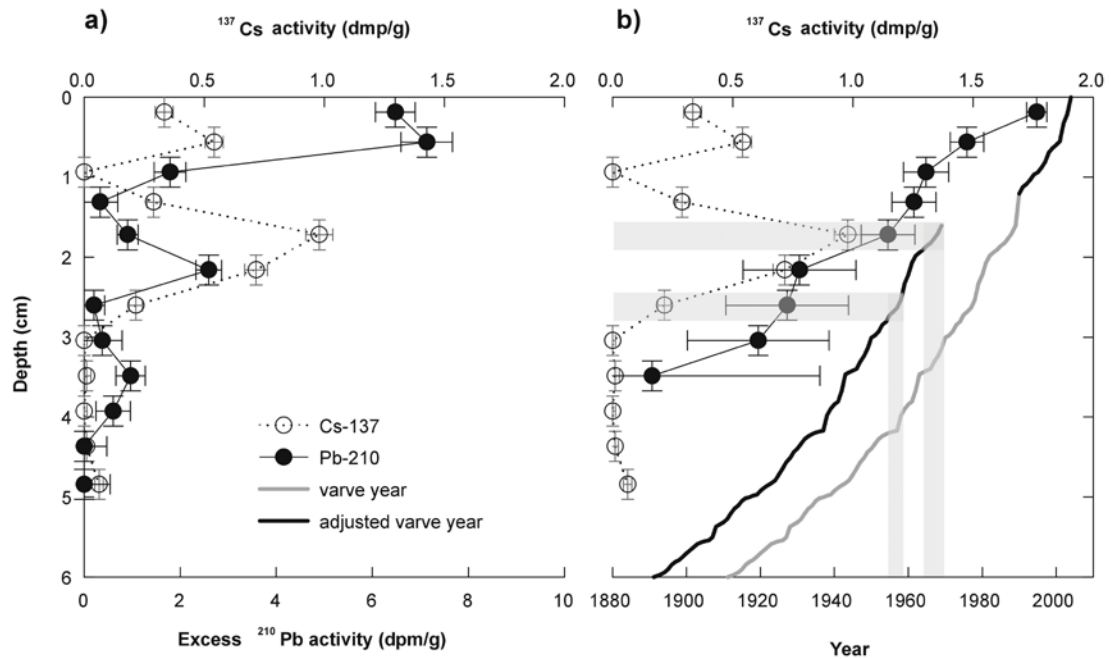
Figure 3.4 (a) ^{210}Pb and ^{137}Cs activity versus depth for core LML- 05-C1-E5. The ^{210}Pb minimum between ~1 and 1.5 cm depth suggests non-uniform deposition and is consistent with the depth of a turbidite observed in the sediment. (b) Comparison of the varve chronology with the ^{210}Pb age model (CRS model) and ^{137}Cs activity. Horizontal error bars are 1 σ uncertainties and vertical error bars represent the sampling interval. The gap in the varve chronology reflects suspected erosion resulting from a ca. 1990 turbidite, which likely contributes to the discrepancy between the varve and ^{210}Pb chronologies. Shaded regions indicate the first occurrence (~1954) and peak (1963) horizons of ^{137}Cs activity in the sediment, and their general agreement with the varve chronology.
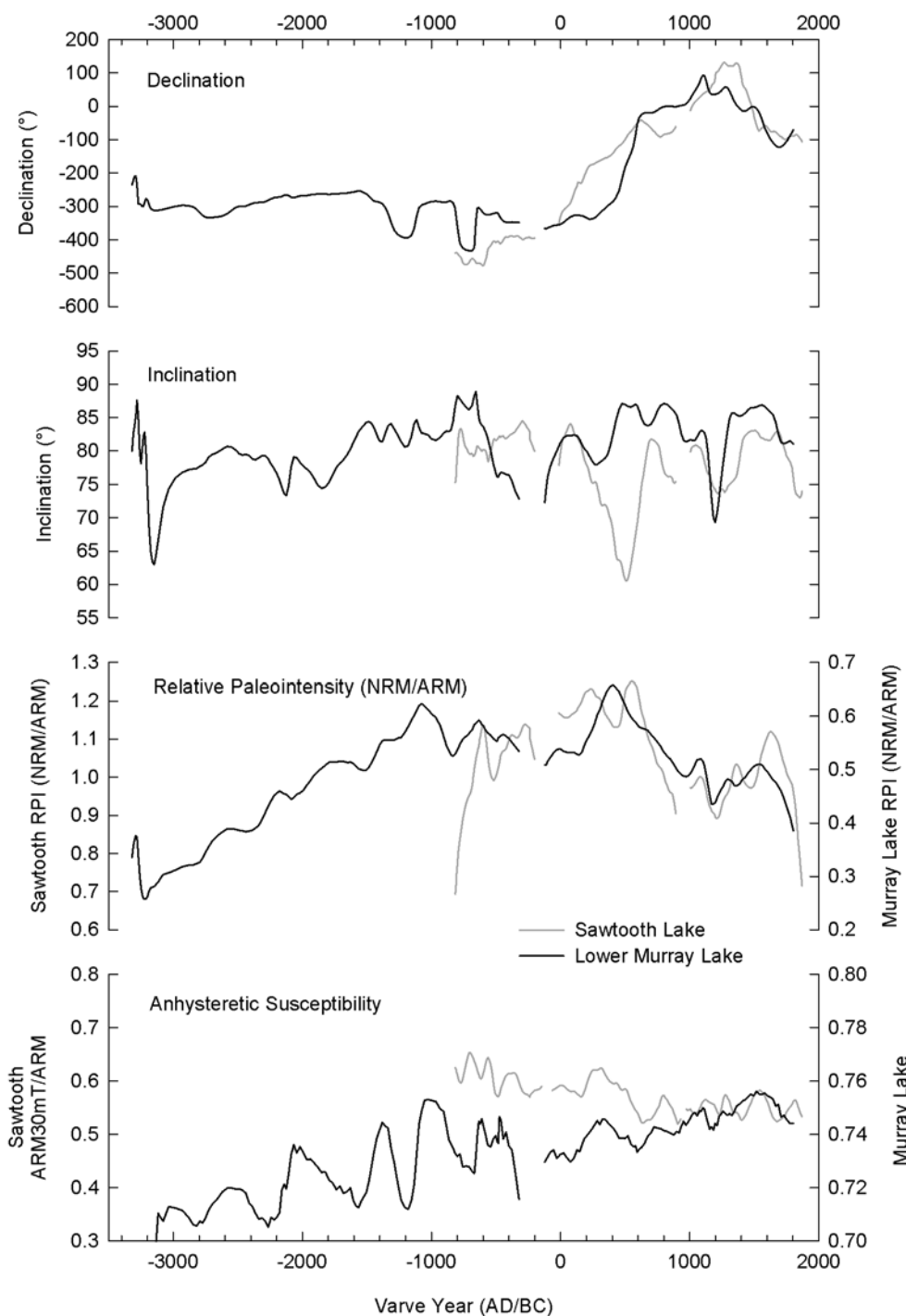
Figure 3.5 Comparison of paleomagnetic secular variation records in sediment cores from Lower Murray Lake and South Sawtooth Lake on their independently derived varve-based chronologies. From top to bottom, the records include: the characteristic remanent magnetization (ChRM) declination; ChRM inclination; relative paleointensity estimated using the mean of the natural remanent magnetization (NRM) intensity normalized by anhysteretic remanent magnetization (ARM) over a range of progressive alternating field demagnetization steps; the ratio of ARM after 30 mT demagnetization to the ARM before demagnetization. See Stoner and St-Onge (2007) for further explanation of these measurements. Due to the higher rate of sedimentation in Sawtooth Lake, those data have been smoothed with a 20 point running mean filter.
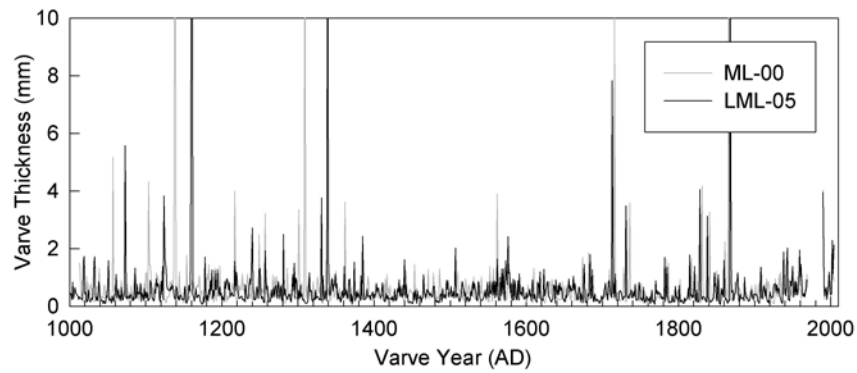
Figure 3.6 Comparison of the independently derived varve chronologies from cores collected in 2005 (LML-05; this study) and 2000 (ML-00; Besonen et al. 2008). Offset between the two records illustrates the uncertainty in varve delineation and reflects error in both the chronology and thickness measurements. Total offset after 1000 varve years is <20 years or 2%. Most of the offset can be isolated within a single portion of the record where laminae are particularly diffuse and difficult to distinguish. Adjusting one record to match the other is difficult to justify.
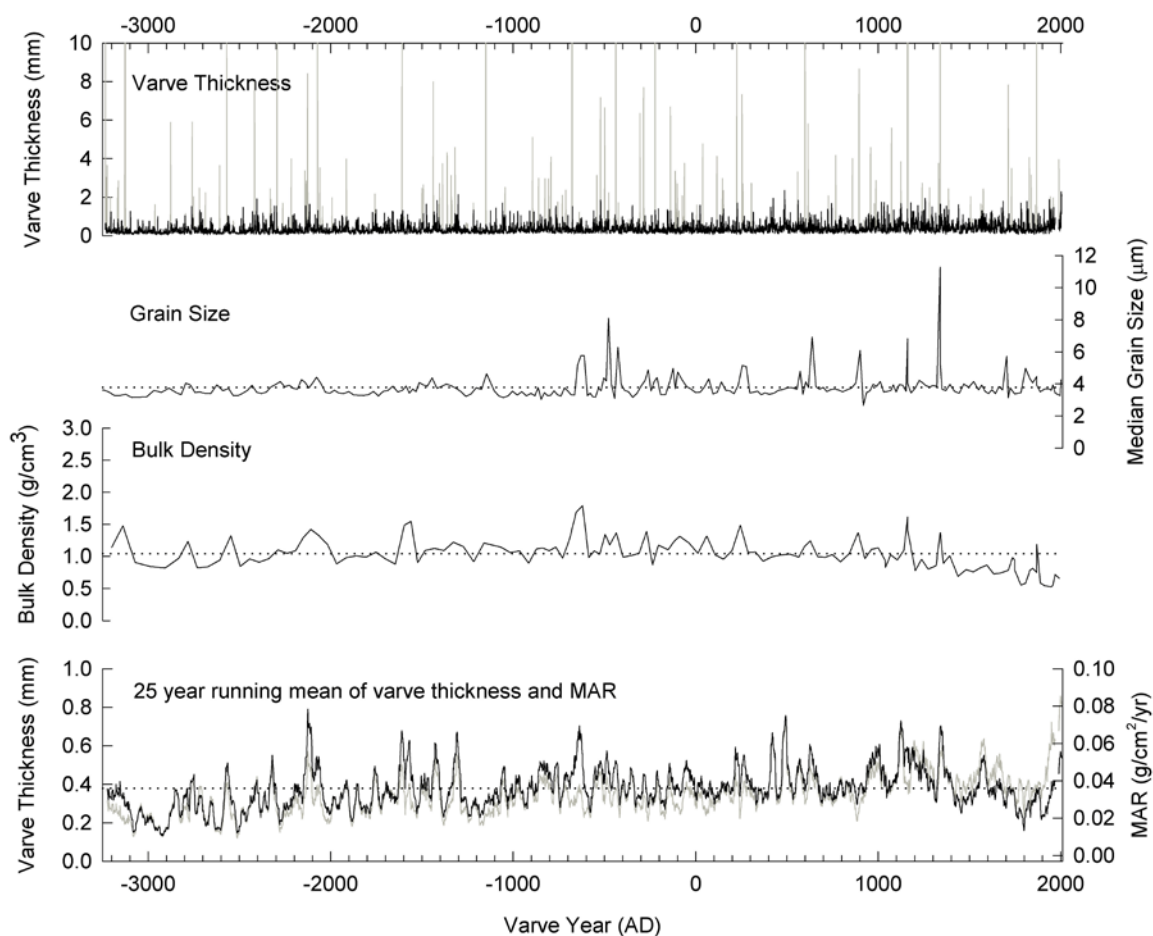
Figure 3.7 Sedimentological results from Lower Murray Lake. Time-series data are a combination of the least disturbed sections of multiple cores. Top panel shows raw varve thickness measurements (grey) and varve thickness after anomalous depositional units have been removed (black). Bottom panel shows varve thickness (grey) and mass accumulation (black) after the data have been smoothed with a 25 year running mean filter. Mass accumulation is calculated from the varve thickness and bulk density measurements. Dotted lines in each panel reflect the series mean value.
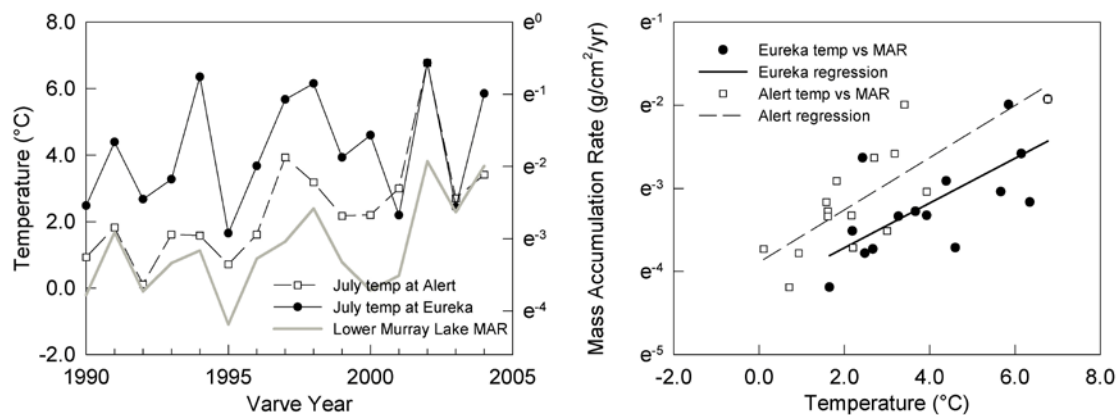
Figure 3.8 (a) Time-series of Lower Murray Lake mass accumulation and 600 m temperatures recorded by radiosondes at Alert and Eureka. (b) Scatter plot showing the relationship between Alert and Eureka 600 m temperatures and mass accumulation rates in Lower Murray Lake.
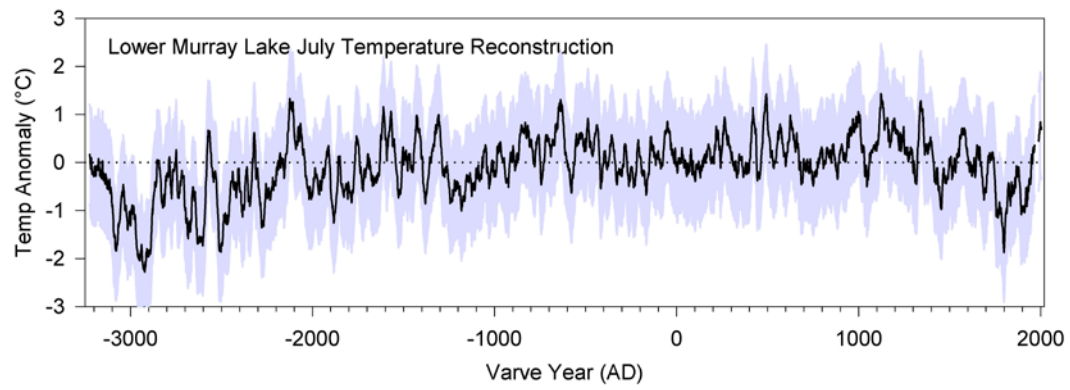
Figure 3.9 Lower Murray Lake temperature reconstruction based on the calibration between mass accumulation rate and July 600 m temperatures at Alert. 25 year running mean temperatures are plotted as anomalies relative to the 1001– 2000 AD mean. Shaded gray region reflects ±1.04°C standard error of the regression equation.
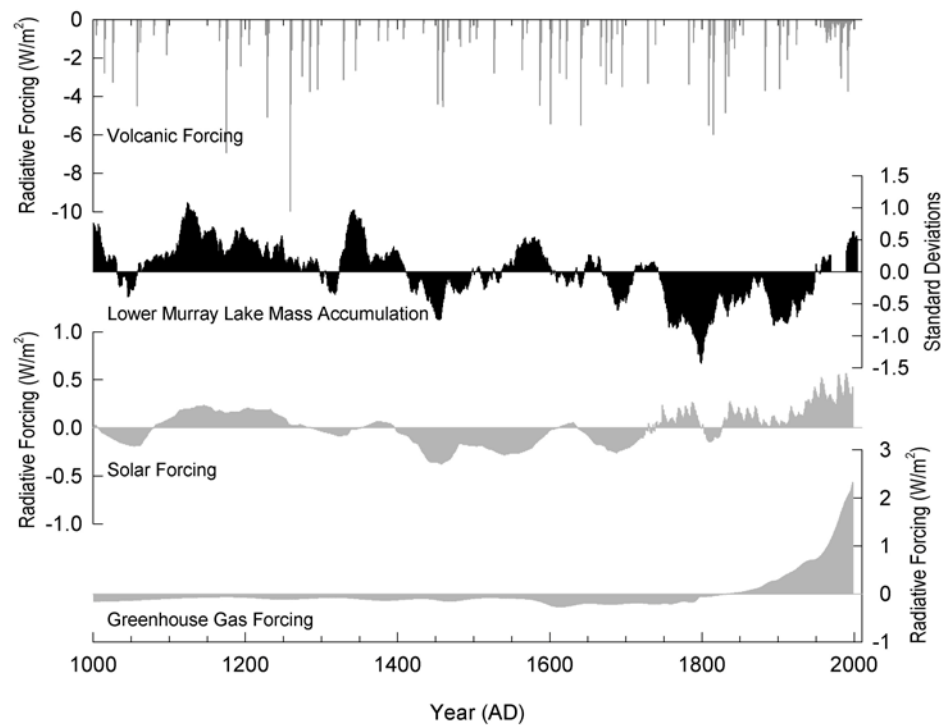
Figure 3.10 Lower Murray Lake mass accumulation over the past 1000 varve years (black) relative to external forcings of global temperatures (Crowley 2000): volcanic forcing (top panel), solar variability (third from top), and greenhouse gasses (bottom panel). Note the different scales for radiative forcing by the different variables. Lower Murray Lake mass accumulation, radiative forcing from greenhouse gasses, and solar variability are plotted relative to their 1001–2000 AD mean. Periods of increased mass accumulation in the twelfth to fourteenth centuries coincide with episodes of elevated solar activity and reduced volcanic activity, whereas reduced mass accumulation around 1450, 1700, and 1800 AD coincides with periods of enhanced volcanism and reduced solar activity. Increased mass accumulation in the twentieth century coincides with anthropogenic forcing of greenhouse gas concentrations.
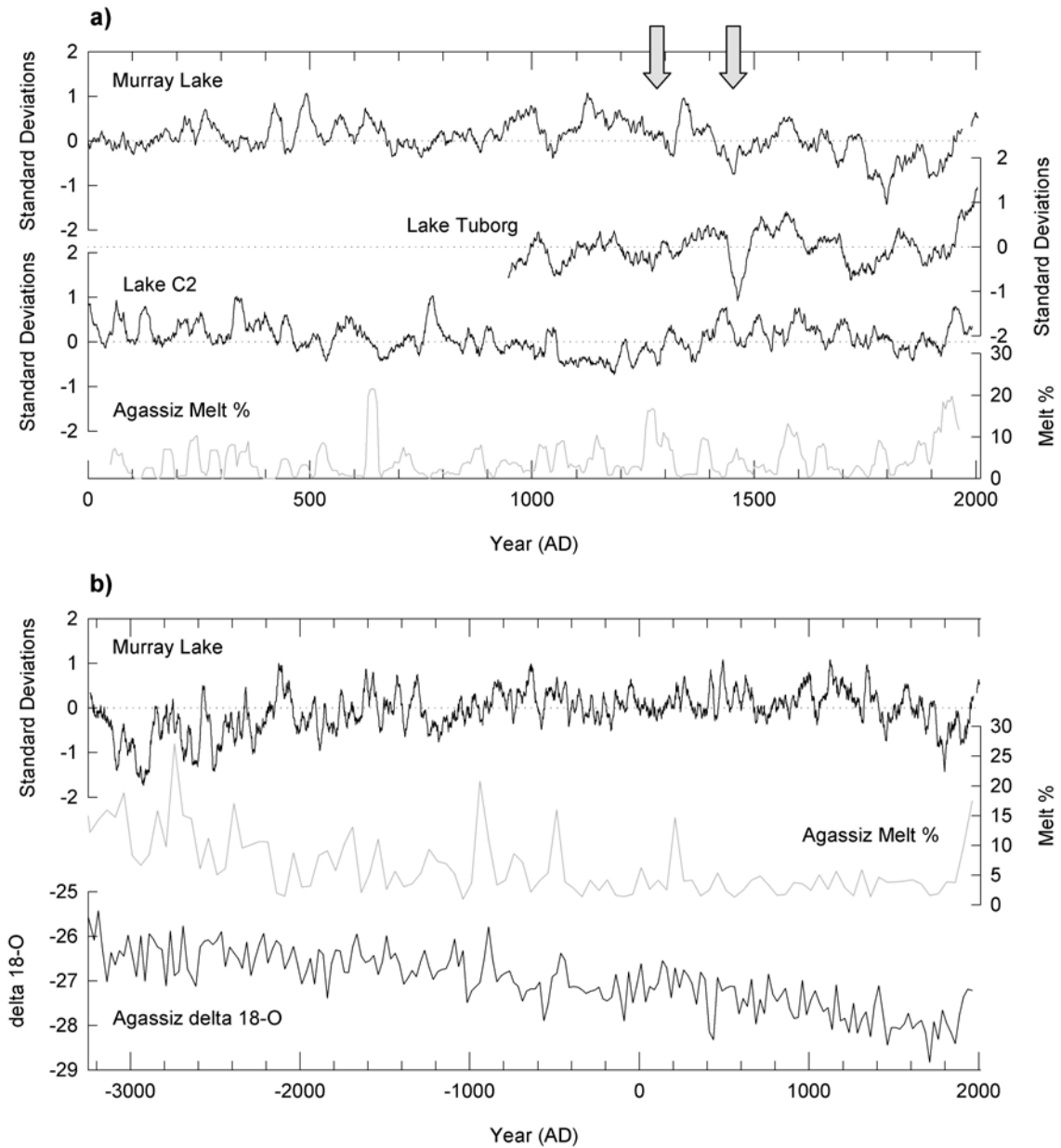
Figure 3.11 (a) Comparison of the last 2000 years of Lower Murray Lake mass accumulation with Lake Tuborg (T. Lewis, unpublished data) and Lake C2 (Lamoureux and Bradley 1996) varve thickness and Agassiz Ice Cap melt percentage (Fisher et al. 1995; Fisher and Koerner 1994). Running means (25 year) are plotted for each record; varve data are log transformed, normalized departures from 1000 to 2000 AD mean. Arrows indicate periods of widespread ice-cap expansion identified in northern Baffin Island ca. ~1280 and ~1450 AD (Anderson et al. 2008). (b) Long-term, 5,200 year record of Lower Murray Lake mass accumulation compared to Aggasiz Ice Cap melt percentage and d18O (Fisher et al. 1995; Fisher and Koerner 1994).

CHAPTER 4

RECENT ADVANCES AND LIMITATIONS IN QUANTITATIVE TEMPERATURE RECONSTRUCTIONS FROM THE CANADIAN ARCTIC

<u>**Introduction**</u>

Accurate predictions of future climate changes and their impacts on the environment require a thorough understanding of both the processes controlling modern climatic conditions and the causes and impacts of past climate variability. Instrumental data collected from networks of meteorological stations provide the basis for our understanding of climate variability on short time scales. In the Canadian Arctic the instrumental record is severely limited in terms of its spatial coverage and the length of the available records. All of the permanent weather stations in the Canadian Arctic are located in low elevation, coastal sites which may not accurately reflect the climatic conditions in inland, high-elevation locations that characterize much of the Canadian Arctic Archipelago. In addition, continuous instrumental records in the Canadian Arctic date predominantly to the late 1940s and early 1950s, with only limited data available as early as the 1920s. These data make it impossible to describe climate variations with periods greater than a few decades and provide only a limited view of the full range of climatic conditions which characterize the Canadian Arctic. Consequently, a longer perspective on climatic variability must be obtained by studying natural archives that have preserved some aspect of past environmental conditions. Such long-term proxy records of climate may be derived from a variety of sources based on the dependence of many physical, chemical, and biological processes on climatic conditions.

Substantial evidence from both observational data (e.g. Serreze et al., 2000) and proxy paleoclimate records (e.g. Overpeck et al., 1997) indicate that the Arctic has warmed considerably over the past few decades. This warming trend is manifested in observations of declining sea ice thickness and extent (Serreze et al., 2007), increases in the duration of ice free conditions on arctic lakes (e.g. Chapter 5; Mueller et al., *in review*), negative trends in the mass balance of small glaciers and ice caps (Dowdeswell et al., 1997; Serreze et al., 2000; Braun et al., 2004), the rapid demise of northern Ellesmere Island ice shelves (Mueller et al., 2003; Copland et al., 2007; England et al, 2008), and unprecedented regime shifts in the

biological communities of arctic lakes (Smol et al., 2005). Although the degree to which these recent changes can be attributed to human activity is uncertain, the continued accumulation of greenhouse gases in the atmosphere over the next century is expected to produce considerable warming in the future (Solomon et al., 2007).

Understanding the context of recent warming and accurately forecasting future temperature changes require long term records of climatic conditions from which the underlying causes of past temperature changes may be evaluated. Specifically, a large network of quantitative estimates of absolute temperature values in the past are needed to determine the sensitivity of the climate system to different forcing mechanisms, distinguish patterns of forced climate change from internal variability within the climate system, and to validate the output of climate models. The varve-based temperature reconstruction from Lower Murray Lake (as described in the previous chapter) was part of a collaborative initiative with the stated goal of addressing this need for additional high-resolution, quantitative temperature reconstructions from the Arctic, the ARCSS 2 kyr project, funded in 2005 by the Arctic System Sciences (ARCSS) Program of the US National Science Foundation. The objective of this chapter is therefore to evaluate advances and limitations in our ability to quantitatively reconstruct past temperature conditions in the Canadian Arctic and adjacent Greenland in light of recent studies. Specifically, this chapter includes a review of potential quantitative indicators of past temperature conditions that are applicable to arctic regions and in the process provides a brief summary of our current understanding of Holocene temperature variability in the region. The records discussed in this chapter are derived from a variety of sources and locations throughout the Canadian Arctic and Greenland as listed in Table 1 and illustrated in Figure 4.1.

Quantitative Indicators of Past Temperature

Ice cores

The ratio of $^{18}O/^{16}O$ isotopes in precipitation is largely dependent on the temperature at which it forms (Dansgaard, 1964). As temperature decreases the isotopic composition of precipitation is increasingly depleted of "heavy" isotopes of deuterium and ^{18}O. As a result, the accumulation of precipitation in the form of ice in polar ice caps provides an archive of past temperature conditions.

Validation of the relationship between temperature and isotopic composition in Greenland Ice cores (Jouzel et al., 1997) has allowed for the production of long-term, calibrated reconstructions of past temperature conditions over Greenland (e.g. Figure 4.2; Cuffey and Clow, 1997; Alley, 2000; Johnsen et al., 2001; Alley, 2004). In the Canadian Arctic, oxygen isotope records are available from ice cores through the Devon Island ice cap (Figure 4.2; Patterson et al., 1977), the Agassiz ice cap on Ellesmere Island (Figure 2; Koerner and Fisher, 1990), the Barnes (Hooke and Clausen, 1982) and Penny (Fisher et al, 1998) ice caps on Baffin Island, and the Meighen Island ice cap (Koerner et al., 1973). In addition, the Hans Tausen ice cap in northwest Greenland is relevant to the regional paleoclimate history (Figure 4.2; Clausen et al., 2001; Hammer et al., 2001).

Holocene oxygen isotope records from ice cores in the Canadian Arctic, indicate a general pattern of elevated $\delta^{18}O$ values during the early Holocene, minimum values between ~1650 and 1900 AD, and a 20th century increase. This pattern indicates that the warmest conditions of the Holocene likely occurred 8-10 kyrs BP and the coldest as recently as 150 years BP. Koerner and Fisher (1990) estimate a cooling of approximately 2.5°C from 9.5 kyrs BP to the present based on the observed 4 ‰ decrease in $\delta^{18}O$ in the Agassiz ice core. This value is comparable with a ~2.0°C cooling suggested by the trend in melt percentage of annual layers in the same core (Figure 2; Koerner and Fisher, 1990). In general, ice core records from the Canadian Arctic have provided considerable insight into past climatic and environmental conditions in the region. However, interpretation of $\delta^{18}O$ values in ice cores of the Canadian Arctic strictly in terms of past temperature variability is non-trivial. A number of factors, other than temperature changes, can alter $\delta^{18}O$ values. These include changes in the $\delta^{18}O$ of source precipitation due to changes in atmospheric circulation (Charles et al., 1994); changes in the seasonality of precipitation (Steig et al., 1994); partial melting and or ablation of annual layers during warm intervals (Koerner et al., 1973); changes in the surface elevation of the ice cap over time (Paterson et al., 1977); and the effects of wind scouring and redeposition of snow (Fisher et al., 1983). Consequently continuous, calibrated temperature records have not been derived from ice cores in the Canadian Arctic.

Boreholes

Temperature conditions at Earth's surface propagate slowly downward into ice sheets or rocks beneath the surface and modify the subsurface thermal regime. Consequently, the present day subsurface thermal profile provides evidence of temperature changes that have occurred at the surface in the past (e.g. Dahl-Jensen et al., 1998; Pollack et al., 1998). An advantage of borehole temperatures reconstructions relative to other proxy indicators, such as tree rings, ice cores, faunal assemblages, is that they rely on direct measurements of temperature and thus do not require calibration against independent surface temperature data (Mann et al., 2003). Majorowicz et al. (2004) evaluated temperature logs from 61 boreholes located between 60° and 82°N in northern Canada and produced a temperature reconstruction spanning the past 500 years that indicates minimum temperatures occurred around 1800 AD and were followed by a subsequent warming of approximately 2°C. Dahl-Jensen et al. 1998 produced a temperature reconstruction spanning the past 100,000 years from boreholes through the Greenland ice sheet (Figure 4.2). Reconstructed temperatures during the Holocene indicate maximum temperatures 4 to 8 kyrs BP that are approximately 1.0 to 1.5°C warmer than present. Neoglacial cooling was interrupted by a significant (+1°C temperature increase lasting ~400 years) warm interval centered around 900 AD and another shorter warm interval around 1700 AD. Minimum "Little Ice Age" temperatures occurred around 1850 AD and were ~1.0 to 1.5°C cooler than present (Dahl-Jensen et al., 1998). These borehole records provide important constraints on the magnitude and timing of past temperature changes and they are particularly sensitive to long term trends. However, they are limited in their ability to detect temperature changes that occur over short time periods and their temporal resolution is reduced further back in time (Pollack et al., 1998).

Changes in Ice Extent

Large scale changes in the spatial extent of glaciers, ice caps, and ice sheets offer an additional indicator of climatic variability. In the Canadian Arctic a number of studies have addressed the impacts of recent warming on the behavior of terrestrial ice masses (e.g. Dowdeswell *et al.*, 1997; Burgess and Sharp, 2004; Braun *et al.*, 2004; Burgess *et al.*, 2005; Mair *et al.*, 2005; Shepherd *et al.*, 2007). Determination of the past configuration of ice masses can provide important information regarding corresponding climatic

conditions. The maximum extent of Neoglacial ice in the Canadian Arctic (post 4.5 kyrs BP) is widely

regarded to have occurred during the Little Ice Age (LIA; ~AD 1250-1900; England, 1977; Blake, 1981;

Bradley, 1990; Grove, 2001; Miller et al., 2005). The culmination of the LIA is considered the coldest

interval of the Holocene (Bradley, 1990; Koerner and Fisher 1990) and as such provides an important

benchmark against which recent warming can be evaluated. Wolken (2005) validated the interpretation of

lichen free zones around ice caps as an indication of snow and ice expansion during the LIA. Use of remote

sensing techniques (Wolken, 2006) allowed the large scale reconstruction of past ice extent and

equilibrium-line altitudes (ELAs) throughout the Queen Elizabeth Islands (Wolken et al., 2008a).

Comparison of modern (ca. 1960) ELAs with reconstructed LIA ELAs allowed Wolken et al. (2008b) to

determine regional-scale spatial variations in surface temperature trends between the LIA and 1960.

Resulting mean temperature change for the Queen Elizabeth Islands was +1.1°C, and ranged from <0.5°C

along northwestern Axel Heiberg and Ellesmere Islands and western Melville Island, to >2.9°C in localized

areas of Devon and Ellesmere Islands. Some degree of change in ELAs may be attributed to changes in

precipitation and changes in ice-extent provide only a snapshot of temperature conditions during a single

interval in the past. Nonetheless, the regional-scale spatial variations determined through this type of

analysis provide important insight into synoptic scale patterns of atmospheric circulation and their

influence on climate variability.

Dendroclimatology

Dendroclimatology studies have produced extensive records of past climatic conditions,

particularly near the northern treeline where tree growth is effectively limited by temperature (e.g. Briffa et

al., 1994). North of the treeline however, the application of dendroclimatology is limited by the scarcity of

vegetation. Nonetheless, exploratory studies on Ellesmere Island have demonstrated the potential for

dendroclimatology studies in the Arctic. Woodcock and Bradley (1994) analyzed ring widths of the arctic

ground willow *Salix arctica* and although the time-series spanned only a few decades, the study

demonstrated the potential to extend the climate record into the past if suitable fossil wood could be found.

Rayback and Henry used retrospective analysis of the widespread evergreen dwarf-shrub, *Cassiope*

tetragona, to reconstruct average summer air temperatures for Alexandra Fiord, Ellesmere Island from

1895 through 1994. Their reconstruction accounted for 45% of the variance in the instrumental record and revealed an increase in summer temperature from ~1905 to the early 1960s, a cooling trend from the mid-1960 to the 1970s, and an increase in temperature after 1980. Although dendroclimatology studies in the Canadian Arctic are unlikely to extend the record of past temperatures beyond the culmination of the LIA, an annual temperature record extending through the 20th century is double the length of the instrumental record in most arctic locations and provides a valuable data set for calibration of other proxy records.

Lake sediments

Studies of lake sediments have a long history in paleo-environmental analysis (Cohen, 2003) and are particularly relevant in arctic regions because of the common and widespread occurrence of lakes in glaciated landscapes (Wolfe and Smith, 2004). Considerable progress has occurred in the development of quantitative paleotemperature indicators based on biological, chemical, and physical characteristics of lake sediments. Andrews et al. (1981) applied a transfer function to polled assemblages from 9 peat and lake sediment sequences from northern Canada and Baffin Island and estimated an approximately 2 to 3°C cooling in July temperatures between 6 kyrs BP and present (Figure 4.3). Kerwin et al. (2004) reconstructed July temperatures from 7 lakes on Baffin Island, most of which showed maximum Holocene warmth 4 to 6 kyrs BP which was ~1 to 2°C above modern (1951-1980) temperatures (Figure 4.3). Peros and Gajewksi (2008) used pollen assemblages to reconstruct July temperatures on western Victoria Island. Their data indicate that July temperatures were approximately 4.0°C 10.2 kyrs BP, rose by approximately 2°C between ~8.7 and 9.7 kyrs BP and then gradually decreased to ~4.5°C during the Little Ice Age, before warming almost 1.0°C during the last 100 years (Figure 4.3). These examples, as well as shorter duration reconstructions (e.g. Peros and Gajewski, 2009; Figure 4.3), demonstrate the utility of pollen data for quantifying past temperature conditions. However, it should be noted that the limited supply of pollen to arctic lakes and the delayed response of terrestrial vegetation to climate fluctuations limits the ability of pollen resolve short period climate variations.

Organisms with shorter lifecycles respond more rapidly to climate variations and thus considerable effort has focused on reconstructing temperatures based on variations in the assemblages of diatoms and midges (chironomidae) preserved in lake sediments (Battarbee, 2000). Joynt and Wolfe (2001)

analyzed surface sediment samples from 61 lakes across Baffin Island to develop a model linking diatom

assemblage to surface water temperature. Applied to Fog Lake on eastern Baffin Island the model indicates

~4.0°C range in summer water temperatures since 5 kyrs BP (Figure 4.4; Joynt and Wolfe, 2001).

Minimum temperatures occured ca. 1400 AD, followed by warm intervals centered around 1100 AD and

400 AD and then increased by ~2.0°C in the past 150 years (Joynt and Wolfe, 2001). Francis et al. (2006)

produced a midge-inferred summer temperature reconstruction extending into the previous interglacial

from Fog and Brother of Fog Lakes on Baffin Island. The two records indicate that summer temperatures

during the last interglacial were higher than at any time in the Holocene, and 5 to 10°C higher than present.

The warmest conditions in the Holocene occurred in the first half of the period and have decreased since

about the mid-Holocene. Additional midge studies from Baffin Island have provided further insight into

Holocene temperature variability. Chironomid-inferred July air temperatures from Lakes CF8 and CF3

record peak Holocene temperatures 8 to 10 kyrs BP that are 5°C higher than present (Figure 4.4; Briner et

al., 2006; Axford et al., 2009). This early Holocene warm interval is interrupted by abrupt cold intervals (3-

4°C temperature reduction) centered around 8.6 and 9.2 kyrs BP (Axford et al., 2009). Analyses of recent

chironomid trends in Lake CF8 indicate ~2.0°C increase in summer water temperatures over the past 100

years (Figure 4.4; Thomas et al., 2007). The success of the these studies and the widespread distribution of

midges throughout the Arctic, in addition to their ability to rapidly colonize water bodies, suggests that

chironomids may prove to be one of the more widely applicable temperature proxies in the Arctic.

As discussed previously in regards to ice cores, the $\delta^{18}O$ of precipitation is highly correlated to

mean annual air temperatures (Dansgaard, 1964). In suitable lakes with short residence times the $\delta^{18}O$ of

lake water is controlled by the $\delta^{18}O$ of precipitation and influenced by the temperature at which the

precipitation forms. Consequently, sedimentary records of lakewater $\delta^{18}O$ provide a means for

reconstructing past temperatures. Lakewater $\delta^{18}O$ in Arctic lakes has been inferred from the $\delta^{18}O$ of

authigenic calcite (e.g. Anderson et al., 2001), aquatic cellulose (e.g. Wolfe et al., 2001), diatoms (e.g.

Schiff et al., 2009), and chironomids head capsules (e.g. Wooller et al., 2004). Preliminary work by

Wooller et al. (2004) demonstrated the potential for quantitative reconstructions of mean annual air

temperature from chironomid head capsules in two arctic lakes, but additional work is needed to produce a

continuous paleotemperature record that spans the Holocene. Nonetheless, further pursuit of this proxy is warranted.

In the marine environment, the U^{K}_{37} index of long-chain alkenones has proven a reliable indicator of sea surface temperatures (Brassell et al., 1986; Prahl and Wakeman, 1987; Muller et al., 1998). Recent work in Greenland lakes has illustrated the potential for the use of lacustrine alkenones as a paleotemperature proxy in arctic lakes (D'Andrea and Huang, 2005; D'Andrea 2009). D'Andrea (2009) reconstructed surface water temperatures for the past 6000 years in two lakes in southwestern Greenland (Figure 4.4). The millennial scale trend and some centennial scale variability in D'Andrea's (2009) alkenone record is consistent with temperature estimates from a Greenland ice core (Cuffey and Clow, 1997; Alley, 2000) and a qualitative record of past temperatures based on loss-on-ignition in another nearby Greenland lake (Willemse and Tornqvist, 1999). Alkenone peleothermometry offers considerable potential to provide further quantitative estimates of past temperatures around the Arctic and work is currently ongoing to explore alkenone variability in the cores collected from Lower Murray Lake as part of this study.

Due to their widespread occurrence and the potential for high temporal resolution, annually laminated (varved) lake sediments are increasingly being utilized as an important source of paleoclimatic information in the High Arctic. Climate reconstructions from laminated lake sediments are based on the relationship between the characteristics of an individual lamination, such as thickness or grain size, and some aspect of the weather during the corresponding year. Considerable effort has focused on correlating varve characteristics with instrumental climate records (Hughen et al., 2000; Moore et al., 2001; Francus et al., 2002; Hambley and Lamoureux, 2006) and monitoring the meteorological and hydrological processes controlling sediment transfer and deposition in arctic lakes (e.g. Hardy 1996; Hardy et al., 1996; Cockburn and Lamoureux 2007; 2008). Although these studies have highlighted the complexity of the climate-sedimentation system, they have also illustrated that on a site-specific basis varve records may provide quantitative estimates of past summer temperature variability (Lamoureux and Bradley, 1996; Hughen et al., 2000; Moore et al., 2001; Smith et al., 2004; Cook et al., 2009; Thomas and Briner, 2009). Because varve records provide annual resolution they offer the potential to identify short period climate fluctuations not recorded by other proxies and in particular, to determine the range of interval variability within the

climate system. However, comparison of the available varve based temperature reconstructions (Figure 4.5) illustrates a high degree of variability of among the individual records and it is difficult to identify consistent patterns or trends in the records.

Limitations In our Current Understanding of Past Temperatures

Comparison of the available quantitative temperature reconstructions from the Canadian Arctic illustrates considerable differences among both those records using similar proxy indicators and those based on different proxies (Figures 4.2 through 4.5). However, some consistent patterns do emerge and these patterns are considerably strengthened when combined with the more numerous qualitative records of past temperature variability in the arctic (cf. Bradley, 1990; Gajewski and Atkinson, 2003; Wolfe and Smith, 2004; Smol et al., 2005). Consistent features include: warm conditions in the early Holocene (and in general the warmest conditions of the entire period), a period of Neoglacial cooling paralleling the decrease in summer insolation at high latitudes (Figure 4.2), several significant warm intervals within the past 2000 years, and minimum temperatures between 100 and 200 years BP that are followed by considerable warming in the past century. However, the amplitude and timing of these events varies significantly among the individual records. Estimates of the range of post LIA warming range from approximately 1 to 3°C. Similarly, estimates of the Holocene cooling trend also range from approximately 1 to 3°C. Although it is seemingly impressive to be able to identify temperatures variations 10,000 years in the past that were on the order of 1 to 3°C the discrepancies in the amplitude of past changes are in the order of the total variability estimated over Holocene. On their own, such poor quantitative constraints on past temperatures provide little guidance for efforts to model future temperature trends.

Past temperature changes should not be expected to be entirely consistent over an area as vast as the Canadian Arctic and the wide spatial distribution of the available proxy temperature reconstructions (Figure 5.1) is likely responsible for some of the discrepancies among the records. This is especially true for the Holocene period in the Canadian Arctic where the gradual retreat of the Innuitian ice sheet would have had a significant effect on regional atmospheric circulation, ocean currents and sea ice as deglaciation and isostatic uplift influenced the surface albedo, topography, and bathymetry of the region. Consequently,

the role of local landscape evolution, particularly during the early Holocene, may have impacted regional climatic conditions on the same order as external forcing mechanism related to radiative forcing.

The instrumental climate record also provides considerable insight into possible spatial patterns of temperature variability. Between 1966 and 1995 trends in mean annual temperature were positive in the northern and western sectors of the Canadian Arctic and negative in the southeastern region (Serreze et al., 2000). Satellite observations of regional temperature conditions on an annual basis indicate that positive temperature anomalies can occur simultaneously with negative temperature anomalies in different regions of the Canadian Arctic (Comiso, 2003). Correlation coefficients determined between instrumental temperature records from the Canadian Arctic and western Greenland as well as a principle component based index of the North Atlantic Oscillation (NAO; Hurrell et al., 2003) indicate two distinct regions of temperature response to changes in synoptic scale circulation (Table 4.2). Correlation coefficients were determined for mean summer (June-August) conditions because most of the proxy indicators discussed in this chapter are sensitive only to summer temperature conditions. The results indicate a "seesaw" pattern in the temperature conditions in the western portion of the Canadian Arctic relative to the northern and easternmost regions. Specifically, the positive phase of the NAO translates into cooler conditions in the northern and eastern regions of the Canadian Arctic and warmer conditions in the southern and western regions. The positive phase of the NAO is characterized and a strengthened Icelandic low which brings cold polar air across the northern and eastern portion of the Canadian Arctic (Hurrell, et al., 2003). Consequently, past changes in the dominant mode of atmospheric circulation are likely to have produced significant regional differences in the pattern of temperature variability recorded in proxy records.

An important consideration when evaluating proxy temperature reconstructions is to understand the nature of the proxy indicator's response to climatic forcing. For example, variations of $\delta^{18}O$ in ice cores reflect changes in temperature at the time the precipitation forms, with mean values of $\delta^{18}O$ in annual snow deposits reflecting mean annual temperatures (Jouzel et al., 1997). In contrast, changes in faunal assemblages of diatoms and chironomids reflect summer conditions (e.g. Francis et al., 2006), when the organisms are actively growing and reproducing. Similarly, the temperature signal in varve records is sensitive to conditions during the melt season when sediment is actually delivered to the lakes (Hardy, 1996; Hardy et al., 1996; Cook et al., 2009; Thomas et al., 2009). Given that recent surface temperature

trends in the Arctic vary widely according to seasons (e.g. Serreze et al., 2000), past temperature reconstructions based on proxy indicators sensitive to different seasons should not be expected to show similar patterns in the amplitude or even the sign of the temperature change. In addition, orbital conditions in the early Holocene produced greater seasonality than at present (Berger and Loutre, 1991), thus the amplitude of reconstructed temperature changes will differ according to the seasonal sensitivity of the individual proxies.

Even individual proxies that are sensitive to conditions during the same season may respond differently to similar temperature changes. Although melt percentages measured in ice cores are not a quantitative paleothermometer, they provide a useful example of the limitations of proxy temperature indicators. The maximum scale of variance in melt percentage measurements ranges from 0 to 100%. If temperatures remain below freezing for many years, no amount of annual temperature variability will be recorded by melt percentage measurements. Similarly, once temperatures are warm enough to melt 100% of the annual snow accumulation each year (resulting in net ablation) no additional temperature variability will be recorded. The quantitative temperature proxies discussed in this chapter each have their own analogous limitations. For example, the maximum response of annual sediment accumulation recorded in varves may be limited by sediment availability. If a watershed is starved for sediment, further melting and runoff will deliver no additional sediment to the lake and the amplitude of the warmest intervals may be underestimated by varve measurements. Additionally, little or no sediment may be delivered to the lakes during cold years in which temperatures remain below fresezing. Proxies that are sensitive to water temperature (e.g. diatoms and chironomids) may also be expected to have reduced sensitivity to cold conditions. For example the minimum optimum water temperature for an individual midge taxon in the transfer function developed by Francis et al. (2006) was 5.4°C, whereas, temperatures in many arctic presently remain below 4°C throughout the year. Thus, past climatic conditions significantly colder than modern conditions are potentially beyond the range of available transfer functions.

The Holocene period in the Canadian arctic is marked not only by significant climate variability, but also by profound landscape changes as the Innuitian ice sheet retreated in response to climatic conditions. The lakes and biological communities targeted as indicators of past temperature variability evolved following their emergence from beneath the Innuitian ice sheet. The sensitivity and response of

these systems to climatic changes during the early stages of their evolution likely differs from their response as more mature systems. For example, lakes on the Hazen Plateau of north-central Ellesmere Island were deglaciated ca. 8.5 kyrs BP, but diatom populations did not become established until ca. 5.5 kyr BP (Smith, 2002). Thus, these lakes show no paleolimnological response to warm early Holocene conditions as recorded elsewhere in the region.

A considerable portion of the temporal differences in the pattern of past temperature changes in different records, and especially the time transgressive nature of the Holocene thermal maximum observed in the early part of most records (Kaufman et al., 2004), is likely a result of the gradual evolution of the arctic landscape in response to deglaciation. Nonetheless, it is important to consider chronological uncertainties inherent in paleoclimate reconstructions. The Agassiz ice core record has now been synchronized to the Greenland GICC05 timescale linking it to the NGRIP, GRIP, GISP2, DYE-3 and Renland chronologies (Vinther et al., 2008). Thus, regional climatic differences recorded in the Agassiz and Greenland ice cores can be readily identified. In contrast, each of the paleolimnological records described in this chapter relies on an individual chronology with inherent uncertainties in its absolute age.

Dating of arctic lake sediments using traditional methods is often problematic. In many arctic watersheds, terrestrial organic matter apparently resides on land for long periods of time before being transported into lakes, producing anomalously old radiocarbon dates from organic material recovered from lake sediments (Abbott and Stafford, 1996; Zolitschka, 1996; Wolfe et al., 2004; Oswald et al., 2005; Besonen et al., 2008). In additional the low productivity within arctic lakes and in the surrounding landscape often limits the availability of suitable organic material for successful radiocarbon dating (e.g. Lamoureux and Bradley, 1996; Cook et al., 2009). Consequently, large inferences are often required to estimate the age of sedimentary deposits between known age horizons, leading to difficulties in the correlation of regionally significant climate events between individual records (cf. Axford et al., 2009).

Low productivity in arctic lakes results in very low accumulation rates in non-glaciated lakes (Wolfe and Smith, 2004), the most important consequence of which is low temporal resolution of paleolimnological reconstructions due to the sample sizes necessary for analyzing fossil pollen, chrionomids and diatoms, or conducting analyses requiring significant pretreatment (e.g. isotopes in diatom extracts). Bioturbation of lake sediments further limits the resolution of paleolimnological reconstructions

and mutes the response to short period events (Cohen, 2003). Although varved sediments offer the potential for extremely precise age control, varve chronologies are often difficult to verify because lakes conducive to varve accumulation are often limited in organic matter deposition (e.g. Lamoureux and Bradley, 1996; Lewis et al., 2008; Cook et al., 2009). Recent efforts using paleomagnetic secular variations to correlate between individual varve chronologies shows considerable promise (Besonen et al., 2008; Cook et al., 2009) and as more independently dated records become available it should be possible to create a regional paleomagnetic data set that can be used to date new records. The high precision provided by varve records means that small errors in chronology will have a significant impact on the correlation of climatic events between individual records. This factor alone could be responsible for the apparent out of phase behavior among some of the varve records shown in Figure 4.5. Because it is possible to retrieve more accurate regional climate signals by stacking cross-dated records (e.g. Vinther et al., 2008), a similar approach may be appropriate for varve records from the Canadian Arctic. However, additional records are needed before this approach could be implemented.

Summary and Conclusions

Exciting developments in paleoclimatic studies in the Canadian Arctic have produced quantitative estimates of past temperature conditions throughout the Holocene period. However, significant discrepancies exist between the available records in terms of both the timing and amplitude of past climatic fluctuations. The limited number of paleotemperature records from the Canadian Arctic is currently inadequate to address these discrepancies and identify spatial patterns of past temperature conditions. Because individual proxies have differing sensitivity to past climatic conditions, paleotemperature reconstructions should rely on multiple proxies to better capture the full range of climatic variability. Two clear objectives emerge from this review of current paleotemperature records from the Canadian Arctic: (1) Additional spatial coverage is needed in the distribution of proxy reconstructions. Because lakes are widely distributed throughout the region, paleolimnological studies likely provide the best opportunity for increased spatial coverage. (2) Replication of temperature reconstructions is necessary within a given region. This includes the production of additional records using the same proxies at different sites and new

records which combine multiple proxies. These records should provide better insight into the full range of temperature variability, including both long-term trends and short period variations, allowing the amplitude of past changes to be better constrained. It is important to point out that many of the quantitative proxies discussed in this chapter are being applied to the Arctic for the first time. As techniques are refined and additional study sites are located, more consistent patterns are likely to emerge and our ability to truly quantify past temperature changes will improve. In addition, this discussion has focused only on quantitative indicators of past temperatures while neglecting numerous qualitative paleoenvironmental indicators that are vital to our current understanding of Holocene climatic conditions in the Canadian Arctic. Thus future efforts to quantify past climatic conditions should continue to incorporate qualitative paleoenvironmental information.

It is somewhat ironic that where the impacts of future climate change are expected to be most severe (Solomon et al., 2007) we have such a limited perspective on past climatic variability. This is partly due to the inaccessibility of the region and also due to climatic and environmental constraints on the availability of many proxy indicators of climate change used elsewhere. Recent studies have demonstrated considerable potential for refining our understanding of past climatic conditions and quantifying the amplitude of past changes. However, continued effort is needed to utilize these new information sources through the concentrated development of additional paleoclimate reconstructions.

Table 4.1 List of study locations discussed in text and shown on map in Figure 1. Site numbers listed in bold have established quantitative paleotemperature records that have been reproduced in Figures 4.2 through 4.5.

Site #	Site Name	Proxy Type	References
1	GISP2	$\delta^{18}O$ (temp calibrated)	Cuffey & Clow, 1997; Alley, 2000; 2004
2	GRIP	borehole temp	Dahl-Jensen et al., 1998
3	Dye-3	borehole temp	Dahl-Jensen et al., 1998
4	Hans Tausen ice cap	$\delta^{18}O$	Clausen et al., 2001; Hammer et al., 2001
5	Agassiz ice cap	$\delta^{18}O$, melt percentage	Koerner & Fisher, 1990; Vinther et al., 2008
6	Meighen Island ice cap	$\delta^{18}O$	Koerner et al., 1973
7	Devon Island ice cap	$\delta^{18}O$	Patterson et al., 1977
8	Barnes ice cap	$\delta^{18}O$	Hooke and Clausen, 1982
9	Penny ice cap	$\delta^{18}O$	Fisher et al, 1998
10	Lake C2	varve	Lamoureux & Bradley, 1990
11	Lower Murray Lake	varve	Cook et al., 2009
12	Lake Tuborg	varve	Lewis et al., 2008
13	Big Round Lake	varve	Thomas & Briner, 2009
14	Donard Lake	varve	Moore et al., 2001
15	Lake KR02	pollen	Peros & Gajewski, 2008
16	Lake MB01	pollen	Peros & Gajewski, 2009
17	Lake SLO6	pollen	Peros & Gajewski, 2009
18	Hikwa Lake	pollen	Kerwin et al., 2004
19	Lake Jake	pollen	Kerwin et al., 2004
20	Iglutalik Lake	pollen	Kerwin et al., 2004
21	Patricia Lake	pollen	Kerwin et al., 2004
22	Lake CF3	chironomid	Axford et al., 2009
23	Lake CF8	chironomid	Briner et al., 2006; Thomas et al., 2008
24	Dyer Lake	pollen	Kerwin et al., 2006
25	Fog Lake	pollen, diatoms	Joynt & Wolfe, 2001; Kerwin et al., 2004
26	Kangerlussuaq	alkenones	D'Andrea, 2009
27	Hazen Plateau Lakes	diatoms	Smith, 2002

Table 4.2 Correlation coefficients determined between June-August temperatures at various stations around the Canadian Arctic and western Greenland and a principle component based June-July-August NAO index. Correlation coefficients were determined on 5-year running means of annual June-August values. Canadian station data is from Environment Canada National Climate Data and Information Archive (www.climate.weatheroffice.ec.gc.ca). Greenland temperature records are from Vinther et al. (2005). NAO Index Data provided by the Climate Analysis Section, NCAR, Boulder, USA, Hurrell (1995).

	Qaqortoq	Nuuk	Ilulissat	Alert	Baker Lake	Camb. Bay	Clyde River	Coral Harbor	Eureka	Iqaluit	Resolute
Nuuk	0.78										
Ilulissat	0.75	0.81									
Alert	0.47	0.31	0.54								
Baker Lake	0.03	-0.16	-0.24	-0.30							
Cambridge Bay	0.20	-0.11	0.01	0.09	0.83						
Clyde River	0.61	0.39	0.56	0.50	0.46	0.75					
Coral Harbor	0.31	0.03	0.10	-0.03	0.88	0.83	0.69				
Eureka	0.67	0.49	0.77	0.67	0.05	0.44	0.79	0.33			
Iqaluit	0.46	0.33	0.40	0.56	0.18	0.28	0.63	0.60	0.43		
Resolute	0.43	0.44	0.66	0.54	-0.05	0.30	0.60	0.20	0.73	0.32	
NAO Index	-0.65	-0.80	-0.78	-0.50	0.43	0.25	-0.27	0.21	-0.51	-0.16	-0.61
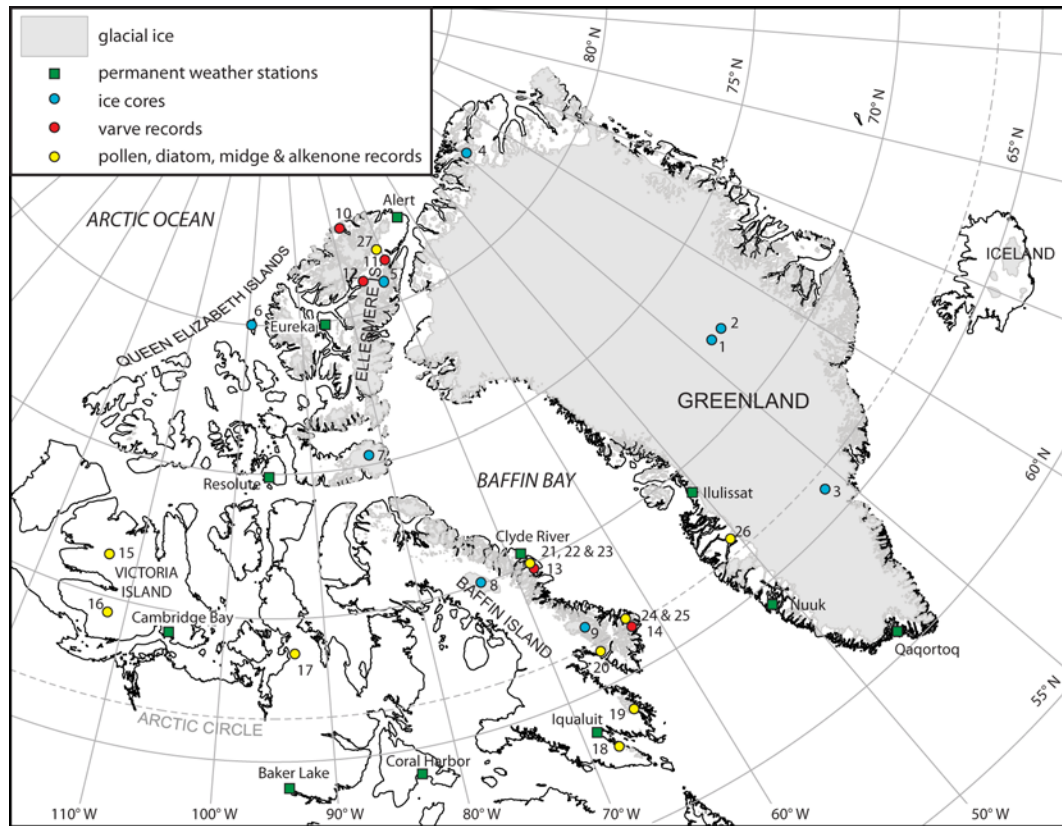
Figure 4.1 Regional map of the Canadian Arctic and Greenland depicting study locations discussed in the text: (1) GISP2, (2) GRIP, (3) Dye-3, (4) Hans Tausen ice cap, (5) Agassiz ice cap, (6) Meighen Island ice cap, (7) Devon Island ice cap, (8) Barnes ice cap, (9) Penny ice cap, (10) Lake C2, (11) Lower Murray Lake, (12) Lake Tuborg, (13) Big Round Lake, (14) Donard Lake, (15) Lake KR02, (16) Lake MB01, (17) Lake SLO6, (18) Hikwa Lake, (19) Lake Jake, (20) Iglutalik Lake, (21) Patricia Bay Lake, (22) Lake CF3, (23) Lake CF8, (24) Dyer Lake, (25) Fog Lake, (26) Kangerlussuaq, (27) Hazen Plateau Lakes.
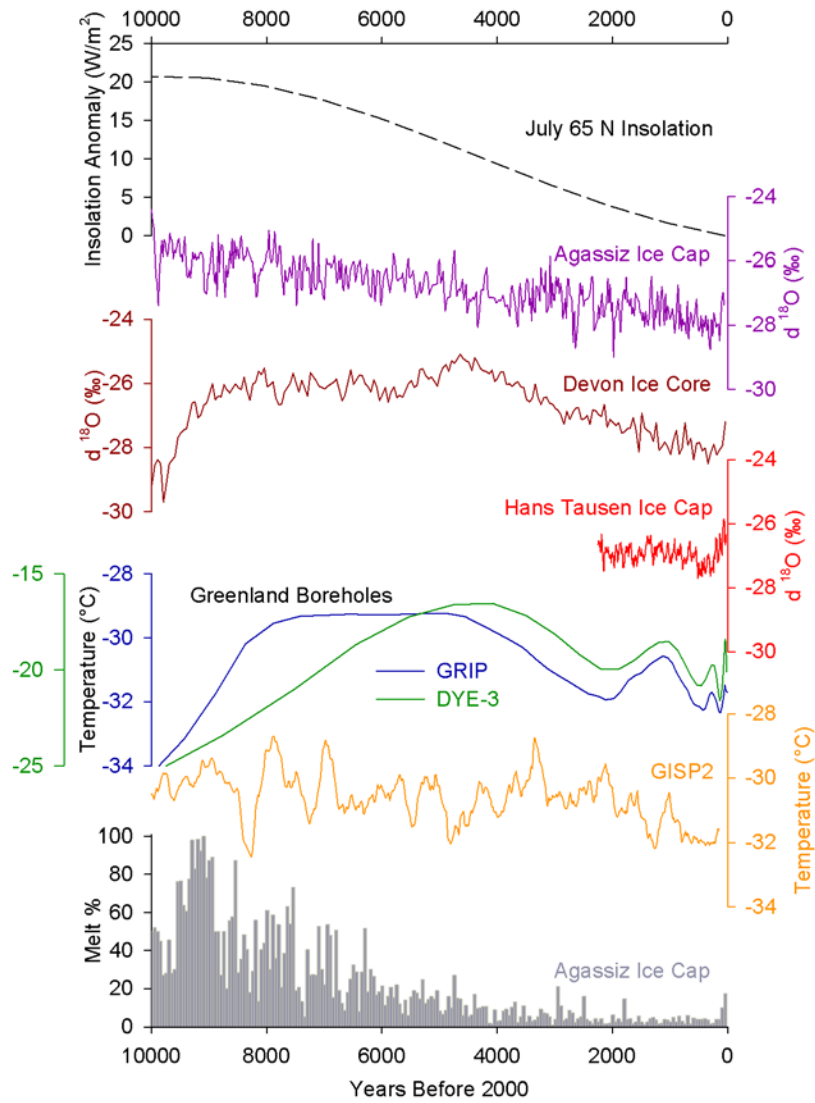
Figure 4.2 Proxy paleotemperature records from ice cores in the Canadian Arctic and Greenland. Shown from top to bottom are Agassiz ice cap $\delta^{18}O$ (Fisher and Koerner, 1990); Devon Island ice cap $\delta^{18}O$ (Patterson et al., 1977); Hans Tausen ice cap $\delta^{18}O$ (Claus et al., 2001; Hammer et al., 2001); Greenland borehole temperatures from GRIP and Dye-3 (Dahl Jensen et al., 1998); GISP2 temperature reconstruction (Cuffey and Clew, 1997; Alley, 2001; 2004) Also shown are July insolation anomalies relative to 1950 values (Berger and Loutre, 1991); Agassiz ice cap percent melt (Koerner and Fisher; 1990). The main Holocene trend in temperatures largerly parallels the gradual decrease in summer through the Holocene.
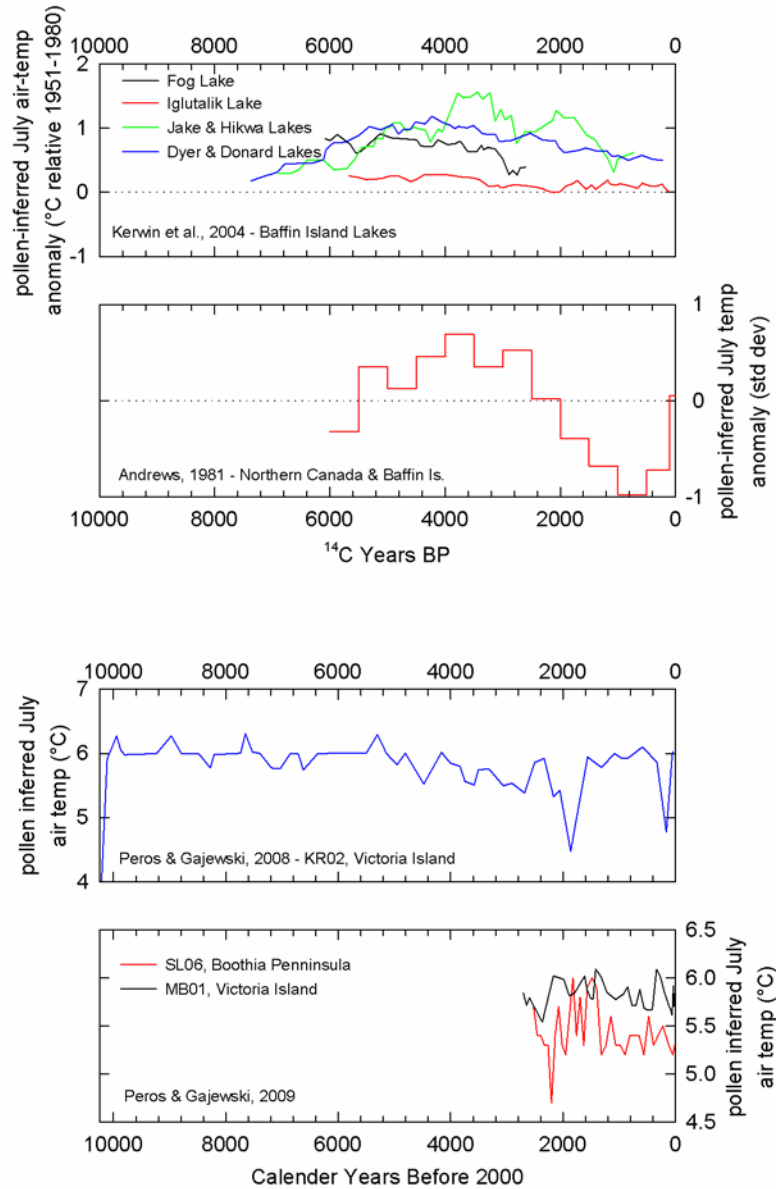
Figure 4.3 Pollen based paleotemperature reconstructions from the Canadian Arctic. Shown from top to bottom are smoothed composite July temperature anomalies from Baffin Island lakes (Kerwin et al., 2004; plots reflect the thick black lines in their Figure 5); composite northern Canada temperature anomalies (Andrews, 1991); mean July temperatures from Lake KR02, Victoria Island (Peros and Gajewski, 2009); and mean July temperatures from Lake SL06, Boothia Peninsula and Lake MB01, Victoria Island (Peros and Gajewski, 2008). Note that temperatures in the top two panels are plotted according to ^{14}C years before 2000, whereas the bottom two records are plotted according to calendar years before 2000.

106
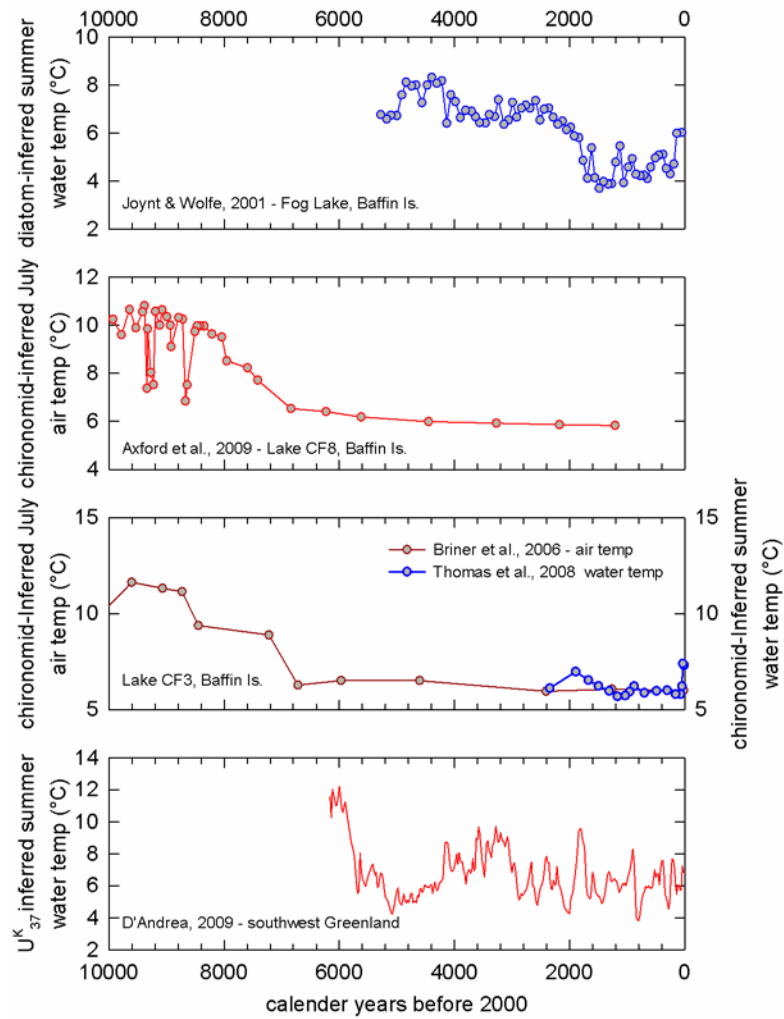
Figure 4.4 Assorted paleotemperature reconstructions from the Canadian Arctic and southwestern Greenland. Shown from top to bottom are diatom-inferred summer water temperatures from Fog Lake, Baffin Island (Joynt and Wolfe, 2001); chironomid-inferred July air temperatures from Lake CF8, Baffin Island (Axford et al., 2009); chironomid-inferred July air temperature (early and mid Holocene) and water temperature (late Holocene) from lake CF3, Baffin Island (Briner et al., 2006; Thomas et al., 2008); and Alkenone based summer water temperature from two lakes near Kangerlussuaq, southwest Greenland (D'Andrea, 2009).
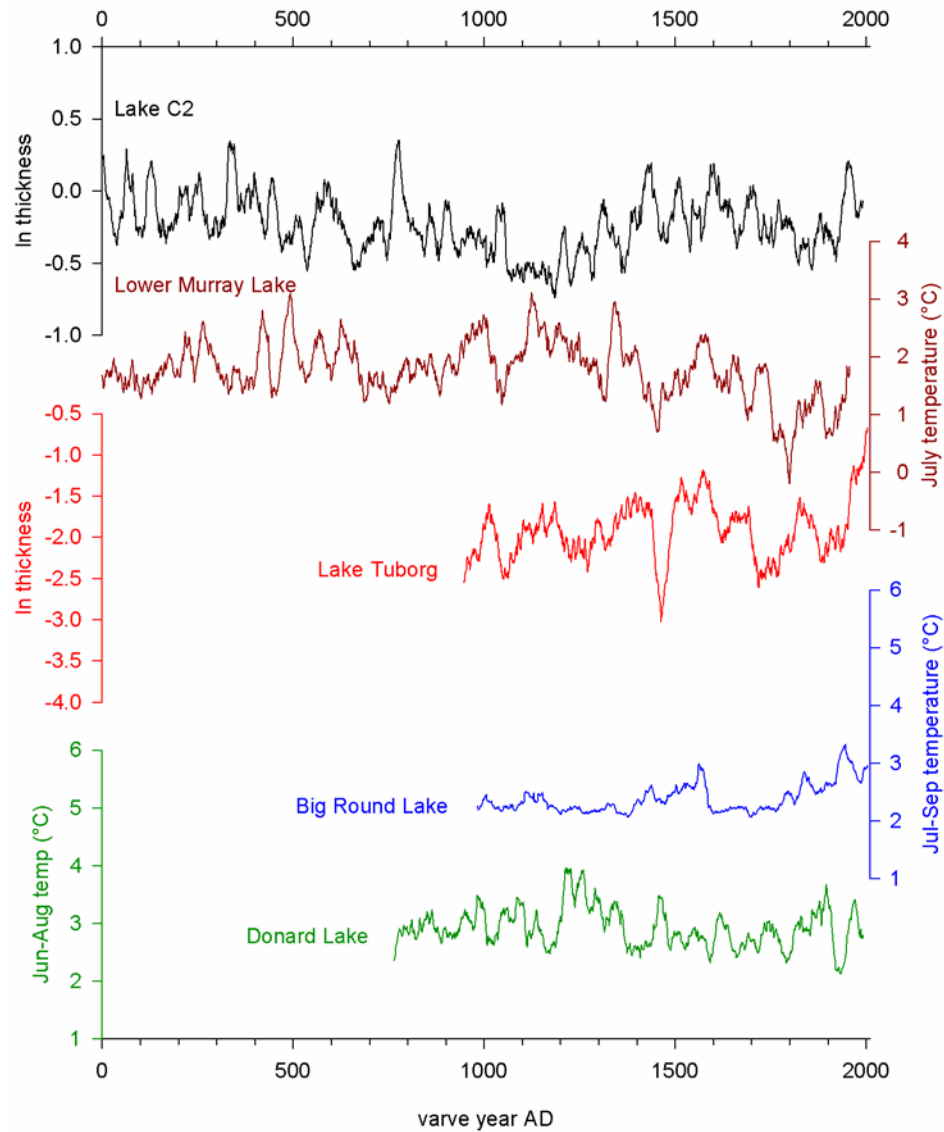
Figure 4.5 Varve records from the Canadian Arctic considered to reflect past temperature variability. Annual data have been smoothed with a 25 year running mean filter to highlight decadal scale variability. Varves characteristics in Lower Murray Lake (Cook et al., 2009), Big Round Lake (Thomas and Briner, 2009), and Donard Lake (Moore et al., 2001) have all been correlated to summer temperatures. Lake C2 (Lamoureux and Bradley, 1996) and Lake Tuborg (Lewis et al., 2008) varve characteristics have not been calibrated to temperature values, but are considered sensitive to past temperature variability.

CHAPTER 5

PAST AND FUTURE CHANGES IN THE ICE COVER OF HIGH-ARCTIC LAKES:
EVIDENCE FROM UPPER & LOWER MURRAY LAKES, ELLESMERE ISLAND, CANADA

Abstract

Space-borne synthetic aperture radar (SAR) data provide a record of the rate and timing of annual ice melt

on high-latitude lakes. Here, we use SAR data for Upper and Lower Murray Lakes (81°20'N, 69°30'W) in

the Canadian High Arctic to demonstrate its utility in assessing changes that have taken place over the last

decade, and use these observations to assess likely effects of rising temperatures on lake-ice conditions in

the future. Under current climatic conditions the Murray Lakes average several weeks of ice-free conditions

in August and early September, although in some years a partial ice cover persists throughout the year. The

relationship between summer temperature and ice melt at Upper and Lower Murray Lakes suggests that

recent warming in the High Arctic has forced the lakes across a threshold from a state of perennial ice

cover to seasonal melting. Projected future warming will significantly increase the duration of ice free

conditions on Upper and Lower Murray Lakes. Ice-out is predicted to occur between 6 and 28 days earlier

for every 1°C of warming.

Introduction

The duration of ice cover on lakes is of fundamental importance to physical, chemical, and biological processes in lake systems. Specifically, ice cover limits the exchange of water, nutrients, gases, and light and heat energy between a lake and its surroundings (Adams, 1981). In high-arctic lakes, changes in ice cover are believed to be a dominant factor controlling shifting biological communities (Smol, 1983; Smol, 1988; Douglas and Smol, 1999), and a number of studies have attributed recent changes in the sedimentary records of high-arctic lakes to changing ice conditions (e.g. Perren et al., 2003; Besonen et al., 2008; Tomkins et al., 2009). On a larger scale, changes in lake-ice duration influence the regional hydrologic-cycle and can affect the regional surface energy balance (Jeffries et al., 1999).

The timing of lake ice formation and break-up are highly sensitive to climatic conditions, with the dominant factor being surface air temperature (Palecki and Barry, 1986; Vavrus et al., 1996; Weyhenmeyer et al., 2004). As a result, records of lake-ice phenology have proven to be a useful indicator of climatic changes (e.g. Assel and Robertson, 1995; Magnuson et al., 2000). In the Arctic, where instrumental climate data are limited, remote sensing of lake-ice conditions can provide valuable insight into climatic conditions and how lake systems respond to climate change. Observational and proxy climate records indicate that recent temperatures in the Canadian High Arctic are the warmest of the last century (e.g. Kalnay et al., 1996; Rayback and Henry, 2006) and likely the warmest of the past several hundred years (e.g. Overpeck et al., 1997; Cook et al., 2008). Projections of future temperature change in the High Arctic indicate the potential for continued warming in excess of 5°C by the end of the 21st century (Christensen et al., 2007).

Recent climate warming is likely to have produced significant changes in Arctic lake-ice conditions, with even greater changes in lake- ice conditions expected due to future warming. Yet, despite the importance of ice cover to lacustrine environments, our understanding of lake-ice conditions in the High Arctic has been limited by a lack of regular observations. Notable exceptions to this are studies by Heron and Woo (1994), Adams et al. (1989), and Doran et al. (1996). Consequently, this study aimed to improve our understanding of the sensitivity of lake ice cover to both past and future changes in climatic conditions by using remote sensing data to evaluate recent changes in the ice cover of Upper and Lower Murray Lakes in the Canadian High Arctic.

Study Area

Upper and Lower Murray Lakes are long, narrow fjord-like lakes on northeastern Ellesmere Island, Nunavut, Canada (81°20'N, 69°30'W, Figure 5.1; Figure 5.2). Upper Murray Lake (UML) has a surface area of ~7.6 km^2 and a maximum depth of 83 m. Lower Murray Lake (LML) has a surface area of ~5 km^2 and a maximum depth of 46 m. The two lakes occupy a narrow, glacially carved valley with a maximum relief of approximately 1000 m. The Murray Lakes valley trends north-south along the length of the lower lake and northwest-southeast along the length of the upper lake. The surrounding land rises most steeply along the western shore of the lower lake where the slope rises >700 m over a distance ~1 km providing a local horizon ~35° above horizontal. Consequently, significant shading of Lower Murray Lake occurs in the afternoon and early evening when the sun is in the west (Figure 5.2). In other directions and around most of the upper lake, the local horizon is generally less than 20° and shading is much less of a factor. Climatically, the region is a polar desert with a mean annual temperature around -19°C, and mean annual precipitation (mostly in the form of snow) < 150 mm water equivalent (Maxwell 1981). Temperatures above freezing occur only from early June through late August. Maximum daily temperatures during the summer typically range between 0 and 10°C and occasionally reach as high as 20°C. The combination of a long, cold winter and a brief summer melt season currently leads to the development of a thick ice cover and limited ice-free conditions. Ice thickness at the start of the melt season in early June 2005 ranged from ~1.5 to 2.2 m.

Data and Methods

Changes in lake-ice coverage were analyzed using space-borne synthetic aperture radar (SAR) data from the Canadian Space Agency (CSA) RADARSAT-1 satellite. The combination of an orbital geometry and beam positions that provide a 1-2 day revisit cycle at high northern latitudes and the ability to return data regardless of sun or cloud conditions make the RADARSAT-1 satellite particularly well suited to monitoring changes in the ice cover of arctic lakes. Archived SAR data for the period 1997 through 2007 were provided by the Alaska Satellite Facility (ASF). A total of 115 images, including RADARSAT-1 fine

and standard beam and ScanSAR Wide B images (8, 25, and 100 m resolution, respectively) provided approximately weekly coverage of ice conditions during the melt season of each year in the record.

The difference in the amplitude of the SAR backscatter signal produced by open water and decaying lake ice allows the two features to be distinguished in SAR imagery (Figure 5.3). Calm, open water has a low backscatter signal due to a lack of internal reflectors and produces a dark, textureless tone in the SAR imagery. In contrast, decaying ice has a higher backscatter signal and produces a gray, textured tone in the SAR imagery. For example, the increase in the area of the dark, textureless region in the sequence of SAR image sub-scenes in Figure 5.3 reflects the increase in the area of open water on Upper and Lower Murray Lakes during the year 2000 melt season.

The rate and timing of ice decay was quantified by measuring changes in the area of ice cover recorded in the sequence of SAR images from each melt season. SAR byte-scaled amplitude images were geocoded to an Albers equal area projection and then analyzed using image analysis software. A polygon or series of polygons outlining regions of open water in each image were digitized and then the area of the polygons relative to the total surface area of the lake was used to calculate the percentage of ice cover remaining. The end of ice break-up, or simply ice-out as used herein, was defined as the time when the lake was 100 % ice free. The ice-out date was estimated by interpolating between the date of the last SAR image depicting partial ice cover and the date of the first ice-free SAR image based on the trend in the rate of ice cover reduction observed in the preceding images. Because of the low backscatter contrast between open water and newly formed ice, the precise timing of lake freeze-up proved more difficult to identify in the SAR imagery. Consequently, ice formation is not discussed further. However, temperatures at the Murray Lakes typically fall below freezing by the end of August and it can be assumed that ice growth is initiated shortly thereafter.

Instrumental climate data were obtained from two permanent weather stations operated by Environment Canada that are located at Alert and Eureka, Nunavut (Figure 5.1). In addition, reanalysis data were obtained from the National Centers for Environmental Prediction / National Center for Atmospheric Research (NCEP/NCAR; Kalnay et al., 1996). These data provide a daily mean surface air temperature value for a 2.5 x 2.5 degree grid box based on the blending of a combination of a global numerical weather prediction model and observational data. Upper and Lower Murray Lake fall within the grid box centered

on 82.5°N 70°W, but are very near the southern boundary of this box (Figure 5.1). Consequently reanalysis data from the adjacent grid box centered at 80°N 70°W was also acquired. Fourteen months (June 10, 2005 through August 4, 2006) of surface air temperature measurements were recorded at the Murray Lakes field site with an Onset Computer Corporation HOBO Pro Temp H08-030-08 temperature logger. According to the manufacturer, the stated accuracy of the logger is better than ± 0.5°C for temperatures between 0° and 40°C and between 0° and -40°C accuracy decreases to approximately ±1.25°C. No additional verification of the accuracy of the temperature loggers was conducted. The temperature logger was placed in a solar radiation shield 2 m above the ground surface and sited on the isthmus between Upper and Lower Murray Lakes at 81.35492°N 69.53679°W. This site was approximately 50 m north of the Lower Murray Lake shoreline. Temperature was recorded at 1 hour intervals from which mean daily temperatures were calculated.

The local observational data were used to evaluate the reliability of the various long-term temperature records in terms of their ability to accurately reflect daily temperatures at the field site. Specifically, we compared the Murray Lake observational data with mean daily temperature records from Alert, Eureka, and the NCEP/NCAR reanalysis data from grid boxes centered on 82.5°N 70°W and 80°N 70°W. Prior to comparison, low frequency (seasonal) variability was removed from each record by producing a spline curve that fit the individual record and then calculating residual daily temperatures relative to the spline value (Figure 5.4). Correlation coefficients were then calculated between each of the regional records and the Murray Lake record using the residual temperature values. Results of the correlation analyses indicate that daily temperatures at Murray Lake are most accurately predicted by the NCEP/NCAR reanalysis data from the grid box centered at 82.5°N 70°W (R = 0.770; Table 1). However, comparison of the reanalysis data and the Murray Lake data indicates that the reanalysis data systematically underestimates local Murray Lake temperatures during the months of May through September (Figure 5.5). This discrepancy may be a consequence of the location of the grid box relative to the Murray Lakes and the large geographic and topographic variability within the grid box which includes much of the upland, glaciated interior of northern Ellesmere Island as well as several hundred square kilometers of the Arctic Ocean. In order to account for the temperature difference during the months of May through September, a

linear regression was calculated between the reanalysis and Murray Lake records using only the data from those months (Figure 4). The equation of the regression line,

$$\text{Murray Lake Temp} = 3.146 + (0.958 \times \text{Reanalysis Temp}) \quad (R = 0.922)$$

was then used to adjust the daily reanalysis temperature data from the months of May through September in each year of the record (Figure 5.5). All further use and discussion of the reanalysis temperature data refers to the adjusted record. Cumulative melting degree days (CMDD) were calculated on an annual basis by calculating a running total of daily reanalysis temperatures for each day where the mean temperature was above 0°C.

Results and Discussion

Annual ice break-up

Observations of ice coverage on Upper and Lower Murray Lake during the period 1997 through 2007 show a wide range of variability in both the rate and timing of ice break-up (Figure 5.6). Ice melt likely begins in early June when temperatures start to exceed 0°C, however a decrease in total ice surface area was not discernable in the SAR imagery until early July. Ice-out dates typically ranged from early August through early September with the mean date of ice-out August 16 on Upper Murray Lake and August 24 on Lower Murray Lake. However, ~50 to 75 % of the ice cover on Upper Murray Lake remained throughout the 1999 and 2004 melt seasons and ~30 to 80 % of the ice cover remained on Lower Murray Lake throughout the 1997, 1999, and 2004 melt seasons.

Air temperature during the preceding days, weeks, or months is generally considered the dominant climatic variable affecting the timing of ice breakup (Palecki and Barry, 1986; Vavrus et al., 1996; Weyhenmeyer et al., 2004). The timing and length of the interval over which air temperatures influence ice break-up is highly dependent on the region of interest (Palecki and Barry, 1986). The dominant time period controlling ice break-up at Upper and Lower Murray Lakes was evaluated by calculating Pearson product moment correlations between the Julian dates of ice-out and mean air temperatures over a variety of time

114

periods (Table 2). The highest correlation was associated with mean temperatures from June through July (R = -0.786 for UML and R = -0.791 for LML), although June temperatures on their own produce nearly as strong a correlation. The negative coefficient indicates that higher mean temperatures in June and July correspond to earlier ice break-up. The two month interval over which air temperatures strongly influence ice break-up reflects the length of time required to melt the thick ice-cover of Upper and Lower Murray lakes.

In general, the timing of ice out on Upper and Lower Murray lakes closely tracks mean June and July temperatures (Figure 5.7). Early (late) ice-out dates coincide with higher (lower) June and July temperatures. However, deviations from this pattern and uncertainty in the relationship between air temperatures and ice decay stem from two sources. The first source of uncertainty stems from variations in local temperature conditions relative to the reanalysis temperature record used in this study. Another source of uncertainty stems from the complexity of the processes influencing ice formation, growth, and decay throughout a given year. The melting of ice occurs at a rate controlled by the energy balance of the ice sheet (e.g. Ashton, 1983; Heron and Woo, 1994; Liston and Hall, 1995; Duguay et al., 2003) with the rate of ice break-up further influenced by dynamic processes related to wind and water currents (Ashton 1980). If the rate of melting and ice break-up remain constant, the timing of ice out will vary according to ice thickness at the start of the melt season which in turn varies in response to winter temperature and snow conditions.

Snow accumulation interacts with the underlying ice sheet in a complex, nonlinear manner which can both increase the overall ice thickness and/or slow its growth and decay (Vavrus et al., 1996). Specifically, the accumulation of snow can lead to the formation of superimposed snow-ice when the ice sheet gets depressed below the hydrostatic water level and the snow cover becomes water saturated and then freezes (Adams and Roulet, 1980, Duguay et al., 2003). On the other hand, snow cover insulates the underlying ice sheet, limiting conductive heat loss from the lake to the atmosphere in autumn and reducing warming in spring. As a result, lakes with a thicker snow cover will tend to have thinner ice and an earlier break-up date relative to similar lakes that have less snow cover (Vincent et al., 2008). Field observations by the authors of completely clear ice (ie. lacking a layer of superimposed snow-ice) on the Murray Lakes in 2005 and other Ellesmere Island lakes including Lake Tuborg, South Sawtooth Lake, and Lakes C1, C2

and C3 suggests that the formation of snow-ice is not a significant process on these large, high arctic lakes, although further observations are required to confirm this. Limited snow-ice formation may reflect low winter snow accumulation, which is typically less than 150 mm weq, relative to the thick (~2 m) ice cover on these lakes. Variations in snow accumulation during the study period are not known, limiting our ability to fully evaluate the role of snow accumulation on the timing of ice break-up.

Physical processes related to wind and water currents play a significant role in delaying the onset of ice formation during autumn and enhancing ice break-up during spring, with the influence of wind generally being more pronounced on lakes with a larger surface area (Ashton 1980). Comparison of SAR images corresponding to the initial break-up period on the Murray Lakes highlights the role of dynamic processes in ice break-up. Observations of the initial break-up of ice cover in mid to late July of each year for which data are available reveal a consistent pattern of ice break-up, with open water initially forming in the center of Upper Murray Lake and in the south end of Lower Murray Lake (Figure 5.8). These regions correspond to the locations of the inlets of the main tributaries draining into each of the lakes, and likely reflect the influence of warmer inflowing water and/or the physical break-up of the ice sheet by water currents. Consequently, some of the variability in the timing of ice break-up in the Murray Lakes likely results from non temperature-related, mechanical processes.

An interesting feature of the Murray Lakes ice decay record is the consistent delay in the timing of ice out on Lower Murray Lake relative to Upper Murray Lake. On average Lower Murray Lake ice out occurs ~8 days after ice out on Upper Murray Lake. Because the two lakes are essentially responding to the same climatic forcings, other factors must be responsible for the difference in the timing of ice out. All other factors being similar, ice out on deeper lakes typically occurs later as some of the energy that would go to melting ice is lost to the heating of the underlying water column (Vincent et al., 2008). However, Upper Murray Lake is considerably deeper than Lower Murray Lake (83 m versus 46 m maximum depth), so lake depth cannot be the controlling factor. Instead, it seems likely that the significant afternoon shading which occurs on Lower Murray Lake (cf. Figure 5.2) reduces surface air temperatures over the lake and limits the absorption of solar radiation, which in turn reduces the rate of ice decay. Astronomical tables can be used to determine the angle of the sun above the horizon at different times of day at the Murray Lakes field site (Figure 5.9; http://aa.usno.navy.mil/data/docs/AltAz.php; last accessed December 31, 2008). As

the local horizon to the west of Lower Murray Lake is ~35° above horizontal, the sun would be below the local horizon for much of the afternoon and evening, whereas the much lower local horizon around the upper lake indicates that shading is much less of a factor on Upper Murray Lake. Differences in the surface area of the two lakes may play an additional role as the larger surface of the upper lake provides a larger fetch and increases the potential for physical breakdown of ice by wind and wave action. Consequently, the combination of reduced sunlight and limited wind action likely delays the rate of ice break-up on Lower Murray Lake. Furthermore, it is possible that differences in ice growth on the two lakes, which is also influenced by lake volume, surface area, and shading, leads to different initial ice conditions at the onset of the ice melt in the spring. Consequently, the combination of these factors adds additional uncertainty to the relationship between air temperature and ice decay.

The current pattern of ice cover on Upper and Lower Murray lakes, characterized by a very brief period of open water and the occasional occurrence of ice cover throughout the year, suggests that the Murray Lakes are presently in a marginal climatic setting where slightly colder climatic conditions could lead to the establishment of a perennial ice cover. Perennial (multiyear) ice covers have been observed at several other locations in the High Arctic and also in parts of Antarctica. In particular, Lakes A, B, C1, C2, and C3 along the northern coast of Ellesmere Island have typically maintained year round ice covers in the past (Belzile et al., 2001; Lenormand et al., 2002; Jeffries et al., 2005), and Colour Lake on Axel Heiberg Island has occasionally maintained an ice cover through the summer, although not in consecutive years (Adams et al., 1989; Doran et al., 1996). Doran et al., (1996) suggested that an ice cover that lasted through the summer at Colour Lake effectively trapped water that had been warmed during that summer and led to elevated water temperatures the following spring, limiting the tendency of a multiyear ice cover to persist. This interpretation is consistent with observations at Upper Murray Lake which show early ice-out dates in 2000 and 2005, the two years following residual ice years. Ice out in 2000 (on August 4) was the earliest observed in the record and occurred during a year characterized by abnormally low ice-cover on other northern Ellesmere Island lakes (Jeffries et al., 2005), suggesting that changes in the ice cover on the Murray Lakes are consistent with regional conditions.

Past ice conditions

Observational and proxy climate records indicate that recent temperatures in the Canadian High Arctic are the warmest of the last century (e.g. Kalnay et al., 1996; Rayback and Henry, 2006; Figure 9) and likely the warmest of the past several hundred years (e.g. Overpeck et al., 1997; Cook et al., 2008). The impact of recent warming on the ice cover of the Murray Lakes was evaluated based on the relationship between the area of ice cover remaining and the cumulative melting degree days (CMDD) at that time (Figure 5.11). Figure 5.11 includes all of the ice cover data points from Figure 5.6 plotted as a function of CMDD instead of time. As melting degree days accumulate there is a clear decreasing trend in the area of ice cover remaining. During the period 1997-2007 a minimum of 286 and a mean of 325 CMDD were required to reach complete ice out on Upper Murray Lake and a minimum of 294 and a mean of 353 CMDD were required to reach complete ice out on Lower Murray Lake (Table 3).

Cummulative melting degree days provide a reasonable approximation of the energy available for melt processes (Billelo, 1980). As ice decay evolves and ice becomes weakened and is able to move about the lake surface, dynamic processes become increasingly important to ice break-up (Michel et al., 1986). Thus, the increase in the size of the envelope of ice-cover values as CMDDs increase likely reflects the increasing importance of dynamic processes to ice-breakup as well as variations in initial ice conditions resulting from differences in winter ice growth. Nonetheless the trend of the ice cover-CMDD relationship can be used to evaluate the influence of changing climatic conditions on ice decay and the envelope of values provides an indication of the range of internal variability within the system.

A mean cumulative melting degree day curve was determined from mean daily temperatures during the period 1997-2007 (Figure 5.11). Also determined were CMDD curves calculated based on 0.5°C, 1.0°C, and 1.5°C reductions in mean daily temperatures, which result in 295, 257, and 221 total CMDD, respectively (Figure 5.11). The total CMDD based on mean 1997-2007 temperatures (336 CMDD) is only slightly above the mean number of CMDD needed to reach ice out on Upper Murray Lake (325 CMDD) and below the mean number of CMDD needed to reach ice out on Lower Murray Lake (353 CMDD) during the observation period. Consequently a temperature reduction of less than 1.0°C, relative to the 1997-2007 mean, would produce a CMDD total well below the minimum value required for ice out on either Upper or Lower Murray Lakes during the period of record.

These results suggest that only a minor change in mean temperature is required to shift the Murray Lakes system between states characterized by 100% open water conditions or significant residual ice cover at the end of the melt season. Furthermore, comparison with 20th century observations of summer temperature changes (Figure 5.10) suggests that recent warming in excess of 1.0°C may have forced Upper Murray Lake across a threshold leading away from a state of perennial ice cover. A similar transition has been observed at other lakes along the north coast of Ellesmere Island (Lakes A, B, C1, C2, and C3) which have traditionally been covered by a perennial ice cover (Belzile et al., 2001; Lenormand et al., 2002; Jeffries et al., 2005), but have recently been experiencing ice free conditions during the summer (D. Mueller, *personal communication*). Transitions in ice-cover of this nature are consistent with paleolimnological observations from other High Arctic lakes in which recent, unprecedented shifts in biological communities have been attributed to changes in the duration and extent of summer ice cover (e.g. Perren et al., 2003; Smol et al., 2005). In fact, analysis of a 1000 year sedimentary record from Lower Murray Lake identified the first appearance of diatoms in the lake as recently as 1998 (Besonen et al., 1998), supporting our interpretation that significant changes in the lake system have occurred in recent years.

Future Ice conditions

Projections of future temperature change in the High Arctic indicate the potential for mean annual temperatures to increase by as much as 5°C by the end of the 21st century (Christensen et al., 2007). Although warming is expected to be highest in winter (>7°C), summer warming is likely to exceed 2°C (Christensen et al., 2007). The relationship between ice-out dates and mean June and July temperatures was used to evaluate the impact of future warming on the ice-cover of Upper and Lower Murray Lakes (Figure 5.12). As noted previously, surface air temperatures for the period spanning June and July showed the strongest correlation with the timing of ice out (cf. Table 2). A linear regression between mean June and July temperatures and ice-out dates indicates that for each 1.0°C increase in temperature the timing of ice-out will be ~14 days earlier for Upper Murray Lake and ~ 18 days earlier for Lower Murray Lake. Consequently, future warming in the High Arctic will result in significantly longer periods of ice free conditions on these lakes. The standard errors associated with these regressions (±7.7 for UML and ±9.8

LML) reflect the limited data set and the influence of non temperature-related processes on ice decay. Given this range of uncertainty, the expected rate of change in the timing of ice-out on the Murray Lakes varies anywhere from ~6 to 28 days per 1.0°C change in temperature, although the actual rate is likely closer to the observed trends at the two lakes.

Recent work has suggested that the timing of ice out may not respond linearly to changes in temperature (Weyhenmeyer et al., 2004), thus the 14 and 18 day per 1.0°C relationships determined in this study may change as temperatures shift beyond the range of observations. By comparison, historical trends in the ice cover of lower latitude lakes have shown a mean shift in the timing of ice out by ~5 days per 1.0°C temperature change (e.g. Assel and Robertson, 1995; Magnuson et al., 2000). In a comprehensive study of past ice conditions on Swedish lakes, Weyhenmeyer et al. (2004) observed ice breakup dates that were 4 to 17 days earlier following a temperature increase of 0.8°C. The largest changes were observed in the warmest locations, thus Weyhenmeyer et al. (2004) concluded that future changes in ice conditions due to increased warming are likely to be less drastic in colder regions, which is inconsistent with the large temperature dependence of ice out identified in this study. However, the coldest site examined by Weyhenmeyer et al. (2004) had a mean annual air temperature near -1.0°C, whereas mean annual temperature at Upper Murray Lake is -19°C. Consequently, it is possible that the climatic conditions at the Murray Lakes, near the threshold necessary for perennial ice cover, lead to an amplified change in the timing of ice out for a given change in temperature. Quantitative relationships between air temperature and ice break-up are applicable only within specific geographic and climatic settings (e.g. Palecki and Barry 1986; Weyhenmeyer et al., 2004). In addition morphometric characteristics of individual water bodies (ie. depth, surface area) further influence ice decay (Stewart and Haugen, 1990; this study). Consequently, caution must be used when applying the results of this study to other lakes. Nonetheless, the magnitude of the ice-out response to temperature changes as reported here highlights the impacts of future warming on High Arctic lake systems and emphasizes the need for continued study of ongoing environmental changes in the Arctic.

Conclusions

Space-borne synthetic aperture radar data have provided a valuable tool for interpreting the climatic sensitivity of the ice-cover on remote high-arctic lakes. Comparison with reanalysis air temperature records allowed for quantification of the relationship between ice cover and climatic conditions. The summer temperature conditions necessary for the complete melting of the ice covers on Upper and Lower Murray Lakes are very near current mean climatic conditions, suggesting that the two lakes are at or near a threshold between a state of perennial ice cover and regular seasonal melting of their ice covers. Recent (20th century) warming has likely forced the Murray Lakes across this threshold, and projected future warming due to anthropogenic causes will further increase the duration of ice free conditions on these lakes. Although the exact response of lake ice to temperature changes will vary according to the local geographic and climatic setting as well as the characteristics of the individual lake, the results presented here indicate that profound changes in the ice cover of high-arctic lakes have recently occurred and that even greater changes should be expected in the future. Given the significance of the timing of ice out and the length of open water conditions to so many physical, chemical, and biological processes acting both within and beyond the lake, future changes in lake ice cover are likely to have a significant impact on high-arctic environments.

Table 5.1 Results of correlation analysis between the mean daily temperature record at the Murray Lakes and the available long-term regional records.

Temperature Series	Correlation Coefficient – r	Significance – p value
Alert	0.752	<0.001
Eureka	0.704	<0.001
Reanalysis (82.5°N 70°W)	0.770	<0.001
Reanalysis (80° N 70°W)	0.631	<0.001

Table 5.2 Pearson product moment correlation results between the timing of ice-out on Upper (UML) and Lower (LML) Murray Lakes mean temperatures over various time intervals. Significant correlations are in bold.

Temperature Variable	Correlation Coefficient – r		Significance – p value	
	UML	**LML**	**UML**	**LML**
Mean June Temp	**-0.716**	**-0.777**	**0.030**	**0.0233**
Mean July Temp	-0.501	-0.426	0.170	0.293
Mean August Temp	-0.152	0.196	0.697	0.641
Mean Annual Temp (Sep – Aug)	-0.499	-0.425	0.172	0.294
Mean Winter Temp (Sep – May)	-0.418	-0.332	0.263	0.422
Mean June & July Temp	**-0.786**	**-0.791**	**0.012**	**0.0193**
Mean June, July, August Temp	-0.612	-0.586	0.080	0.127

Table 5.3 Ice-out dates and the total cumulative melting degree days (CMDD) required to reach ice out on Upper and Lower Murray during each year of the record. Missing values indicate complete ice-out did not occur.

Time Period	Upper Murray Lake		Lower Murray Lake	
	Ice-Out Date	CMDD to Ice-Out	Ice-Out Date	CMDD to Ice-Out
1997	240	286	-	-
1998	222	354	228	374
1999	-	-	-	-
2000	217	301	218	305
2001	218	284	231	348
2002	232	326	247	351
2003	217	351	226	402
2004	-	-	-	-
2005	222	342	228	355
2006	248	292	264	294
2007	239	391	243	396
1997-2007 Mean	228	325	236	353

Figure 5.1 Regional map showing the location of Upper and Lower Murray Lakes as well as other high-arctic lakes mentioned in the text. Also shown is the grid box associated with NCEP/NCAR reanalysis temperature data used in this study.

Figure 5.2 Aerial photograph looking north across Lower Murray Lake in the foreground and Upper Murray Lake which wraps behind the hill to the left in the background. Note the significant shadow across much of Lower Murray Lake which occurs in the afternoon.
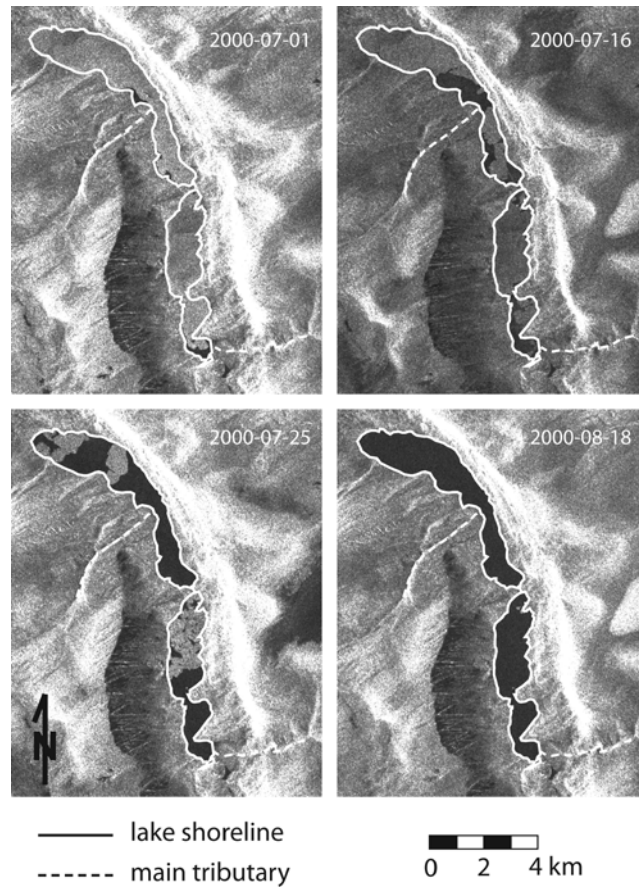
Figure 5.3 Sequence of RADARSAT-1 SAR image sub-scenes showing an increase in the percentage of open water (dark, textureless tone) on Upper and Lower Murray Lakes during the year 2000 melt season. The original RADARSAT-1 data (©Canadian Space Agency – CSA) were provided by the Alaska Satellite Facility (ASF).
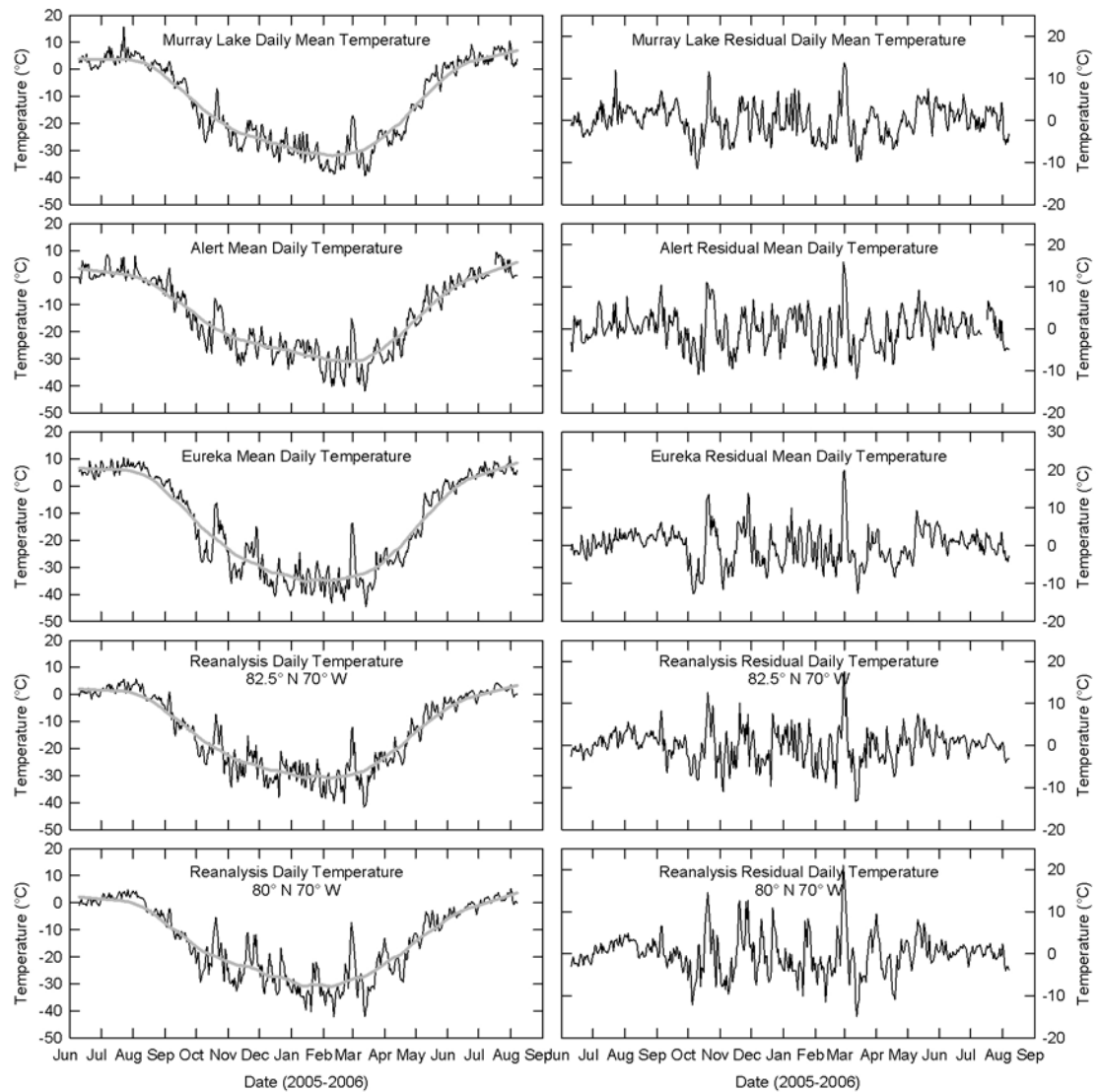
Figure 5.4 Comparison of mean daily surface air temperature observation at the Murray Lakes field site with the available long term regional temperature records. Plots along the left show mean daily temperatures (in black) and the spline curve (in grey) fit to each time series in order remove seasonal variability. Plots along the right show residual daily temperatures relative to the spline value.
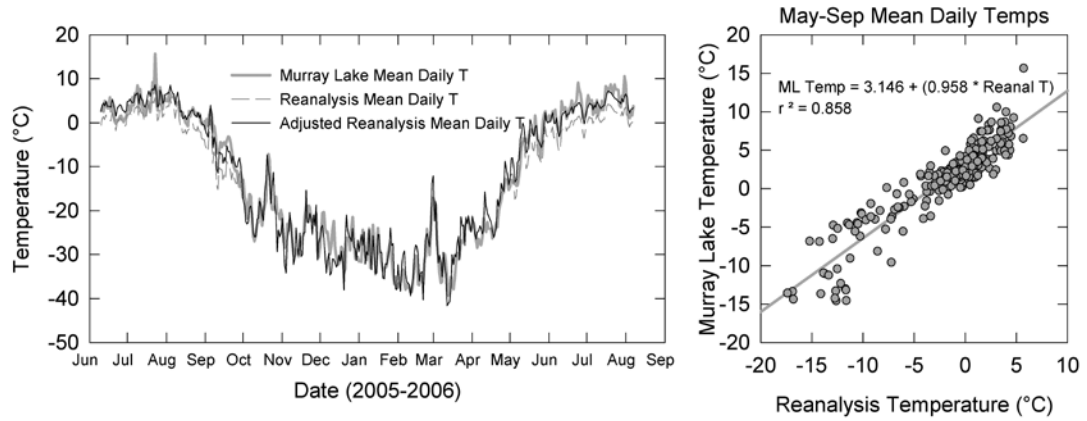
Figure 5.5 (left) Mean daily temperature at Murray Lakes compared to the reanalysis temperature data from the grid box centered on 82.5°N 70°W. The reanalysis data systematically underestimated May-September temperatures at the Murray Lakes. Consequently, the reanalysis temperature record was adjusted based on a linear regression of the May through September temperature data (right). The adjusted reanalysis temperature series is plotted in red on the upper panel and shows much better agreement with the local observations.
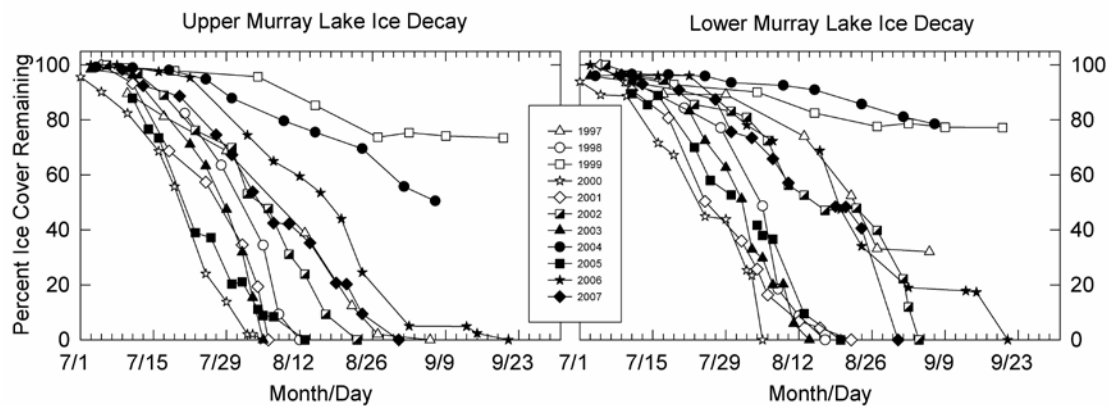
Figure 5.6 Annual record of ice decay on Upper and Lower Murray Lakes showing changes in the area of the lake covered by ice during each summer from 1997 through 2007.
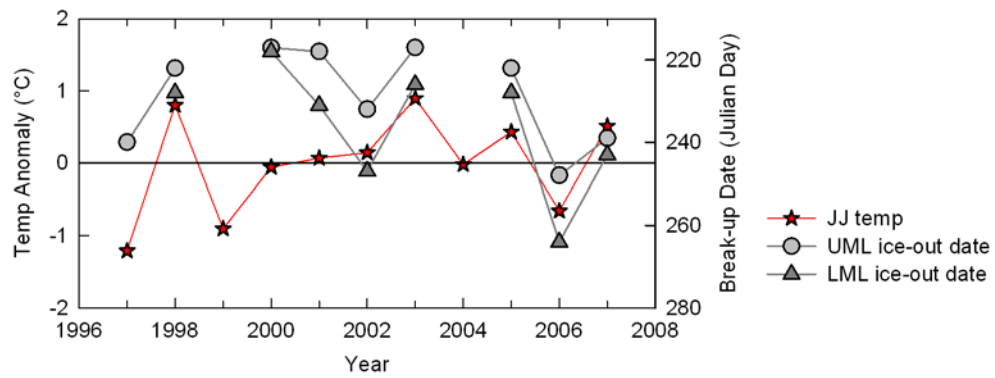
Figure 5.7 Plot showing mean June and July temperatures anomalies (relative to 1997-2007 mean) and ice-out dates for the each year of the record. Note that the ice-out date scale has been reversed in order to emphasis the consistent relationship between summer temperatures and the timing of ice-out.
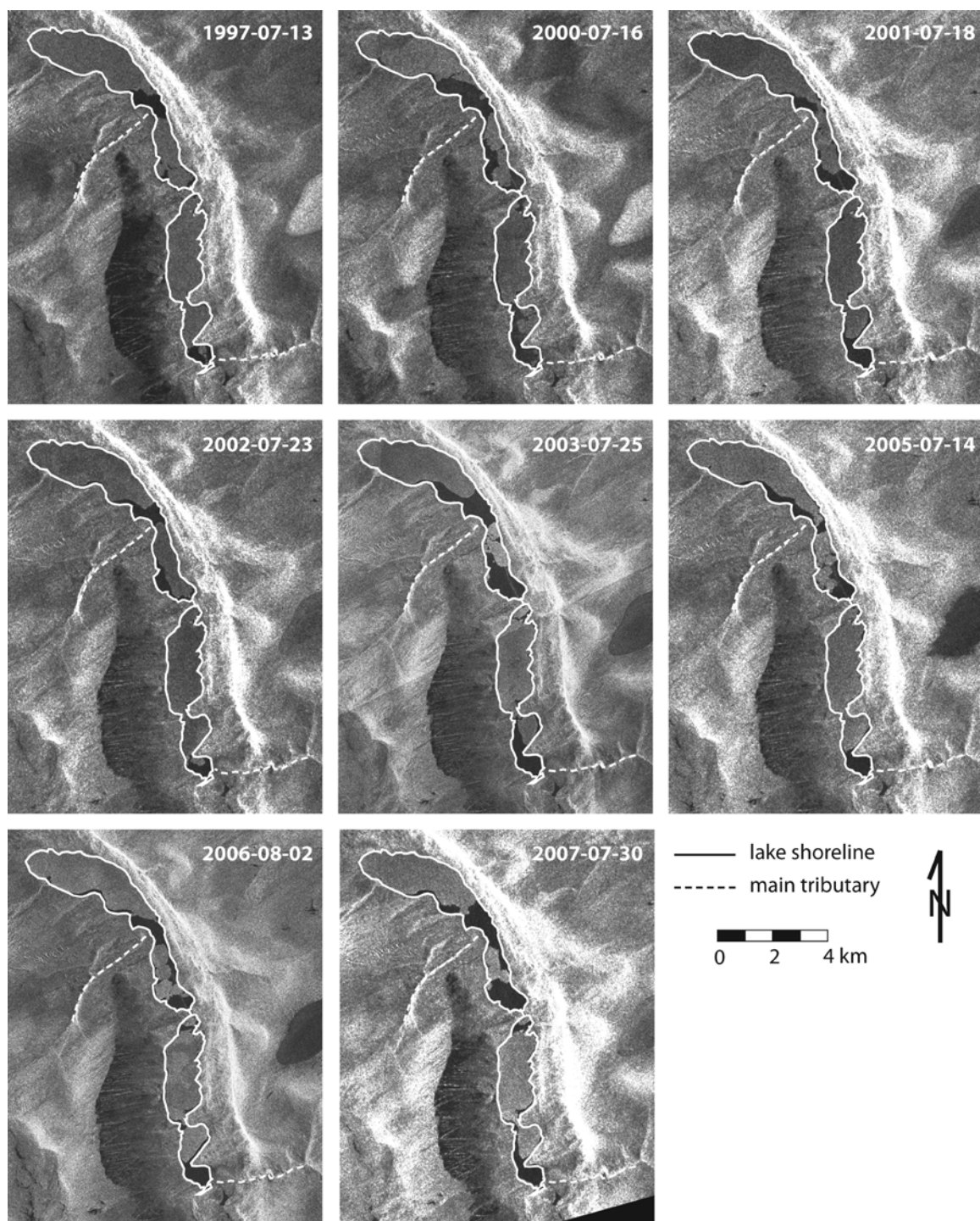
Figure 5.8 RADARSAT-1 SAR image sub-scenes showing initial ice break-up on Upper and Lower Murray Lakes. Note the consistent pattern of open water first occurring near the center of the Upper Murray Lake and the south end of Lower Murray Lake. The original RADARSAT-1 data (©Canadian Space Agency – CSA) were provided by the Alaska Satellite Facility (ASF).
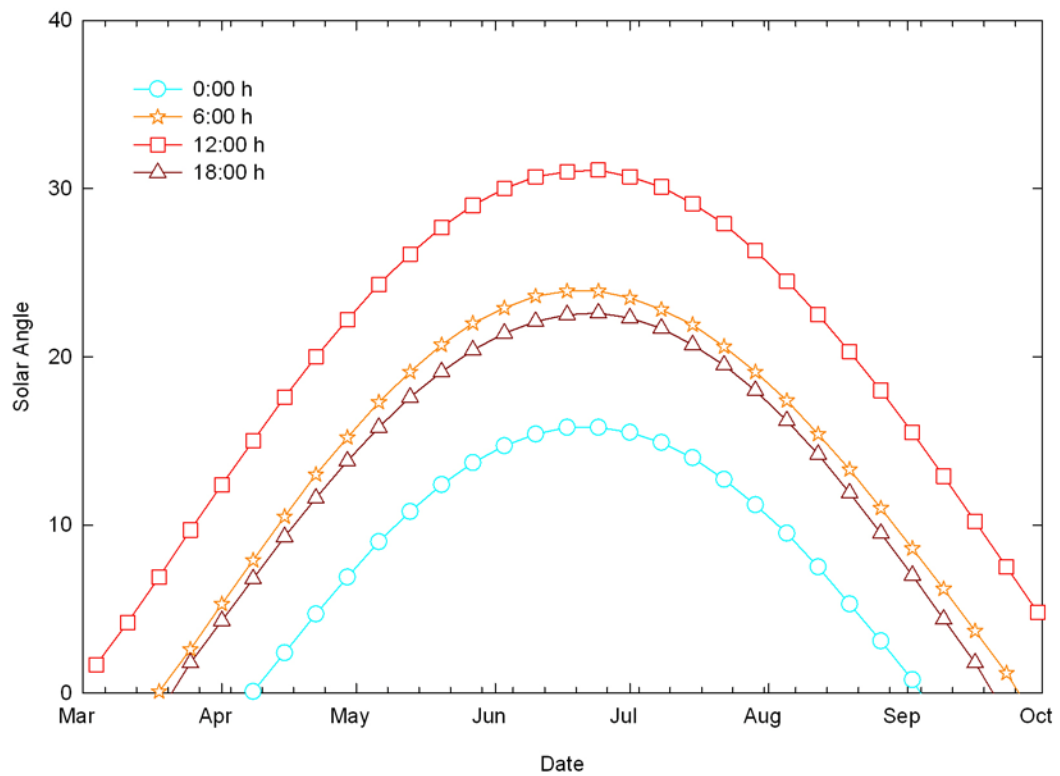
Figure 5.9 Seasonal variations in the angle of the sun above the horizon for different times of day at the Murray Lakes field site.
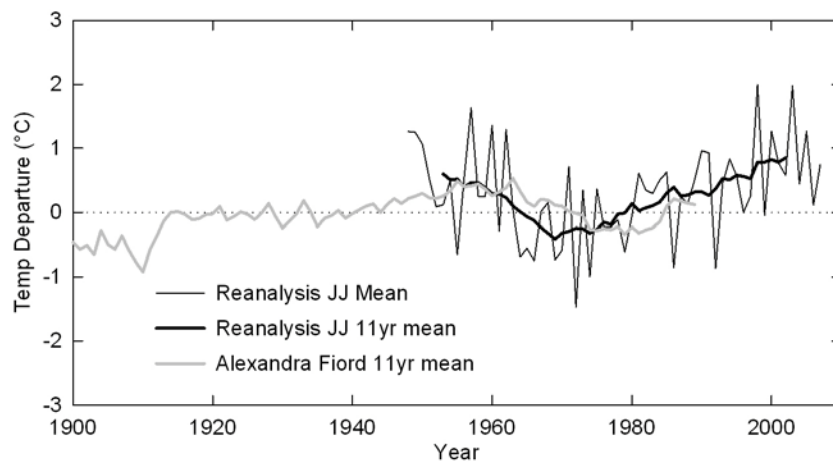
Figure 5.10 Recent summer temperature anomalies (relative 1961-1990 means) from Ellesmere Island, including annual and 11-yr mean June and July reanalysis temperature records (Kalnay et al., 1996) and 11 yr mean reconstructed July-September temperatures from Alexandra Fiord (Rayback and Henry, 2006).
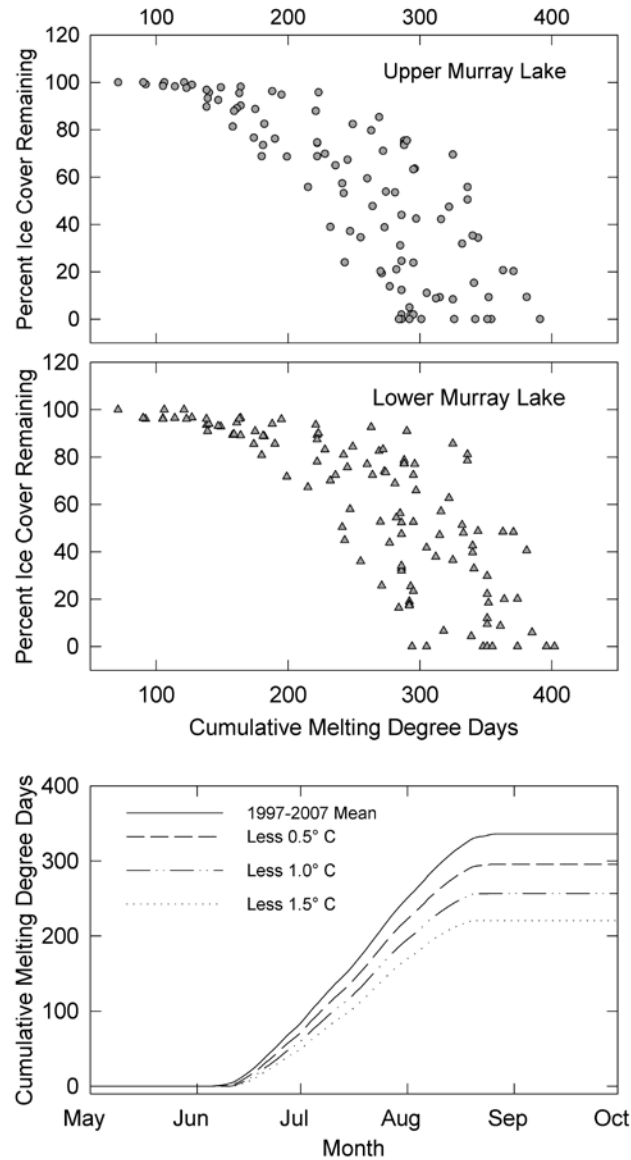
Figure 5.11 (top) Percent ice cover remaining on Upper and Lower Murray Lakes plotted as a function of cumulative melting degree days (CMDD). Plots include all data from 1997-2007, with each data point reflecting the percentage of ice cover remaining and the total CMDD on the date the SAR image was acquired. (bottom) Cumulative melting degree days calculated based on mean daily temperatures during 1997-2007 and 0.5, 1.0, and 1.5°C reductions from this mean. Comparison of the top and bottom panels indicate that complete melting of Upper and Lower Murray Lakes is unlikely to occur if temperatures are reduced by 1.0°C, resulting in an end of melt-season total of only ~250 cumulative melting degree days.
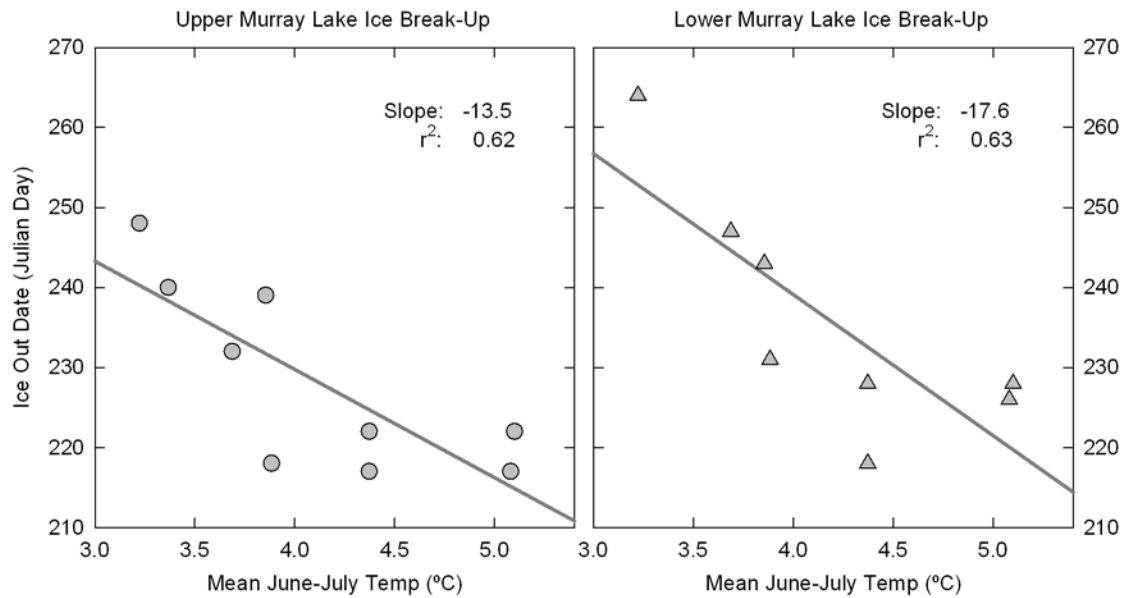
Figure 5.12 Plots showing the relationship between the timing of ice out and mean June and July surface air temperatures. Linear regression lines indicated that ice out occurs ~14 and ~18 days earlier on Upper and Lower Murray Lakes, respectively, per 1.0°C temperature increase.

CHAPTER 6

SUMMARY & CONCLUSIONS

This study was initially motivated by uncertainties related to projections of future changes in the global climate system. Knowledge of how the Earth system has responded to various forcing mechanisms in the past provides a useful baseline for assessing how the Earth may respond to anticipated changes in the future. By focusing on climate and environmental change in the High Arctic, this study examined a region that is particularly sensitive to global climate change – a region that is likely to have experienced large changes in the past and which should demonstrate the first telltale signs of ongoing and future changes. Because of the high sensitivity of the Arctic to climate change, the impacts of global warming on humans and the environment are likely to be particularly severe. While global surface temperatures are projected to rise by 1.1 to 6.4°C during the 21st century (Solomon et al., 2007), warming in the Arctic is expected to be two to three times this global average (Holland and Bitz, 2003).

Despite the potential impacts of climate change on the Arctic, and the significance of the Arctic to the global climate system, our understanding of the Arctic climate system has been severely limited by a lack of information pertaining to past climatic conditions. Consequently, this study was designed with the overarching goal of improving our understanding of the nature, causes, and impacts of past climatic conditions in the High Arctic and to evaluate the potential impacts of future climatic warming. These goals were addressed by focusing on Upper and Lower Murray Lakes (81° 21' N, 69° 32' W) on northern Ellesmere Island, Nunavut, Canada. The sedimentary archives preserved in these lakes were used to reconstruct past environmental conditions in the High Arctic and the response of these lakes to ongoing climate change was evaluated using recent observations derived from remotely sensed satellite data. The results described herein present critical new insight into past environmental change in the High Arctic and provide important details about ongoing changes to arctic lake systems. Specifically, this study produced the longest annually resolved, quantitative temperature reconstruction yet recovered from the high Arctic and documented recent changes in the characteristics of the ice cover of arctic lakes.

The climatic setting of the Murray Lakes, characterized by extreme seasonality, and the physical characteristics of the lakes, including an extended ice cover, reduced mixing, and oxygen depleted bottom

waters have led to the formation and preservation of annually laminated sediments (varves). Varved sediments provide a valuable paleolimnologic tool because they provide precise chronological control and can be used as an indicator of past environmental conditions. The varved sediments in Lower Murray Lake were used to evaluate the first two hypotheses outlined in the introduction to this study:

1. The physical characteristics of annually laminated sediments in high Arctic lakes are a sensitive indicator of past climate variability.

2. Changes in summer climate in the High Arctic are related to shifts in radiative forcing caused by variations in solar irradiance, explosive volcanism, and the concentration of greenhouse gases in the atmosphere.

The physical and chemical characteristics of the sediments in Lower Murray Lake record the evolution of the lake basin following the retreat of the Innuitian Ice Sheet ca. 6000 ^{14}C years BP. These data indicate a period of rapid deposition of coarse clastic material during the early history of the lake, followed by a transitional period marked by decreasing grain size and sediment accumulation. These changes occur simultaneously with the onset of anoxia in bottom waters attributed to enhanced productivity and reduced mixing of the water column. Varve deposition began ca. 5200 calendar years BP and continued through 2004 AD. Relative to the earlier portion of the record, the physical and chemical characteristics of the sediments remain relatively stable throughout the period of varve deposition, suggesting that weathering, erosion, and sediment transport processes in the watershed, as well as physical, chemical, and biological conditions within the lake have not undergone major changes during this period.

Lower Murray Lake varves contain an annual record of sediment mass accumulation spanning the past ~5200 years. In general, periods of elevated sediment accumulation coincide with periods of presumed warm conditions in the past. Likewise, suspected cold periods in the past are associated with low rates of sedimentation in Lower Murray Lake. Lower Murray Lake mass accumulation rates were positively correlated with mean July 600 m free air temperatures at the two nearest permanent weather stations at Alert and Eureka. Calibration of the MAR timeseries provided a quantitative estimate of the magnitude of past temperature variability. These results indicate that decadal-scale patterns of sedimentation in Lower Murray Lake are influenced by regional temperatures driven by radiative forcing mechanisms including variations in solar irradiance, explosive volcanism, and greenhouse gas concentrations. The lowest rates of

sediment accumulation, and by inference the coldest periods occurred around varve year 1800 AD and prior to ~4200 varve years ago. In contrast, periods of increased sedimentation, and by inference the warmest conditions, occurred in the twelfth, fourteenth, and twentieth centuries, and throughout the middle portion of the record, approximately 1000 to 4200 varve years ago.

Lower Murray Lake sediments maintain a consistent pattern of deposition throughout the period of record and respond predictably to presumed climatic conditions in the past. Despite the complexity and inherent uncertainty in the varve-climate process network, the stability of the Lower Murray Lake sedimentary system supports the use of annual mass accumulation as a proxy indicator of climatic conditions in the past. Nonetheless, discrepancies between the Lower Murray Lake varve record and other regional paleoclimate records highlight the need to validate varve-based climate reconstructions using multiple lines of evidence from numerous locations.

Quantitative estimates of past temperature variability are now available from a variety of proxy indicators. However, significant discrepancies exist between the available records in terms of both the timing and amplitude of past climatic fluctuations. The limited number of paleotemperature records from the Canadian Arctic is currently inadequate to address these discrepancies and identify spatial patterns of past temperature conditions. Because individual proxies have differing sensitivity to past climatic conditions, paleotemperature reconstructions should rely on multiple proxies to better capture the full range of climatic variability. Two clear objectives emerge from this review of current paleotemperature records from the Canadian Arctic: (1) Additional spatial coverage is needed in the distribution of proxy reconstructions. Because lakes are widely distributed throughout the region, paleolimnological studies likely provide the best opportunity for increased spatial coverage. (2) Replication of temperature reconstructions is necessary within a given region. This includes the production of additional records using the same proxies at different sites and new records which combine multiple proxies. These records should provide better insight into the full range of temperature variability, including both long-term trends and short period variations, allowing the amplitude of past changes to be better constrained.

The possibility exists for continued work on the Murray Lakes which may provide further insight into past environmental change in the region. Although the nature and preservation quality of the sediment cores recovered from Upper Murray Lake were not conducive to a varve analysis, a reasonably robust

radiocarbon chronology was derived from these sediments. Should a suitable proxy be identified, these sediments could produce a valuable paleoenvironmental record based on a chronology completely independent of the varve and paleomagnetic chronology used in this study. One possible proxy indicator includes the U^K_{37} index of long-chain alkenones. Alkenone peleothermometry offers the potential to provide an independent, quantitative estimate of past temperature from the Murray Lakes which could be compared with the varve-based record from Lower Murray Lake. Ongoing work by William D'Andrea at the University of Massachusetts is currently exploring the potential for alkenone peleothermometry in the cores from Lower Murray Lake.

Recent environmental changes in the High Arctic are evident within the observational period of satellite and instrumental measurements providing a means of evaluating the third hypothesis outlined in the introduction of this study: Ice cover on high arctic lakes is sensitive to small temperature changes and recent warming has caused a significant reduction in the duration of ice cover on high arctic lakes. Space-borne synthetic aperture radar data were used to interpret the climatic sensitivity of the ice-cover on Upper and Lower Murray Lake. Comparison with reanalysis air temperature records allowed for quantification of the relationship between ice cover and climatic conditions. The summer temperature conditions necessary for the complete melting of the ice covers on Upper and Lower Murray Lakes are very near current mean climatic conditions, suggesting that the two lakes are at or near a threshold between a state of perennial ice cover and regular seasonal melting of their ice covers. Recent (20th century) warming has likely forced the Murray Lakes across this threshold, and projected future warming due to anthropogenic causes will further increase the duration of ice free conditions on these lakes. Although the exact response of lake ice to temperature changes will vary according to the local geographic and climatic setting as well as the characteristics of the individual lake, the results presented here indicate that profound changes in the ice cover of high-arctic lakes have recently occurred and that even greater changes should be expected in the future. Given the significance of the timing of ice out and the length of open water conditions to so many physical, chemical, and biological processes acting both within and beyond the lake, future changes in lake ice cover are likely to have a significant impact on high-arctic environments.

APPENDIX 1

THIN SECTION PHOTOGRAPHS

Appendix 1 Ordered sequence of thin section images used in the construction of the Lower Murray Lake varve chronology. Labeled features denote marker beds used to tie the sequence together between successive images.

01-LML-001_XP.tif   02-LML-080_XP.tif   03-LML-002_XP.tif   04-LML-010_XP.tif   05-LML-003_XP.tif

06-LML-083_XP.tif   07-LML-084_XP.tif   08-LML-004_XP.tif   09-LML-005_XP.tif   10-LML-006_XP.tif

11-LML-007_XP.tif

12-LML-008_XP.tif

13-LML-009_XP.tif

14-LML-093_XP.tif

15-LML-094_XP.tif

16-LML-095_XP.tif

17-LML-024_XP.tif

18-LML-096_XP.tif

19-LML-097_XP.tif

20-LML-098_XP.tif
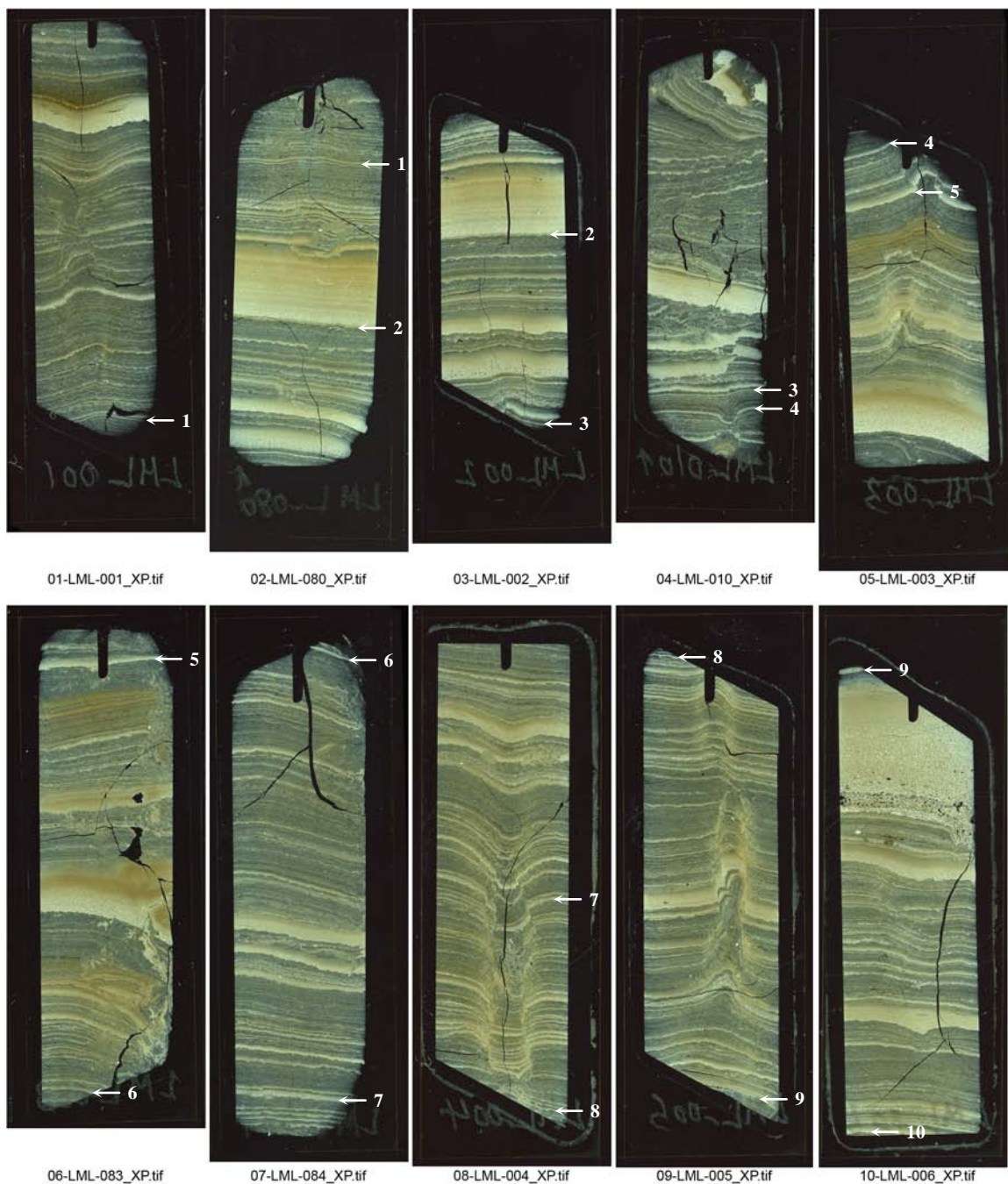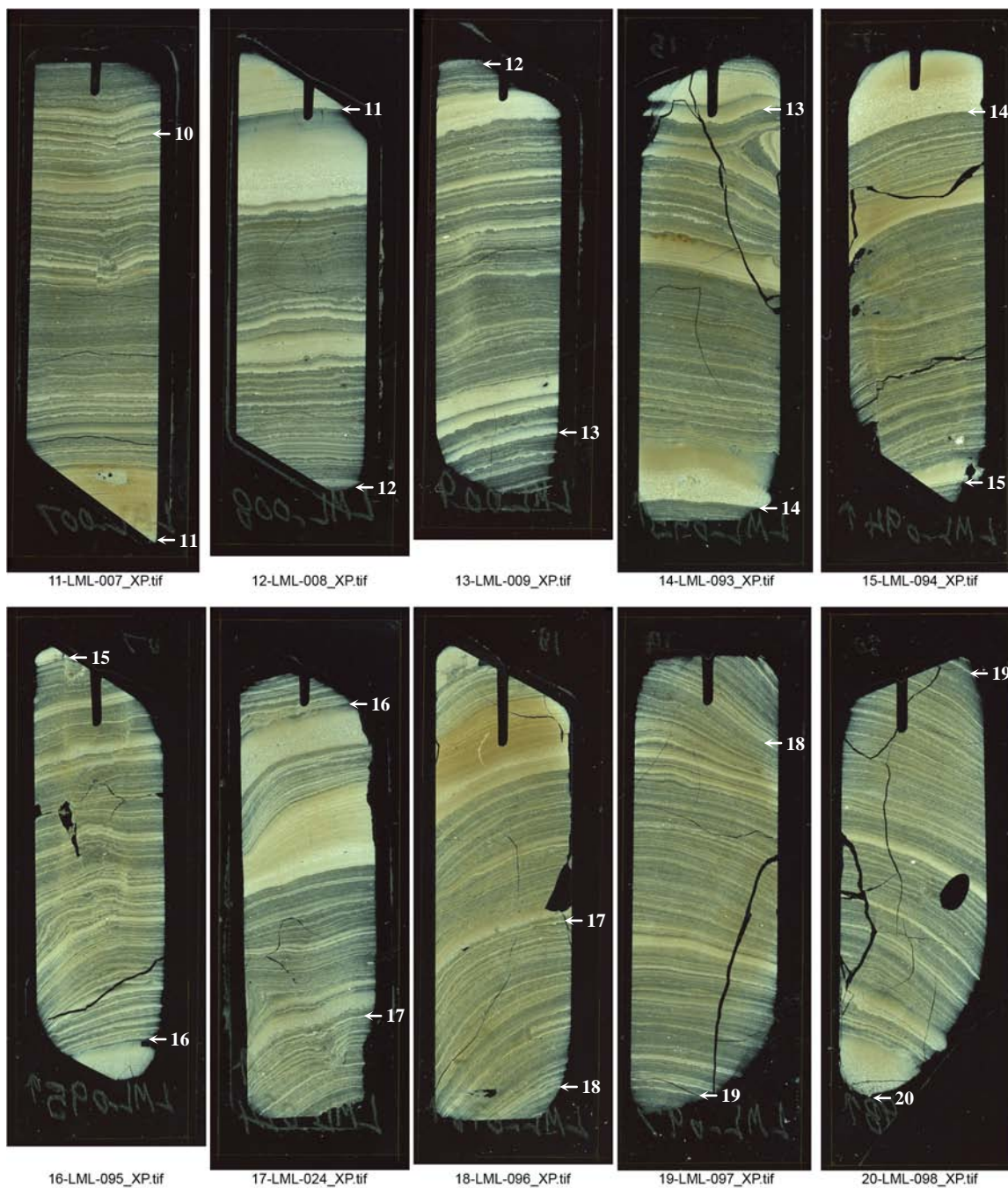
(Appendix 1, continued)

21-LML-099_XP.tif   22-LML-100_XP.tif   23-LML-101_XP.tif   24-LML-029_XP.tif   25-LML-102_XP.tif

26-LML-030_XP.tif   27-LML-055_XP.tif   28-LML-031_XP.tif   29-LML-056_XP.tif   30-LML-032_XP.tif

31-LML-057_XP.tif 32-LML-058_XP.tif 33-LML-034_XP.tif 34-LML-059_XP.tif 35-LML-035_XP.tif

36-LML-036_XP.tif 37-LML-061_XP.tif 38-LML-062_XP.tif 39-LML-040_XP.tif 40-LML-063_XP.tif

41-LML-064_XP.tif   42-LML-065_XP.tif   43-LML-066_XP.tif   44-LML-067_XP.tif   45-LML-045_XP.tif

46-LML-068_XP.tif   47-LML-046_XP.tif   48-LML-069_XP.tif   49-LML-070_XP.tif   50-LML-071_XP.tif

51-LML-049_XP.tif   52-LML-072_XP.tif   53-LML-073_XP.tif   54-LML-051_XP.tif   55-LML-074_XP.tif

56-LML-075_XP.tif   57-LML-076_XP.tif   58-LML-077_XP.tif

APPENDIX 2

INDEX OF THIN SECTIONS

Appendix 2 Index of all thin sections produced from Upper and Lower Murray Lake Sediments.

Thin Section ID	Core Section	Depth Interval w/in section (cm)	Thin Section ID	Core Section	Depth Interval w/in section (cm)
LML-001	LML-05 Ekman4	0-7	LML-052	LML-05 C1-A2	73.5-80
LML-002	LML-05 Ekman4	6-11.5	LML-053	LML-05 C1-A2	80-85.5
LML-003	LML-05 Ekman4	10.5-16	LML-054	LML-05 C1-A2	85.5-91.5
LML-004	LML-05 Short Core 2	19-26	LML-055	LML-05 C2-A2	0-7
LML-005	LML-05 Short Core 2	25-32	LML-056	LML-05 C2-A2	6-13
LML-006	LML-05 Short Core 2	31-38	LML-057	LML-05 C2-A2	12.5-19.5
LML-007	LML-05 Short Core 2	37-44	LML-058	LML-05 C2-A2	18.5-25.5
LML-008	LML-05 Short Core 2	43-50	LML-059	LML-05 C2-A2	24.5-31
LML-009	LML-05 Short Core 2	49-56	LML-060	LML-05 C2-A2	31-37
LML-010	LML-05 Short Core1	0-6.5	LML-061	LML-05 C2-A2	36.5-43
LML-011	LML-05 Short Core1	6.5-12.5	LML-062	LML-05 C2-A2	42.5-49
LML-012	LML-05 Short Core1	12.5-19.5	LML-063	LML-05 C2-A2	49-55.5
LML-013	LML-05 Short Core1	16-23	LML-064	LML-05 C2-A2	55-62
LML-014	LML-05 Short Core1	22-28	LML-065	LML-05 C2-A2	61.5-68
LML-015	LML-05 Short Core1	27.5-35	LML-066	LML-05 C2-A2	67.5-74.5
LML-016	LML-05 C1-A1	0-7	LML-067	LML-05 C2-A2	73-80
LML-017	LML-05 C1-A1	6-13	LML-068	LML-05 C2-A2	80-86
LML-018	LML-05 C1-A1	12-19	LML-069	LML-05 C2-A2	86-92
LML-019	LML-05 C1-A1	18-25	LML-070	LML-05 C2-A2	91-97.5
LML-020	LML-05 C1-A1	24-31	LML-071	LML-05 C2-A2	98.5-104
LML-021	LML-05 C1-A1	30-37.5	LML-072	LML-05 C2-A2	104-110
LML-022	LML-05 C1-A1	37.5-44	LML-073	LML-05 C2-A2	109-115.5
LML-023	LML-05 C1-A1	44-50	LML-074	LML-05 C2-A2	116-122
LML-024	LML-05 C1-A1	50-56.5	LML-075	LML-05 C2-A2	122-128
LML-025	LML-05 C1-A1	56-63	LML-076	LML-05 C2-A2	125.5-132
LML-026	LML-05 C1-A1	62.5-69.5	LML-077	LML-05 C2-A2	132-138
LML-027	LML-05 C1-A1	68.5-74.5	LML-078	LML-05 C2-A2	138-144
LML-028	LML-05 C1-A1	74-81	LML-079	LML-05-Ekman 5	0-6.3
LML-029	LML-05 C1-A1	81-87	LML-080	LML-05-Ekman 5	5.8-12
LML-030	LML-05 C1-A1	87-94	LML-081	LML-05 Short Core 2	0-7
LML-031	LML-05 C1-A1	93-99.5	LML-082	LML-05 Short Core 2	6-13
LML-032	LML-05 C1-A1	99.7-106.2	LML-083	LML-05 Short Core 2	9-16
LML-033	LML-05 C1-A1	106.5-112.2	LML-084	LML-05 Short Core 2	15.5-23
LML-034	LML-05 C1-A1	111.7-118.7	LML-085	LML-05-C2-A1	0-7
LML-035	LML-05 C1-A1	118.5-125	LML-086	LML-05-C2-A1	6.5-13
LML-036	LML-05 C1-A1	124.5-131	LML-087	LML-05-C2-A1	13-19.5
LML-037	LML-05 C1-A1	125-130	LML-088	LML-05-C2-A1	19-24.5
LML-038	LML-05 C1-A1	130-135.5	LML-089	LML-05-C2-A1	24.5-31.5
LML-039	LML-05 C1-A1	136-140	LML-090	LML-05-C2-A1	31-37.5
LML-040	LML-05 C1-A2	0-7	LML-091	LML-05-C2-A1	37-43.5
LML-041	LML-05 C1-A2	7.5-13	LML-092	LML-05-C2-A1	43.5-49.5
LML-042	LML-05 C1-A2	13-19	LML-093	LML-05-C2-A1	50-56.5
LML-043	LML-05 C1-A2	18.5-25	LML-094	LML-05-C2-A1	55-62
LML-044	LML-05 C1-A2	25-31	LML-095	LML-05-C2-A1	61.5-68
LML-045	LML-05 C1-A2	31-37.5	LML-096	LML-05-C2-A1	67.5-74
LML-046	LML-05 C1-A2	37-43.5	LML-097	LML-05-C2-A1	73.5-79.5
LML-047	LML-05 C1-A2	43.5-50	LML-098	LML-05-C2-A1	79.5-85.5
LML-048	LML-05 C1-A2	49.5-56	LML-099	LML-05-C2-A1	85.5-92
LML-049	LML-05 C1-A2	55-61.5	LML-100	LML-05-C2-A1	89.5-95.5
LML-050	LML-05 C1-A2	61-67	LML-101	LML-05-C2-A1	95-101.5
LML-051	LML-05 C1-A2	67.5-74	LML-102	LML-05-C2-A1	101-107.5

(Appendix 2, continued)

Thin Section ID	Core Section	Depth Interval w/in section (cm)
UML-001	UML-05 Grab A-1	0-5.5
UML-002	UML-05 Grab A-1	4.5-10
UML-003	UML-05 AR-1	0-7
UML-004	UML-05 AR-1	6-13
UML-005	UML-05 AR-1	12-19
UML-006	UML-05 AR-1	15.5-22.5

BIBLIOGRAPHY

Abbott, M. B., and Stafford, T. W., 1996. Radiocarbon geochemistry of modern and ancient Arctic lake systems, Baffin Island, Canada, Quaternary Research, 45:300-311.

ACIA, 2004. *Impacts of a Warming Arctic*, Cambridge University Press, Cambridge.

Adams, W. P., 1981. Snow and ice on lakes. In Grey, D. M., and Male, D. H. (eds.), *Handbook of Snow and Ice: Principles, Processes, Management and Use*. Canada: Pergamon, 437-474.

Adams, W. P., Doran, P. T., Ecclestone, M., Kingsbury, C. M., and Allan, C. J., 1989. A rare second year – lake ice cover in the Canadian High Arctic. *Arctic,* 42: 299-306.

Adams, W. P., and Roulet, N. T., 1980. Illustration of the roles of snow in the evolution of the winter cover of a lake. *Arctic,* 33: 100-116.

Alley, R. B., 2000. The Younger Dryas cold interval as viewed from central Greenland. *Quaternary Science Reviews,* 19:213-226.

Alley, R. B., 2004. GISP2 Ice Core Temperature and Accumulation Data. IGBP PAGES/World Data Center for Paleoclimatology Data Contribution Series #2004-013. NOAA/NGDC Paleoclimatology Program, Boulder CO, USA.

Anderson, L., Abbott, M. B., and Finney, B. P., 2001. Holocene climate inferred from oxygen isotope ratios in lake sediments, central Brooks Range, Alaska, *Quaternary Research,* 55: 313-321.

Anderson, N. J., Harriman, R., Ryves, D. B., and Patrick, S. T., 2001. Dominant factors controlling variability in the ionic composition of West Greenland lakes, *Arctic, Antarctic, and Alpine Research,* 33:418-425.

Anderson, R. K., Miller, G. H., Briner, J. P., Lifton, N. A., and DeVogel, S. B., 2008. A millennial perspective on Arctic warming from ^{14}C in quartz and plants emerging from beneath ice caps, *Geophysical Research Letters,* 35, doi:10.1029/2007GL032057.

Appleby, P. G., and Oldfield, F., 1978. The calculation of ^{210}Pb dates assuming a constant rate of supply of unsupported ^{210}Pb to the sediment. *Catena* 5:1-8

Ashton, G. D., 1980. Freshwater ice growth, motion, and decay. In Colbeck, S. C. (ed.), *Dynamics of Snow and Ice Masses*. Academic Press, New York, 261-304.

Ashton, G. D., 1983. Lake ice decay. *Cold Regions Science and Technology,* 8: 83-86.

Assel, R. A., and Robertson, D. M., 1995. Changes in winter air temperatures near Lake Michigan, 1851-1993, as determined from regional lake-ice records. *Limnology and Oceanography*, 40: 165-176.

Axford, Y., Briner, J. P., Miller, G. H., and Francis, D. R., 2009. Paleoecological evidence for abrupt cold reversals during peak Holocene warmth on Baffin Island, Arctic Canada, *Quaternary Research*, 71: 142-149.

Barry. R. G., 2002, The role of snow and ice in the global climate system: a review, *Polar Geopgraphy*, 26:235-246.

Battarbee, R. W., 2000. Paleolimnological approaches to climate change, with special regard to the biological record, *Quaternary Science Reviews,* 19: 107-124.

Belzile, C., Vincent, W. F., Gibson, J. A. E., and Van Hove, P., 2001. Bio-optical characteristics of the snow, ice, and water column of a perennially ice-covered lake in the High Arctic. *Canadian Journal of Fisheries and Aquatic Science*, 58: 2405–2418.

Berger, A. and Loutre, M. F., 1991. Insolation values for the climate of the last 10 million years. *Quaternary Sciences Review*, 10: 297-317.

Besonen, M. R., Patridge, W., Bradley, R. S., Francus, P., Stoner, J., and Abbott, M., 2008. A record of climate over the last millennium based on varved lake sediments from the Canadian High Arctic. *Holocene*, 18: 169-180.

Bilello, M. A., 1980. *Maximum thickness and subsequent decay of lake, river, and fast sea ice in Canada and Alaska, Report 80-6*. Hanover, NH: U.S. Army Cold Regions Research and Engineering Laboratory, 160 pp.

Blake, W. J., 1981. Neoglacial fluctuations of glaciers, Southeastern Ellesmere Island, Canadian Arctic Archipelago, *Geografiska Annaler*, 63: 201-218.

Blass, A., Grosjean, M., Troxler, M., and Sturm, M., 2007. How stable are twentieth-century calibration models? A high-resolution summer temperature reconstruction for the eastern Swiss Alps back to AD 1580 derived from proglacial varved sediments, *Holocene*, 17: 51-63.

Boyle, J. F., 2001. Inorganic Geochemical methods in paleolimnology, In Last, W. M. and Smol, J. P. (eds.), *Tracking Environmental Change Using Lake Sediments Volume 2: Physical and Geochemical Methods*, Dordrecht Kluwer Academic Publishers, pp. 83-142.

Bradley, R. S., 1990. Holocene paleoclimatology of the Queen Elizabeth Islands, Canadian High Arctic, *Quaternary Science Reviews*, 9: 365-384.

Braun, C., 2006. *Sensitivity of the Hazen Plateau and North Coast, Ellesmere Island, Nunavut, Canada to Climate Change*, dissertation, University of Massachusetts Amherst, 519 pp.

Braun, C., Hardy, D. R., Bradley, R. S., Retelle, M. J., 2000a. Streamflow and suspended sediment transfer to Lake Sophia, Cornwallis Island, Nunavut, Canada, *Arctic, Antarctic and Alpine Research*, 32: 45-465.

Braun, C., Hardy, D. R., Bradley, R. S, Retelle, M. J., 2000b. Hydrological and meteorological observations at Lake Tuborg, Ellesmere Island, Nunavut, Canada, *Polar Geography*, 24: 83-97.

Brassell, S. C., Eglinton, G., Marlowe, I. T., Pflaumann, U. and Sarnthein, M., 1986. Molecular stratigraphy: A new tool for climatic assessment. *Nature*, 320: 129.

Briffa, F. R., Jones, P. D., and Schweingruber, F. H., 1994. Summer temperatures across northern North America: regional reconstructions from 1760 using tree-ring indices, *Journal of Geophysical Research*, 99D: 25835-25844.

Briner, J. P., Axford, Y., Formna, S. L., Miller, G. H., Wolfe, A. P., 2008. Multiple generations of interglacial sediment preserved beneath the Laurentide Ice Sheet, *Geology*, 35: 887-890.

Briner, J. P., Michelutti, N., Francis, D. R., Miller, G. H,. Axford, Y., Wooller, M. J., and Wolfe, A. P., 2006. A multi-proxy lacustrine record of Holocene climate change on northeastern Baffin Island, Arctic Canada, *Quaternary Research*, 65: 431-442.

Burgess, D. O., and Sharp, M. J., 2004. Recent changes in areal extent of the Devon Ice Cap, Nunavut, Canada, *Arctic, Antarctic, and Alpine Research* 36, 261–71.

Burgess, D. O., Sharp, M. J., Mair, D. W. F., Dowdeswell, J. A., and Benham, T. J., 2005. Flow dynamics and iceberg calving rates of Devon Ice Cap, Nunavut, Canada. *Journal of Glaciology* 51, 219–30.

Charles, C., Rind, D., Jouzel, J., Koster, R., and Fairbanks, R., 1994. Glacial interglacial changes in moisture sources for Greenland: Influences on the ice core record of climate, *Science*, 261: 508-511.

Christensen, J. H., Hewitson, B., Busuioc, A., Chen, A., Gao, X., Held, I., Jones, R., Kolli, R. K., Kwon, W.-T., Laprise, R., Magaña Rueda, V., Mearns, L., Menéndez, C. G., Räisänen, J., Rinke, A., Sarr, A., and Whetton, P., 2007: Regional Climate Projections. In Solomon, S., Qin, D., Manning, M., Chen, Z., Marquis, M., Averyt, K. B., Tignor M., and Miller, H. L., (eds.), *Climate Change 2007: The Physical Science Basis. Contribution of Working Group I to the Fourth Assessment Report of the Intergovernmental Panel on Climate Change,* United Kingdom and New York, NY: Cambridge University Press, 848-940.

Clausen, H. B., Stampe, M., Hammer, C. U., Hvidberg, C. S., Dahl-Jensen, D., and Steffensen, J. P., 2001. Glaciological and chemical studies on ice cores from Hans Tausen Iskappe, Greenland, *Meddelelser om Grønland, Geoscience,* 39: 123-150.

Cook, T. L., Bradley, R. S., Stoner, J. S., and Francus, P., 2009. Five thousand years of sediment transfer in a High Arctic watershed recorded in annually laminated sediments from Lower Murray Lake, Ellesmere Island, Nunavut, Canada, *Journal of Paleolimnology*, 41: 77-94.

Cockburn, J. M. H., and Lamoureux, S. F., 2007. Hydroclimate controls over seasonal sediment yield in two adjacent High Arctic watersheds. *Hyrdological Processes,* doi:10.1001/hyp.6798.

Cockburn, J. M. H.,and Lamoureux, S. F., 2008. Inflow and lake controls on short-term mass accumulation and sedimentary particle size in a High Arctic lake: implications for interpreting varve lacustrine sedimentary records. *Journal of Paleolimnology*, doi:10.1007/s10933-008-9207-5.

Cohen, A. D., 2003. *Paleolimnology, The History and Evolution of Lake Systems*, Oxford University Press, Oxford, 500 pp.

Copland, L., Mueller, D. R., Weir, L., 2007. Rapid loss of the Ayles Ice Shelf, Ellesmere Island, Canada, *Geophysical Research Letters*, 34: L21501, doi:10.1029/2007GL031809.

Comiso, F. C., 2003. Warming trends in the Arctic from Clear Sky Satellite Observations, *Journal of Climate*, 16: 3498-3510.

Croudace, I. W., Rindby, A., and Rothwell, R. G., 2006. ITRAX: description and evaluation of a new multi-function X-ray core scanner, In: Rothwell, R. G. (ed) *New Techniques in Sediment Core Analysis*, Geological Society, London, Special Publications, 267: 51-63.

Crowley, T. J., 2000. Causes of climate change over the past 1000 years. *Science,* 289: 270-277.

Cuffey, K. M., and Clow, G. D., 1997. Temperature, accumulation, and ice sheet elevation in central Greenland through the last deglacial transition, *Journal of Geophysical Research*, 102:26383-26396.

Dahl-Jensen, D., Mosegaard, K., Gundestrup, N, Clow, G. D., Johnsen, S. J., Hansen, A. W., and Balling, N., 1998. Past temperatures directly from the Greenland ice sheet, *Science*, 282: 268-271.

D'Andrea, W. J., 2009, *Development and Application of Lacustrine Alkenono Paleothermometry in Southwestern Greenland,* PhD thesis, Brown University, Providence, RI, 179 pp.

D'Andrea, W. J., and Huang, Y., 2005. Long-chain alkenones in Greenland lake sediments: low $\delta^{13}C$ values and exceptional abundance. *Organic Geochemistry,* 36: 1234-1241.

Dansgaard, W. 1964. Stable isotopes in precipitation, *Tellus*, 16:436-467.

Davidge, G. D. 1994. *Physical limnology and sedimentology of Romulus Lake: a meromictic lake in the Canadian High Arctic*. M.Sc. thesis, Queen's University, Kingston, Ontario, 114 pp.

Davison, W., 1993, Iron and manganese in lakes, *Earth Science Reviews*, 34: 119-163.

Dean, W. E. J., 1974. Determination of carbonate and organic matter in calcareous sediments and sedimentary rocks by loss on ignition: comparison with other methods. *Journal of Sedimentary Petrology,* 44: 242-248.

Desloges, J. R., Gilbert, R. E., 1991. Sedimentary record of Harrison Lake: implications for deglaciation in Southwestern British Columbia, *Canadian Journal of Earth Sciences*, 28: 800–815.

Dokulil, M. T., 1994. Environmental control of phytoplankton productivity in turbulent turbid systems, *Hydrobiologia*, 289: 65-72.

Doran, P. T., McKay, C. P., Adams, W. P., English, M. C., Wharton Jr., R. A. and Meyer, M. A., 1996. Climate forcing and thermal feedback of residual lake-ice covers in the high Arctic. *Limnology and Oceanography*, 41: 839-848.

Douglas, M. S. V., and Smol, J. P., 1999. Freshwater diatoms as indicators of environmental change in the High Arctic, In Stoermer, E. F. and Smol, J. P. (eds.), *The Diatoms: Applications for the Envrionmental and Earth sciences,* Cambridge University Press, Cambridge, 227-244.

Dowdeswell, J. A., Hagen, J. O., Bjornsson, H., Glazovsky, A. F., Harrison, W. D., Holmlund, P., Jania, J., Koerner, R. M., Lefauconnier, B., Ommanney, C. S. L. and Thomas, R. H., 1997. The mass balance of circum-Arctic glaciers and recent climate change. *Quaternary Research* 48: 1–14.

Duguay, C. R., Flato, G. M., Jeffries. M. O., Ménard, P., Morris, K., and Rouse, W., 2003. Ice-cover variability on shallow lakes at high latitudes: model simulations and observations. *Hydrological Processes,* 17: 3465-3483.

Embody, G. C. 1927. An outline of stream study and the development of a stocking policy, Cornell University Aquaculture Laboratory, Ithaca, New York., 21 pp.

England, J. H., Lakeman, T. R., Lemmen, D. S., Bednarski, J. M., Stewart, T. G., and Evans, D. J A., 2008. A millennial-scale record of Arctic Ocean sea ice variability and the demise of the Ellesmere Island ice shelves, *Geophysical Research Letters*, 35, L19502, doi:10.1029/2008GL034470.

England, J. 1977. The glacial geology of northeastern Ellesmere Island, N. W. T., Canada, *Canadian Journal of Earth Science*, 15: 603-617.

England, J., 1983. Isostatic adjustments in a full glacial sea, *Canadian Journal of Earth Science,* 20: 895-917.

England, J., Atkinson, N., Bednarski, J., Dyke, A. S., Hodgson, D. A., and Cofaigh, C. Ó., 2006. The Innuitian Ice Sheet: configuration, dynamics and chronology, *Quaternary Science Reviews*, 25: 689-703.

Esper, J. E., Frank, D. C., Wilson, R. J. S., Briffa, K. R., 2005. Effect of scaling and regression on reconstructed temperature amplitude for the past millennium. *Geophysi al Research Letters* 32: doi:10.1029/2004GL021236.

Esper, J., Wilson, R. J.S., Frank, D. C., Moberg, A., Wanner, H., Luterbacher, J., 2005. Climate: past ranges and future changes, *Quaternary Science Reviews*, 24: 2164-2166.

Ferris, J. M., Gibson, J. A. E., and Burton, H. R. 1991. Evidence of density currents with the potential to promote meromixis in ice-covered saline lakes, *Palaeogeography, Palaeoclimatology, Palaeoecology*, 84: 99–107.

Forbes, A. C., Lamoureux, S. F., 2005. Climatic controls on streamflow and suspended sediment transport in three large Middle Arctic catchments, Boothia Peninsula, Nunavut Canada. *Arctic, Antarctic, and Alpine Research,* 37: 304-315.

Francis, D. R., Wolfe, A. P., Walker, I. R., and Miller, G. H., 2006. Interglacial and Holocene temperature reconstructions based on midge remains in sediments of two lakes from Baffin Island, Nunavut, Arctic Canada, *Palaeogeography, Palaeoclimatology, Palaeoecology,* 236: 107-124.

Francus, P., and Asikainen, C., 2001. Sub-sampling unconsolidated sediments: a solution for the preparation of undisturbed thin-sections from clay-rich sediments. *Journal of Paleolimnolgy*, 26: 323-326.

Francus, P., Bradley, R. S., Abbott, M. B., Patridge, W., Keimig, F., 2002. Paleoclimate studies of minerogenic sediments using annually resolved textural parameters. *Geophysical Research Letters*, 29: doi:1029/2002GL015082.

Francus, P., Bradley, R. S., Lewis, T., Abbott, M. B., Retelle, M., and Stoner, J. S., 2008. Limnological and sedimentary processes at Sawtooth Lake, Canadian High Arctic, and their influence on varve formation, *Journal of Paleolimnolgy*, 40: 963-985.

Fisher, D. A., and Koerner, R. M., 1994. Signal and noise in four ice-core records from the Agasiiz Ice Cap, Ellesmere Island, Canada: details of the last millennium for stable isotopes, melt and solid conductivity, *Holocene*, 4: 113-120.

Fisher, D. A., Koerner, R. M., Paterson, W. S. B., Dansgaard, W., Gundestrup, N., and Reeh, N., 1983. Effect of wind scouring on climatic records from ice-core oxygen-isotope profiles, *Nature*, 301: 205-209.

Fisher, D. A., Koerner, R. M., and Reeh, N., 1995. Holocene climatic records from Agassiz Ice Cap, Ellesmere Island, NWT, Canada, *Holocene,* 5: 19-24.

Fisher, D. A., Koerner, R. M., Bourgeois, J. C., Zielinski, G., Wake, C., Hammer, C. U., Clausen, H. B., Gundestrup, N., Johnsen, S., Goto-Azuma, K., Hondoh, T., Blake, E., and Gerasimoff M., 1998. Penny Ice Cap cores, Baffin Island, Canada, and the Wisconsinan Foxe Dome connection: two states of Hudson Bay ice cover, *Science,* 279: 692-695.

Gajewski, K., and Atkinson, D. A., 2003. Climatic change in northern Canada. *Environmental Reviews*, 11:69-102.

Gajewski, K., Hamilton, P. B., and McNeely, R., 1997. A high resolution proxy-climate record from an arctic lake with annually-laminated sediments on Devon Island, Nunavut, Canada, *Journal of Paleolimnology,* 17: 215-225.

Gilbert, R., Desloges, J. R., 1992. The late Quaternary sedimentary record of Stave Lake, southwestern British Columbia, *Canadian Journal of Earth Sciences,* 29: 1997–2006.

Grove, J. M., 2001. The initiation of the 'Little Ice Age' in regions round the North Atlantic, *Climatic Change,* 48: 53-82.

Hambley, G. W., and Lamoureux, S. F., 2006. Recent summer climate recorded in complex varved sediments, Nicolay Lake, Cornwall Island, Nunavut, Canada. *Journal of Paleolimnolgy,* 35:629-640.

Hammer, C. U., Johnsen, S. J., Clausen H. B., Dahl-Jensen, D., Gundestrup, N., and Jørgen Peder Steffensen, 2001. The paleoclimatic record from a 345 m long ice core from the Hans Tausen Iskappe, *Meddelelser om Grønland, Geoscience,* 39: 87-96.

Hardy, D. R., 1996. Climatic influences on streamflow and sediment flux into Lake C2, Northern Ellesmere Island, Canada, *Journal of Paleolimnology,* 16: 133-149.

Hardy, D. R., Bradley, R. S., Zolitschka, B., 1996. The climatic signal in varved sediments from Lake C2, northern Ellesmere Island, Canada, *Journal of Paleolimnology*, 16: 227-238.

Heiri, O., Lotter, A. F., and Lemcke, G., 2001. Loss on ignition as a method for estimating organic and carbonate content in sediments: reproducibility and comparability of results, *Journal of Paleolimnolgy*, 25: 101-110.

Heron, R., Woo, M.-K., 1994. Decay of a High Arctic lake-ice cover: observations and modeling, *Journal of Glaciology,* 40: 283-292.

Hodder, K. R., Gilbert, R., and Desloges, J. R., 2007. Glaciolacustrine varved sediment as an alpine hydroclimatic proxy, *Journal of Paleolimnolgy*, 38: 365-394.

Holland, M. M., and Bitz, C. M., 2003. Polar amplification of climate change in coupled models, *Climate Dynamics*, 21: 221-232.

Hooke, R. L., and Clausen, H. B., 1982. Wisconsin and Holocene $\delta^{18}O$ variations Barnes Ice Cap, Canada, *Geological Society of America Bulletin*, 93: 784-789.

Hughen, K. A., Overpeck, J. T., and Anderson, R. F., 2000. Recent warming in a 500-year palaeotemperature record from varved sediments, Upper Soper Lake, Baffin Island, Canada, *Holocene*, 10: 9-19.

Hurrell, J. W., Kushnir, Y., Ottersen, G., and Visbeck, M., 2003. An overview of the North Atlantic Oscillation, In Hurrell, J. W., Kushnir, Y., Ottersen, G., and Visbeck, M., (Eds.), *The North Atlantic Oscillation: Climatic Significance and Environmental Impact*, Geophysical Monograph 134, American Geophysical Union, Washington, 279 pp.

Imboden, D. M., and Wuest, A., 1995. Mixing mechanisms in lakes, In Lerman, A. Imboden, D. M., and Gat, J. R., (eds.) *Physics and Chemistry of Lakes*, Springer Verlag, Dordrecht, 83–138.

Jeffries, M. O., Zhang, T., Frey, K., and Kozlenko, N., 1999. Estimating late winter heat flow to the atmosphere from the lake-dominated Alaskan North Slope, *Journal of Glaciology*, 45, 315-324.

Jeffries, M. O., Morris, K., and Kozlenko, N., 2005: Ice Characteristics and Processes, and Remote Sensing of Frozen Rivers and Lakes. In Duguay, C. R., and Pietroniro, A. (eds.), *Remote Sensing in Northern Hydrology: measuring environmental change*, American Geophysical Union, Washington, 63-90.

Johnsen, S. J., Dahl-Jensen, D., Gundestrup, N., Steffensen, J. P., Clausen, H. B., Miller, H., Masson-Delmotte, V., Sveinbjörnsdottir A. E., and White, J., 2001. Oxygen isotope and paleotemperature records from six Greenland ice-core stations: Camp Century, Dye-3, GRIP, GISP2, Renland and NorthGRIP, *Journal of Quaternary Science*, 16: 299-307.

Jouzel, J., Alley, R. B., Cuffey, K. M., Dansgaard, W., Grootes, P., Hoffmann, G., Johnsen, S. J., Koster, R. D., Peel, D., Shuman, C. A., Stievenard, M., Stuiver, M., and White, J., 1997. Validity of the temperature reconstruction from water isotopes in ice cores, *Journal of Geophysical Research*, 102: 26471-26487.

Joynt III, E. H. and Wolfe, A. P., 2001. Paleoenvironmental inference models from sediment diatom assemblages in Baffin Island lakes (Nunavut, Canada) and reconstruction of summer water temperature, *Canadian Journal of Fisheries and Aquatic Science*, 58: 1222–1243.

Kalnay, E., Kanamitsu, M., Kistler, R., Collins, W., Deaven, D., Gandin, L., Iredell, M., Saha, S., White, G., Woollen, J., Zhu, Y., Leetmaa, A., Reynolds, R., Chelliah, M., Ebisuzaki, W., Higgins, W., Janowiak, J., Mo, K. C., Ropelewski, C., Wang, J., Jenne, R., and Joseph, D., 1996. The NCEP/NCAR 40-year reanalysis project. *Bulletin of the American Meteorological Society*, 77: 437-470.

Kaufman, D. S., Ager, T. A., Anderson, N. J., Anderson, P. M., Andrews, J. T., Bartlein, P. J., Brubaker, L. B., Coats, L. L., Cwynar, L. C., Duvall, M. L., Dyke, A. S., Edwards, M. E., Eisner, W. R., Gajewski, K., Geirsdóttir, A., Hu, F. S., Jennings, A. E., Kaplan, M. R., Kerwin, M. W., Lozhkin, A. V., Macdonald, G. M., Miller, G. H., Mock, C. J., Oswald, W. W., Otto-Bliesner, B. L., Porinchu, D. F., Rühland, K., Smol, J. P., Steig, E. J., and Wolfe, B. B., 2004. Holocene thermal maximum in the western Arctic (0-180°W), *Quaternary Science Reviews*, 23: 529-560.

Kerwin, M. W., Overpeck, J. T., Webb, R. S., and Anderson, K. H., 2004. Pollen-based summer temperature reconstructions for the eastern Canadian boreal forest, subarctic, and Arctic, *Quaternary Science Reviews,* 23: 1901-1924.

Koenig, K. A., Shotyk, W., Lotter, A. F., Ohlendorf, C., and Sturm, M., 2003. 9000 years of geochemical evolution of lithogenic major and trace elements of an alpine lake – the role of climate, vegetation and land-use history, *Journal of Paleolimnology*. 30: 307-320.

Koerner, R. M., and Fisher, D. A., 1990. A record of Holocene summer climate from a Canadian high-Arctic ice core, *Nature*, 343: 630-631.

Koerner, R. M., and Paterson, W. S. B., 1974. Analysis of a core through the Meighen Ice Cap, Arctic Canada, and its paleoclimatic implications, *Quaternary Research*, 4: 254-63.

Koerner, R. M., Paterson, W. S. B., and Krouse, H. R., 1973. A δ^{18}O profile in ice formed between the equilibrium and firn lines, *Nature Physical Science*, 245: 137-140.

Lamoureux, S. F., 1999. Spatial and interannual variations in sedimentation patterns recorded in nonglacial varved sediments from the Canadian High Arctic. *Journal of Paleolimnology*, 21: 73-84.

Lamoureux, S. F., 2000. Five centuries of interannual sediment yield and rainfall-induced erosion in the Canadian High Arctic recorded in lacustrine varves, *Water Resources Research*, 36: 309-318.

Lamoureux, S., 2002. Temporal patterns of suspended sediment yield following moderate to extreme hydrological events recorded in varved lacustrine sediments, *Earth Surface Processes and Landforms*, 27: 1107-1124.

Lamoureux, S. F., 2005, A sediment accumulation sensor for use in lacustrine and marine sedimentation studies, *Geomorphology*, 68: 17-23.

Lamoureux, S. F., and Bradley, R. S., 1996. A late Holocene varved sediment record of environmental change from northern Ellesmere Island, Canada. *Journal of Paleolimnolgy*, 16: 239-255.

Lamoureux, S. F., and Gilbert, R., 2004. A 750-yr record of autumn snowfall and temperature variability and winter storminess recorded in the varved sediments of Bear Lake, Devon Island, Arctic Canada, *Quaternary Research*, 61: 134-147.

Lamoureux, S. F., England, J. H., Sharp, M. J., and Bush, A. B. G., 2001. A varve record of increased 'Little Ice Age' rainfall associated with volcanic activity, Arctic Archipelago, Canada, *Holocene* 11: 243-249.

Laxon, S. W., Walsh, J. E., Wadhams, P., Johannessen, O., and Miles, M., 2003, Sea-ice observations. In Bamber, J. L., and Payne, A. J., (eds.) *Mass Balance of the Cryosphere*, Cambridge University Press, New York, 337-366.

Lenormand, F., Duguay, C. R., and Gauthier, R., 2002. Development of a historical ice database for the study of climate change in Canada. *Hydrological Processes*, 16: 3707–3722.

Lewis, T., Braun, C., Hardy, D. R., Francus, P., and Bradley, R. S., 2005. An extreme sediment transfer event in a Canadian High Arctic Stream, *Arctic, Antarctic, and Alpine Research*, 37: 477-482.

Lewis, T., Francus, P., Bradley, R. S., 2008. Recent occurrence of large jökulhlaups at Lake Tuborg, Ellesmere Island, Nunavut, *Journal of Paleolimnology,* DOI:10.1007/s10933-008-9240-4.

Liston, G. E., and Hall, D. K., 1995: An energy-balance model of lake-ice evolution. *Journal of Glaciology,* 41: 373-382.

Magnuson, J. J., Robertson, D. M., Benson, B. J., Wynne, R. H., Livingstone, D. M.., Arai, T., Assel, R. A., Barry, R. G., Card, V., Kuusisto, E., Granin, N. G., Prowse, T. D., Stewart, K. M., and Vuglinski V. S., 2000. Historical trends in lake and river ice cover in the northern hemisphere, *Science*, 289: 1743-1745.

Mair, D., Burgess, D. and Sharp, M. 2005. Thirty-seven year mass balance of Devon Ice Cap, Nunavut, Canada, determined by shallow ice coring and melt modeling. *Journal of Geophysical Research-Earth Surface* 110, F01011, doi:10.1029/2003JF000099.

Majorowicz, J. A., Skinner, W. R., and Šafanda, J., 2004. Large ground warming in the Canadian Arctic inferred from inversions of temperature logs, *Earth and Planetary Science Letters*, 221: 15-25.

Manabe, S., and Stouffer, R. J. 1980. Sensitivity of a global climate model to an increase of CO_2 concentration in the atmosphere, *Journal of Geophysical Research*, 85: 5529–5554.

Mann, M. E., Rutherford, S., Bradley, R. S., Hughes, M. K., Keimig F. T., 2003. Optimal surface temperature reconstructions using terrestrial borehole data, *Journal of Geophysical Research,* 108, doi:10.1029/2002JD002532.

Mann, M. E., Zhang, Z., Hughes, M. K., Bradley, R. S., Miller, S. K., Rutherford, S., and Ni, F., 2008. Proxy-based reconstructions of hemispheric and global surface temperature variations over the past two millennia, *Proceedings of the National Academy of Sciences*, 105: 13252-13257.

Marshall, S. J., Sharp, M. J., Burgess, D. O., and Anslow, F. S., 2007. Near-surface-temperature lapse rates on the Prince of Wales Icefield, Ellesmere Island, Canada: implications for regional downscaling of temperature, *International Journal of Climatology*, 27: 385-398.

Maxwell, J. B., 1981. Climatic regions of the Canadian Arctic islands, *Arctic*, 34: 225-240.

Michel, B., Ashton, G., Beltaos, S., Davar, K., Frederking, R., Gerard, L., Pratte, B., Tsang, G., and Williams, G., 1986: Hydraulics. In Ashton, G. (ed.), *River and Lake Ice Engineering*, Water Resources Publications, Littleton, CO, 261-371.

Miller, G. H., Mode, W. N., Wolfe, A. P., Sauer, P.E., Bennike, O., Forman S. L., Short, S. K. and Stafford Jr., T. W., 1999. Stratified interglacial lacustrine sediments from Baffin Island, Arctic Canada: chronology and paleoenvironmental implications, *Quaternary Science Reviews*, 18: 789-810.

Miller, G. H., Wolfe, A. P., Briner, J. P., Sauer, P. E., and Nesje, A., 2005. Holocene glaciations and climate evolution of Baffin Island Arctic Canada, *Quaternary Science Reviews*, 24: 1703-1721.

Moore, J. J., Hughen, K. A., Miller, G. H., Overpeck, J. T., 2001. Little Ice Age recorded in summer temperature reconstruction from varved sediments of Donard Lake, Baffin Island, Canada. *Journal of Paleolimnology,* 25: 503-517.

Mueller, D. R., Vincent, W. F., and Jeffries, M. O., 2003. Break-up of the largest Arctic ice shelf and associated loss of an epishelf lake. Geophysical Research Letters, 30, doi:10.1029/2003GL017931.

Mueller, D. R., Van Hove, P., Antoniades, D., Jeffries, M. O., and Vincent, W. F., *in review.* High Arctic Lakes as Sentinel Ecosystems: Cascading Regime Shifts in Climate, Ice-cover and Mixing.

Muller, P. J. et al., 1998. Calibration of the alkenone paleotemperature index U^K_{37} based on core-tops from the eastern South Atlantic and the global ocean (60 degrees N-60 degrees S). *Geochimica Et Cosmochimica Acta,* 62: 1757-1772.

Oechel, W. C., Hastings, S. J., Voulitis, G., Jenkins, M., Reichers, G., and Grulke, N., 1993. Recent change of Arctic tundra ecosystems from a net carbon dioxide sink to a souce, *Nature*, 361: 520-523.

Oswald, W. W., Anderson, P. M., Brown, T. A., Brubaker, L. B., Hu, F. S., Lozhkin, A. V., Tinner, W., and Kaltenrieder, P., 2005. Effects of sample mass and macrofossil type on radiocarbon dating of arctic and boreal lake sediments. *Holocene*, 15: 758–767.

Overpeck, J., Hughen, K., Hardy, D., Bradley, R., Case, R., Douglass, M., Finney, D. B., Gajewski, K., Jacoby, G., Jennings, A., Lamoureux, S., Lasca, A., MacDonald, G., Moore, J., Retelle, M., Smith, S., Wolfe, A., and Zeilinski, G., 1997. Arctic environmental change of the last four centuries, *Science*, 278: 1251-1256.

Palecki, M. A. and Barry, R. G., 1986. Freeze-up and break-up of lakes as an index of temperature changes during the transition seasons: a case study for Finland, *Journal of Climate and Applied Meteorology*, 25: 893–902.

Paterson, W. S. B., 1969. The Meighen Ice Cap, Arctic Canada: accumulation, ablation and flow, *Journal of Glaciology*, 8: 341-352.

Paterson, W. S. B., Koerner, R. M., Fisher, D., Johnsen, S. J., Clausen, H. B., Dansgaard, W., Bucher, P., and Oeschger, H., 1977. An oxygen-isotope climatic record from the Devon Island ice cap, arctic Canada, *Nature,* 266: 508-511.

Perren, B. B., Bradley, R. S., and Francus, P., 2003. Rapid lacustrine response to recent High Arctic warming: A diatom record from Sawtooth Lake, Ellesmere Island, Nunavut. *Arctic, Antarctic, and Alpine Research*, 35: 271-278.

Perros, M. C., and Gajewski, K., 2008. Holocene climate and vegetation changes on Victoria Island, western Canadian Arctic, *Quaternary Science Reviews*, 27: 235-249.

Perros, M. C., and Gajewski, K., 2009. Pollen-based reconstructions of late Holocene climate from the central and western Canadian Arctic, *Journal of Paleolimnology*, 41: 161-175.

Pienitz, R., Douglas M. S. V., and Smol, J.P., 2004. *Long-term environmental change in Arctic and Antarctic lakes*. Springer, Dordrecht, 562 pp.

Pollack, H. N., Huang, S., and Shen, P.-Y., 1998. Climate change record in subsurface temperatures: A global perspective, *Science*, 282: 279-281.

Prahl, F.G., and Wakeham, S.G., 1987. Calibration of unsaturation patterns in longchain ketone compositions for paleotemperature assessment. *Nature,* 330: 367-369.

Przybylak, R., 2002. Variability of total and solid precipitation in the Canadian Arctic from 1950 to 1995. *International Journal of Climatolgy*, 22: 394-420.

Rayback, S. A., and Henry, G. H. R., 2006. Reconstruction of Summer Temperature for a Canadian High Arctic Site from Retrospective Analysis of the Dwarf Shrub, *Cassiope tetragona*, *Arctic, Antarctic, and Alpine Research*, 38: 228-238.

Reimer, P. J., Baillie, M. G. L., Bard, E., Bayliss, A., Beck, J. W., Bertrand, C. J. H., Blackwell, P. G., Buck, C. E., Burr, G. S., Cutler, K. B., Damon, P. E., Edwards, R. L., Fairbanks, R. G., Friedrich, M. Guilderson, T. P., Hogg, A. G., Hughen, K. A., Kromer, B., McCormac, G., Manning, S., Ramsey, C. B., Reimer, R. W., Remmele, S., Southon, J. R., Stuiver, M., Talamo, S., Taylor, F. W., van der Plicht, J., Weyhenmeyer, C. E., 2004. IntCal04 Terrestrial Radiocarbon Age Calibration, 0–26 cal kyr BP, *Radiocarbon*, 46: 1029-1059.

Robock, A., 1980. The seasonal cycle of snow cover, sea ice, and surface albedo, *Monthly Weather Review*, 108: 267-285.

Schiff, C. J., Kaufman, D., Wolfe, A. P., Dodd, J., and Sharp, Z., 2009. Late Holocene storm-trajectory changes inferred from the oxygen isotope composition of lake diatoms, south Alaska, *Journal of Paleolimnology*, 41: 189-208.

Serreze, M. C., Holland, M. M., and Stroeve, J., 2007. Perspectives on the Arctic's shrinking sea-ice cover, *Science*, 315: 1533-1536.

Serreze, M. C., Walsh, J. E., Chapin III, F. S., Osterkamp, T., Dyurgerov, M., Romanovsky, V., Oechel, W. C., Morison, J., Zhang, T., and Barry, R. G., 2000. Observational evidence of recent changes in the northern high-latitude environment, *Climatic Change*, 46: 159-207.

Shepherd, A., Du, Z., Benham, T. J., Dowdeswell, J. A. and Morris, E. M. 2007. Mass balance of Devon Ice Cap, Canadian Arctic, *Annals of Glaciology* 46, 249–54.

Smith, I. R., 1999. Late Quaternary glacial history of Lake Hazen Basin and eastern Hazen Plateau, northern Ellesmere Island, Nunavut, Canada. *Canadian Journal of Earth Sciences*, 36: 1547-1565.

Smith, I. R. 2002. Diatom-based Holocene paleoenvironmental records from continental sites on northeastern Ellesmere Island, high Arctic, Canada. *Journal of Paleolimnology*, 27: 9-28.

Smith Jr., S. V., Bradley, R. S., Abbott, M. B., 2004. A 300 year record of environmental change from Lake Tuborg, Ellesmere Island, Nunavut, Canada, *Journal of Paleolimnolgy* 32: 137-148.

Smol, J. P., 1983. Paleophycology of a high arctic lake Cape Herschel, Ellesmere Island, *Canadian Journal of Botany*, 61: 2195-2204.

Smol, J. P., 1988. Paleoclimate proxy data from freshwater Arctic diatoms. *Verhandlungen - Internationale Vereinigung für theoretische und angewandte Limnologie*, 23: 837-844.

Smol, J. P., Wolfe, A. P., Birks, H. J. B., Douglas, M. S. V., Jones, V. J., Korholai, A., Pienitzj, R., Rühland, K., Sorvarii, S., Antoniades, D., Brooks, S. J., Fallu, M.-A., Hughes, M., Keatley, B. E., Laing, T. E., Micheluttia, N., Nazarova, L., Nyman, M., Paterson, A. M., Perren, B., Quinlan, R., Rautio, M., Saulnier-Talbot, E., Siitonen, S., Solovieva, N., and Weckström, J., 2005. Climate-driven regime shifts in the biological communities of arctic lakes, *Proceedings of the National Academy of Sciences,* 102: 4397-4402.

Solomon, S., D. Qin, M. Manning, R.B. Alley, T. Berntsen, N.L. Bindoff, Z. Chen, A. Chidthaisong, J.M. Gregory, G.C. Hegerl, M. Heimann, B. Hewitson, B.J. Hoskins, F. Joos, J. Jouzel, V. Kattsov, U. Lohmann, T. Matsuno, M. Molina, N. Nicholls, J. Overpeck, G. Raga, V. Ramaswamy, J. Ren, M. Rusticucci, R. Somerville, T.F. Stocker, P. Whetton, R.A. Wood and D. Wratt, 2007. Technical Summary, In Solomon, S., D. Qin, M. Manning, Z. Chen, M. Marquis, K.B. Averyt, M. Tignor and H.L. Miller (eds.), *Climate Change 2007: The Physical Science Basis. Contribution of Working Group I to the Fourth Assessment Report of the Intergovernmental Panel on Climate Change*, Cambridge University Press, Cambridge, United Kingdom and New York, NY, USA.

Steig, E. J., Grootes, P. M., and Stuiver, M., 1994. Seasonal precipitation timing and ice core records, *Science*, 266: 1885-1886.

Stewart, K. M., and Platford, R. F., 1986. Hypersaline gradients in two Canadian High Arctic lakes, *Canadian Journal of Fisheries and Aquatic Science,* 43:1795-1803.

Stewart, K. M. and Haugen, R. K., 1990. Influence of lake morphometry on ice dates: *Internationale Vereinigung fur Theoretische und Angewandte Limnologie:Verhandlungen*, 24: 122–127.

Stocker, T. F., and Wright, D. G., 1991. Rapid transition of the ocean's deep circulation induced by changes in surface water fluxes, *Nature*, 351: 729-732.

Stoner, J. S., and St-Onge, G., 2007. Magnetic Stratigraphy: Reversals, Excursions, Paleointensity and Secular Variation, In Hillaire-Marcel C., and de Vernal, A. (eds) *Developments in Marine Geology: Volume 1, Proxies in Late-Cenozoic Paleoceanography*, Elsevier*, 99-138.

Stuiver, M., and Reimer, P. L., 1993. Extended ^{14}C database and revised CALIB radiocarbon calibration program, *Radiocrabon*, 35:215-230.

Sturm, M., 1979. Origin and composition of clastic varves. In, Schlüchter, C. (ed.), *Moraines and varves*. Balkeema, Rotterdam, 281-285.

Thomas E. K., and Briner, J. P., 2009. Climate of the past millennium inferred from varved proglacial lake sediments on northeast Baffin Island, Arctic Canada, *Journal of Paleolimnology*, DOI:10.1007/s10933-008-9258-7.

Thomas, E. K., Axford, Y., and Briner, J. P., 2007. Rapid 20th century environmental change on Northeastern Baffin Island, Arctic Canada inferred from a multi-proxy lacustrine record, *Journal of Paleolimnology*, 40: 507-517

Trettin, H. P. 1994, Pre-carboniferous geology of the northern part of the Arctic Islands, Hazen Fold Belt and adjacent parts of central Ellesmere Fold Belt, Ellesmere Island, Geological Survey of Canada, Bulletin 430, 260 pp.

Tomkins, J. D., Lamoureux, S. F., Antoniades, D., and Vincent, W. F., 2009. Sedimentary pellets as an ice cover proxy in a High Arctic ice-covered lake. *Journal of Paleolimnology*, 41:225–242.

Van Hove, P., Belzile, C., Gibson, J. A. E., and Vincent, W. F., 2006. Coupled landscape-lake evolution in High Arctic Canada, *Canadian Journal of Earth Science*, 43: 533-546.

Vavrus, S. J., Wynne, R. H., and Foley, J. A., 1996. Measuring the sensitivity of southern Wisconsin lake ice to climate variations and lake depth using a numerical model, *Limnology and Oceanography*, 41: 822– 831.

Vincent, W. F., MacIntyre, S., Spige, R. H., and Laurion, I., 2008. The physical limnology of high-latitude lakes. In Vincent, W. F. and Laybourn-Parry, J., (eds.), *Polar Lakes and Rivers: Limnology of Arctic and Antarctic Aquatic Ecosystems*. Oxford University Press, Oxford, 65-81.

Vinther, B. M., Andersen, K. K., Jones, P. D., Briffa, K. R., and Cappelen, J. 2005. Extending Greenland temperature records into the late 18th Century, *Journal of Geophysical Research,* doi:10.1029/2005JD006810, 111, D11105.

Vinther, B. M., Clausen, H. B., Fisher, D. A., Koerner, R. M., Johnsen, S. J., Andersen, K. K., Dahl-Jensen, S., Rasmusssen, S. O., Steffensen, J. P., and Svensson, A. M., 2008. Synchronizing ice cores from the Renland and Agassiz ice caps to the Greenland Ice Core Chronology, *Journal of Geophysical Research*, 113: D08115, doi:10.1029/2007JD009143.

Wanner, H., Beer, J., Bütikofer, J., Crowley, T. J., Cubasch, U., Flückiger, J., Goosse, H., Grosjean, M., Joos, F., Kaplan, J. O., Kütter, M., Müller, S. A., Prentice, I. C., Solomina, O., Stocker, T. F., Tarasov, P., Wagner, M., Widmann, M., 2008. Mid- to Late Holocene climate change: an overview, *Quaternary Sciecne Reviews*, 27: 1791-1728.

Wetzel, R. G., 2001. *Limnology: Lake and River Ecosystems,3rd edition*, Elsevier, London, 1006 pp.

Weyhenmeyer, G. A., Meili, M., and Livingstone, D. M., 2004. Nonlinear temperature response of lake ice breakup, *Geophysical Research Letters*, 31, L07203, doi:10.1029/2004GL019530.

Willemse, N. W., and Tornqvist, T. E., 1999. Holocene century-scale temperature variability from West Greenland lake records, *Geology,* 27: 580-584.

Wolfe, A. P., Fréchette, B., Richard, P. J. H., Miller, G. H. and Forman, S. L., 2000. Paleoecology of a >90,000-year lacustrine sequence from Fog Lake, Baffin Island, Arctic Canada, *Quaternary Science Reviews,* 19: 1677-1699.

Wolfe, A. P., Miller, G. H., Olsen, C. A., Forman, S. L., Doran, P.T., Holmgren, S. U., 2004. Geochronology of high latitude lake sediments. In Pienitz, R., Douglas, M. S. V.,and Smol, J. P. (eds.), Long-term Environemntal Change in Arctic and Antarctic Lakes. Sprnger, Netherlands, 19-52.

Wolfe, A. P., and Smith, I. R., 2004. Paleolimnology of the middle and high Canadian Arctic, In Pienitz, R., Douglas, M. S. V., and Smol, J. P., (eds.), *Long-term Environmental Change in Arctic and Antarctic Lakes*, Springer, Netherlands, 241-268.

Wolfe, B. B., Edwards, T. W. D., Buening, K. R. M., and Elgood, R. J., 2001. Carbon and oxygen isotope analysis of lake sediment cellulose: methods and applications, In Last, W. M. and Smol, J. P., (eds.), *Tracking Environmental Change Using Lake Sediments*, *Vol. 2, Physical and Geochemical Methods*, Developments in Paleoenvironmental Research, Kluwer Academic Publishers, Dordrecht, pp. 673-400.

Wolken, G. J., 2006. High-resolution multispectral techniques for mapping former Little Ice Age terrestrial Ice cover in the Canadian High Arctic, *Remote Sensing of the Environment*, 101: 104-114.

Wolken, G. J., England, J. H. and Dyke, A. S. 2005. Re-evaluating the relevance of vegetation trimlines in the Canadian Arctic as an indicator of Little Ice Age paleoenvironments, *Arctic* 58: 341–53.

Wolken, G. J., England, J. H. and Dyke, A. S., 2008a. Changes in late-Neoglacial perennial snow/ice extent and equilibrium-line altitudes in the Queen Elizabeth Islands, Arctic Canada. *The Holocene* 18: 615-627.

Wolken, G.J., Sharp, M.J. and England, J.H. 2008b. Changes in late-Neoglacial climate inferred from former equilibrium-line altitudes in the Queen Elizabeth Islands, Arctic Canada. *The Holocene* 18: 629-641.

Woo, M.-K., 1983. Hydrology of a drainage basin the Canadian High Arctic. *Annals of the Association of American Geographers*, 73: 577-596.

Woodcock, H., and Bradley, R., 1994. *Salix arctica* (Pall.): its potential for dendroclimatological studies in the High Arctic, *Dendrochronologia*, 12: 11-22.

Wooller, M . Francis, D., Fogel, M. L., Miller, G. H., Walker, I R., and Wolfe., 2004. Quantitative paleotemperature estimates from δ^{18}O of chironomid head capsules preserved in arctic lakes, *Journal of Paleolimnology,* 31: 267-274.

Zolitschka, B., 1996. Recent sedimentation in a high arctic lake, northern Ellesmere Island, Canada, *Journal of Paleolimnology,*16:169–186.

Zolitschka, B., 2007. Varved Lake Sediments. In Elias, S. A., (ed.), Encyclopedia of Quaternary Science, Elsevier, Amsterdam, 3105-3114.